A Hybrid Neural Network- Mathematical Programming Approach to Design an Air Quality Monitoring Network for an Industrial Complex

by

Suad Al-Adwani

A thesis

presented to the University of Waterloo

in fulfillment of the

thesis requirement for the degree of

Master of Applied Science

in

Chemical Engineering

Waterloo, Ontario, Canada, 2007

I hereby declare that I am the sole author of this thesis. This is a true copy of the thesis, including any required final revisions, as accepted by my examiners.

I understand that my thesis may be made electronically available to the public.

Abstract

Air pollution sampling site selection is one of the most important and yet most vexing of the problems faced by those responsible for regional and urban air quality management and for the attainment and maintenance of national ambient air quality standards. Since one cannot hope to monitor air quality at all locations at all times, selection of sites to give a reliable and realistic picture of air quality becomes a major issue and at the same time a difficult task. The location (configuration) and the number of stations may be based on many factors, some of which may depend on limited resources, federal and state regulations and local conditions. The combination of these factors has made air quality surveys more complex; requiring comprehensive planning to ensure that the prescribed objectives can be attained in the shortest possible time and at the least cost. Furthermore, the choice and siting of the measuring network represents a factor of significant economic relevance for policymakers. In view of the fact that equipment, maintenance and operating personnel costs are increasing dramatically, the possibility of optimizing the monitoring design, is most attractive to the directors of air quality management programs.

In this work a methodology that is able to design an optimal air quality monitoring network (AQMN) is described. The objective of the optimization is to provide maximum information about the presence and level of atmospheric contaminants in a given area and with a limited budget. A criterion for assessing the allocation of monitoring stations is developed by applying a utility function that can describe the spatial coverage of the network and its ability to detect violations of standards for multiple pollutants. A mathematical model based on the Multiple Cell Approach (MCA) was used to create monthly spatial distributions for the concentrations of the pollutants emitted from different emission sources. This data was used to train artificial neural networks (ANN) that were proven to be able to predict very well the pattern and violation scores at different potential locations. These neural networks were embedded within a mathematical programming model whose objective is to determine the best monitoring locations for a given budget. This resulted in a nonlinear program (NLP).

The proposed model is applied to a network of existing refinery stacks and the locations of monitoring stations and their area coverage percentage are obtained.

Acknowledgments

This journey was special to me and my family. It was hard and tough but I have gained many new good friends and now I am attached to them and to a very beautiful city which I believe will become one day the Knowledge Capital of Canada.
I am grateful to my family and friends. Their support and encouragement was essential part of my success. Without them I would not be able to make it.

Special thanks to my supervisors, Prof. Ali El-Kamel and Prof. Thomas Duever. They provided me with their guidance and care. Prof's Duever and El-Kamel taught me the techniques and methodologies to achieve the objectives of our research work. My dear supervisors made each single problem we faced in our research a new interesting challenge and pushed me to find out my way.

I am grateful for Prof. Mazda Biglari and Prof. Jason Grove for their valuable comments and their contribution in my research work.

I will always have you all in my heart

Dedication

To my beloved father,

Mohammed

Table of Contents

List of Figures

List of Tables

Chapter 1– Introduction

1.1 Research Capabilities

Protection of human health and the environment from pollutants effects is the primary goal of all air pollution control programs. In order to evaluate the direct and indirect effects caused by emissions from air pollution sources, The Air Quality Monitoring Network (AQMN) is an essential tool to monitor and control the atmospheric pollution.
Determination of how many monitoring stations to have and on which site to build them is the most important factor to be taken into account when designing these networks.
The AQMN design objective is usually to provide maximum information about the air quality in a given area with minimum number of monitoring stations. It is required to determine the minimum number of monitoring stations due to budget constraints. Providing the minimum number of stations minimizes the installation, maintenance, and management costs.

In this study, the Multiple Cell Model is used to predict the ground level concentration for multiple pollutants such as SO_2, NO_x, CO in a network of refinery stacks. These data are used to evaluate the siting criteria. Two objectives of AQMN design are of interest; representation of spatial-temporal patterns (or pattern score) and the detection of violations of ambient air quality standard (or violation score). These two objectives are incorporated into a Neural Networks (NN) models. The models obtained have strong predictive abilities in modeling the violation and pattern scores as functions of spatial positions (x,y).

The combination of the two objectives for the multiple pollutants represents a utility function. This function is maximized using optimization techniques in order to find the optimal number and location of monitoring stations in an industrial area.

The optimization models which are developed can be implemented and used for as many stations as needed within a prescribed budget constraint and a desired coverage area.

A sensitivity analysis on the optimum location with respect to changes in pollutants weights of pattern scores and violation scores is also given. The coverage area of the monitoring stations is also calculated.

1.2 Research Objectives

The main objectives of this research are as follows:

1. To determine criteria for designing the optimality of air quality monitoring network for multiple pollutants. Two objectives have been considered in this design:
   - Representation of spatial-temporal patterns.
   - Detection of violations of ambient air quality standards.

2. To develop a mathematical model that incorporates the design criteria to find the optimal AQMN

3. To develop a new optimization strategy based on a hybrid neural network-mathematical programming model to find the optimal number and location of monitoring stations in an industrial area.

1.3 Thesis Outlines

The thesis is divided into the following six chapters:

Chapter 1 Focuses on the research capability and the major objectives of the research.

Chapter 2 Presents a literature review. This chapter discusses the air pollution sources, effects, and control. The air pollution dispersion modeling and the optimization of AQMN are also discussed in this chapter.

Chapter 3 Describes a mathematical model based on the Multiple Cell Approach (MCA). Also a multi objectives design criteria for AQMN is outlined.

Chapter 4 Discusses the artificial neural network models that represent the violation scores and pattern scores as functions of the spatial co-ordinates for the purpose of AQMN design.

Chapter 5 Presents the optimization techniques in order to find the optimal number and location of monitoring stations.

Chapter 6 Gives conclusions and recommendations of the research work of this thesis.

Chapter 2- Literature Review

2.1 Introduction

Air pollution maybe defined as the presence in the atmosphere of one or more contaminants in such quantities and duration as may tend to be injurious to human, plant, animal life, property, or which unreasonably interferes with the comfortable enjoyment of life, property or the conduct of business. Air pollution is woven throughout the fabric of our modern life. A by-product of the manner in which we build our cities, air pollution is a waste remaining from the ways we produce our goods, transport ourselves and our goods, and generate the energy to heat and light the places where we live, play and work (Wark et. al., 1998).

The total amount of pollutants emitted into the atmosphere is about 90% gaseous substances and about 10% particulates. It has been estimated that 3×10^{12} kg of gaseous, liquid and solid pollutants enter the earth's atmosphere every year. Human activity now contributes about 10% of this amount. The other is natural processes such as forest fires, decaying vegetation, dust storms, and volcanic eruptions.

The major pollutants are particulate matter less than 10 μm in diameter (PM_{10}), sulphur dioxide (SO_2), nitrogen dioxide (NO_2), carbon monoxide (CO), volatile organic compounds (VOCs), particulate lead and ozone (O_3).

The approximate amounts of emissions resulting from human activity and industrial processes are shown in Tables 2.1 and 2.2.

Table 2.1 Estimated Emissions from Main Pollution Sources Resulting from Human Activity (Bretschneider and Kurfurst, 1987).

Kind of sources	**Estimated amount of pollutant per year (10^9 kg)**					
	Solid	**SO_x**	**NO_x**	**CO**	**C_xH_y**	**Total**
Transport						
Automobiles	0.7	0.3	7	67.3	12.7	88
Other	0.5	0.1	1	3.9	1.1	6.6
Transport total	1.2	0.4	8	71.2	13.8	94.6
Combustion of fuels						
Power stations	2.3	14	3.5	0.1		19.9
Industry	3	5.5	3.1	0.3	0.1	12
Cities	0.4	1.8	0.5	1.3	0.6	4.6
Other	0.3	0.7	0.4	0.2		1.6
Combustion of fuels total	6	22	7.5	1.9	0.7	38.1
Production of goods, treatment of raw materials	5.9	7.2	0.2	7.8	3.5	24.6
Dumping, liquidation, and treatment of wastes	1.2	0.1	0.7	4.5	1.4	7.9
Other	0.4	0.6	0.2	1.2	4.2	6.6
Total	14.6	30.3	16.6	86.6	23.6	172.8

Table 2.2 Contribution of Industrial Processes to Atmospheric Pollution (Bretschneider and Kurfurst, 1987).

Industry	Main pollutants	Total amounts of emissions per year (10^9 kg)
Petroleum refineries	particulates	3.8
	sulphur oxides	
	hydrocarbons	
	carbon monoxide	
Nonferrous metallurgy (Al, Cu, Pb, Zn)	particulates	3.7
	sulphur oxides	
Foundries	particulates	3.3
	carbon monoxide	
Paper mills	particulates	3
	carbon monoxide	
	sulphur oxides	
Grading of coal and wastes	particulates	2.1
	sulphur oxides	
	carbon monoxide	
Coke batteries (steel industry)	particulates	2
	sulphur oxides	
	carbon monoxide	
Iron and steel mills	particulates	1.6
	carbon monoxide	
Milling and treatment of grains	particulates	1
Production of cement	particulates	0.8
Production of phosphate fertilizers	particulates	0.3
	fluorides	

2.2 Air Pollution Emission Sources

There are different ways for characterizing the sources of air pollution. First we will describe the main air pollution sources which could be divided and characterized into point, line, area, or volume sources.

A point source has no geometric dimensions. This type of air pollution source is a single identifiable source of air pollutant emissions (such as a gas stack or chimney). Point sources could be either elevated or at ground-level. Another type is the line source which is a one-dimensional source of air pollutant emission (like vehicular traffic on a roadway, conveyor belt and railway). The third type is the area source which is a two-dimensional source of diffuse air pollutant emissions (such as a forest fire and a landfill). The last type we would like to mention here of the main sources of air pollution is the volume source. The volume source is a three-dimensional source of diffuse air pollutant emissions. It is an area source with a third (height) dimension (such as the fugitive gaseous emissions from piping flanges, valves and oil refineries and petrochemical plants).

There are other ways to characterize the air pollutant emission sources. The other air pollution sources would be:

a. Stationary or mobile; flue gas stacks are examples of stationary sources and buses are examples of mobile sources.
b. Urban or rural; urban areas constitute a so-called heat island and the heat rising from an urban area causes the atmosphere above an urban area to be more turbulent than the atmosphere above a rural area.
c. Sources time duration:
    i. Puff; short term sources (such as, many accidental emission releases).
    ii. Continuous; a long term source (such as, most flue gas stack emissions).

2.3 Air Pollution Effects

The pollutants affect people life and environment on a local and urban scale. Air pollution impacts the health of human and animals, causes the acid rain, damages vegetations, soil and deteriorates materials, affects climate, reduce visibility and solar radiation, impairs production processes, contributes to safety hazards. Air pollution has led to a number of global concerns such as ozone depletion and global climate change.

Stratospheric ozone protects the biosphere from potentially damaging doses of ultraviolet radiation (UV). Depletion of stratospheric ozone is caused by the release of such pollutants such as chlorofluorocarbons (CFCs), halons, methyl bromide, and hydrochlorofluorocarbons (HCFCs) and these substances could be used in many commercial applications such as refrigerants, aerosol propellants, foam-blowing agents, cleaning solvents, air conditioning gases and other substances. CFCs which are stable in the lower atmosphere break down in the stratosphere, releasing chlorine atoms. Chlorine atoms and other radicals remove stratosphere ozone very effectively through a set of catalytic reactions so CFCs can destroy the ozone layer in the stratosphere. Stratosphere ozone is an important key to protect all life on earth since it absorbs ultraviolet (UV) radiation coming into the earth's atmosphere, preventing the UV radiation from reaching ground level.

There is a huge ozone hole over Antarctica. The hole which is as big as the United States leads to a significant increase in UV radiation reaching the earth's surface, which could adversely affect human and animal health, as well as impact the ecosystem. Forty six countries developed a treaty (the Montreal Protocol) to protect the stratosphere ozone layer and reduce the production of these pollutants.

Next we discuss global climate change, also called global warming or the greenhouse effect. The earth's surface and the atmosphere above the earth's surface create a natural effect, referred to as the greenhouse effect. If the earth had no greenhouse effect, the temperature would be much cooler than it is at the present time.

Carbon dioxide and water vapor have the ability to trap heat and warm the climate. With an increase in the concentration of greenhouse gases such as CO_2, trichlorofluoromethane ($CFCl_3$), dichlorodifluoromethane (CF_2Cl_2), methane (CH_4), and nitrous oxide (N_2O) the atmosphere absorption of the infrared is increased. This lead to an increase in the average temperature of the earth's surface and this will increase the frequency of the extremes of weather such as hurricanes, tornados, heat waves, droughts and floods. Carbon dioxide is the main contributor to the global warming. The main source of carbon dioxide emissions is the burning of coal, oil and gas (Cooper and Alley, 2002).

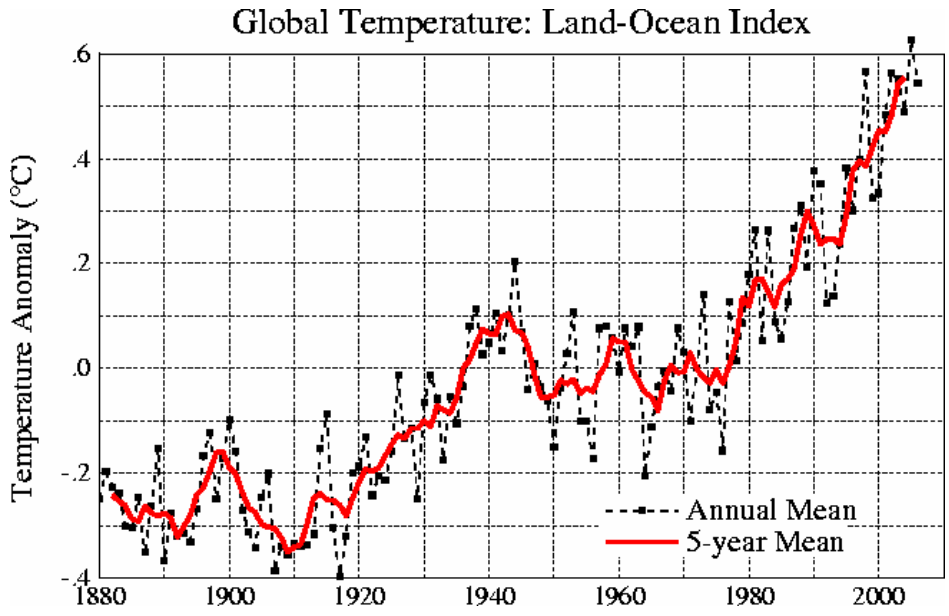

Figure 2.1 Global Annual Mean Surface Air Temperature Change (www.giss.nasa.gov/data/update/gistemp/graphs)

2.4 Air Pollution Control

Air pollution control is an important key to the protection of the atmosphere and demands regulatory acts and engineered solutions.

2.4.1 The Regulatory Control of Air Pollution

Regulation is a driving force in emission reduction programs. Governments impose regulatory control to limit the emission from pollution sources such as chimneys, vents, and stacks. Regulations may limit the quantity or the quality of pollutants.

The pollution prevention limit is based on emission standards, ambient air quality standards and health risk standards. Environmental laws are established to force industry sectors to meet the legal standards and reduce the presence of pollutants. Also the governmental organization should develop and implement action plans and highlight technologies that maybe applicable to pollution prevention opportunities. Optimal solution to pollution problem should be balanced between the financial and environmental benefits in the industrial technology (Cheremisinoff, 2002).

2.4.2 The Engineering Control of Air Pollution

The engineering solutions involve process modifications or process substitutions to eliminate wastes so that pollution does not occur, or is at least kept to a minimum. The air pollution control technologies must not increase pollution in other sectors of the environment but rather should eliminate or convert air pollutants to less polluting forms.

There are two broad approaches to control air pollution depending on the type of pollutants:

1. Particulate control

   The most common and important devices applied in control applications for dust and particulate matter are mechanical separators (such as gravity settlers, or cyclones), fabric filters, electrostatic precipitators, and wet scrubbers.

2. Gases and vapour control

   The reduction of the gases concentration to desirable levels can be accomplished using adsorption, absorption, and incineration (Wark et al., 1998).

2.5 Air Pollution Dispersion Modeling

Air dispersion modelling is the mathematical estimation of pollutant impacts from emissions sources within a study area. Several factors impact the fate and transport of pollutants in the atmosphere including meteorological and geographical conditions, site configuration, and emission release characteristics. The dispersion models are used to estimate or to predict the downwind concentration of air pollutants emitted from sources such as point sources, area sources, and mobile sources. The modeling techniques that will be discussed in this section are limited to point sources and non reactive effluents.

There is a wide array of air dispersion models available to simulate the impacts of emissions of non reactive pollutants. Table 2.3 presents some of these models and their major features.

Table 2.3 Available Models for Modeling Emissions of Non-reactive Pollutants (Seigneur, 1992).

Model	Number of sources	Meteorological conditions	Environmental setting
SCREEN	One	Worst-case	Flat terrain, accepts Terrain elevation
Industrial Source Complex (ISC)	Multiple	Actual	Flat terrain, accepts Terrain elevation, Urban or rural areas
COMPLEX 1	Multiple	Actual	Complex terrain, Rural area
SHORT Z LONG Z	Multiple	Actual	Complex or flat terrain, urban or rural areas
Rough Terrain Dispersion Model (RTDM)	Multiple, Co-located	Actual	Complex terrain
Offshore and Coastal Dispersion (OCD)	Multiple	Actual	Coastal region

The SCREEN model was developed to provide an easy-to-use method of obtaining pollutant concentration estimates. In most cases, it predicts the concentration to be overestimates of actual concentrations. The ISC model predicts the concentrations from a variety of emission sources in a single simulation. This model exists in two versions: short term (ISC-ST) and long term, both have the same atmospheric process treatment but they are different in data treatment. Complex 1, SHORT Z, LONG Z models are used in the areas of complex terrain with elevation that exceeds the pollutant source. RTDM model provides better predictions of pollutant concentration but needs more input data. The OCD model is mainly used in the area near a large body of water. Reactive Plume Model and the PLMSTAR model are providing predictions for the reactive pollutants. In the next section the Gaussian dispersion model will be discussed.

2.5.1 The Gaussian Dispersion Model

The widely used dispersion model to compute pollutant concentration profiles is the Gaussian plume model for single or multiple sources. The Gaussian dispersion equation is the basis for almost all of the computer programs developed by the Environmental Protection Agency (EPA). It predicts the concentration at steady state of non reactive gaseous pollutants from an elevated source;

$$C(x,y,z) = \frac{Q}{2\pi u \sigma_y \sigma_z}\left[\exp -\left(\frac{y^2}{2\sigma_y^{\,2}}\right)\right]\left\{\exp\left[\frac{-(z-H)^2}{2\sigma_z^{\,2}}\right] + \exp\left[\frac{-(z+H)^2}{2\sigma_z^{\,2}}\right]\right\}$$

Where,

C : Steady-state concentration at a point (x,y,z) (g/m^3)

Q: Pollutant emission rate (g/s)

u : Average wind speed at point of release (m/s)

σ_y, σ_z : Horizontal and vertical spread parameters, (m), these are functions of distance, x, and atmospheric stability.

y : Horizontal distance from plume centerline (m)

z : Vertical distance from the ground level (m)

H : Effective height of the centerline of the pollutant plume (H = h + Δh, where h = physical stack height and Δh = plume rise, m)

The wind-oriented coordinate system is shown in Figure 2.2

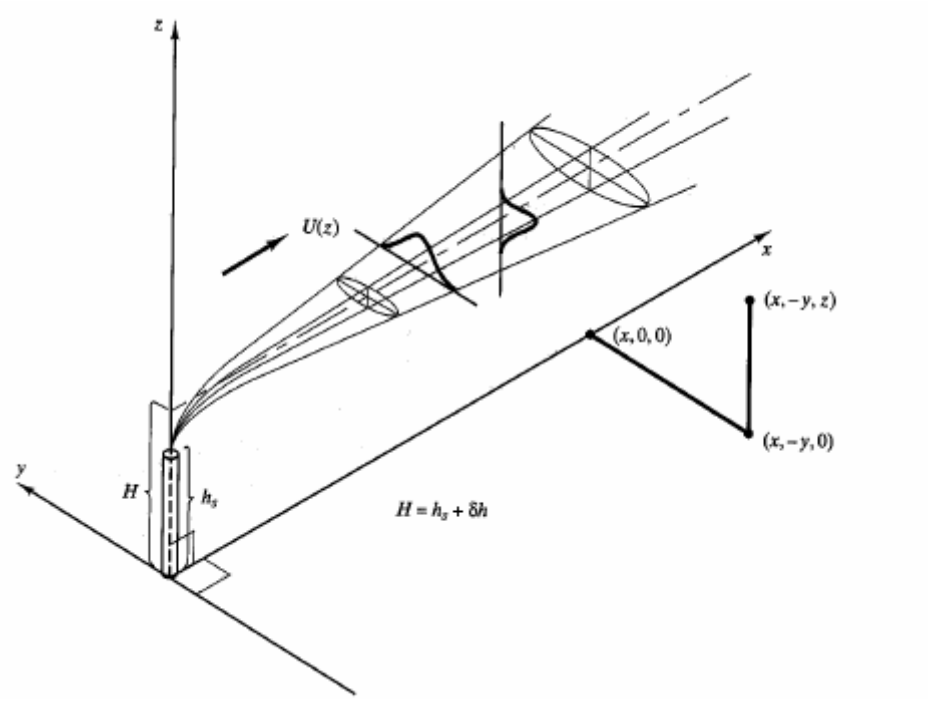

Figure 2.2 Coordinate Systems for Gaussian Plume Model.

Several assumptions are made in this equation:

1. Steady-state concentration to the dispersion of the pollutants in the atmosphere; therefore, $\frac{\partial C}{\partial t}$ is zero.
2. The emission is continuously released.
3. Horizontal advection is balanced by vertical and transverse turbulent diffusion.
4. The dispersion is for non reactive gaseous pollutant.
5. No diffusion along the horizontal axis (no diffusion in the downwind (x) direction).
6. Even though the wind speed does vary in the three coordinate directions, the variation is relatively small. Therefore it is appropriate to assume that the wind speed u is constant (Wark et al., 1998; Cooper and Alley, 2002)

2.5.1.1 Dispersion Coefficient and Atmospheric Stability Classes

It is necessary to determine the dispersion coefficients σ_y, σ_z which are strong functions of atmospheric stability and downwind distance. These parameters are not monitored by meteorological stations and must always be approximated through indirect methods. Using a stability class approach leads to a determination of σ_y and σ_z.

Pasquill (Stern et al., 1984) defined six stability classes ranging from highly stable, low-turbulence Class F, to unstable, highly turbulent Class A**,** and he identified the surface wind speed, intensity of solar radiation, and night time sky cover as being the prime factors controlling atmospheric stability. These stability classes are then correlated with observations of the behaviour of plumes in terms of their dispersion with the identified prime meteorological factors. This system is summarized in Table 2.4.

Table 2.4 The Pasquill Stability Classes

Surface wind speed (m/s)	**Insulation**			**Night**	
	Strong	**Moderate**	**Slight**	**Thinly overcast or ≥ 4/8 cloudy**	**≤ 3/8 clear**
<2	A	A-B	B	---	---
2-3	A-B	B	C	E	F
3-5	B	B-C	C	D	E
5-6	C	C-D	D	D	D
>6	C	D	D	D	D

(For A-B, take the average of values for A and B, etc.)

Alternatively, dispersion coefficients σ_y, σ_z can be calculated using several equations including Briggs, Green, Martin, McMullen, and Turner. Table 2.5 shows empirical formulas for dispersion parameters.

Table 2.5 Empirical Formulas for Dispersion Parameters (Stern et al., 1984).

		σ_y (m)	σ_z (m)
Briggs (rural)	A	$0.22x(1+0.0001x)^{-1/2}$	$0.20x$
	B	$0.16x(1+0.0001x)^{-1/2}$	$0.12x$
10^2 m < x < 10^4 m	C	$0.11x(1+0.0001x)^{-1/2}$	$0.08x(1+0.0002x)^{-1/2}$
	D	$0.08x(1+0.0001x)^{-1/2}$	$0.06x(1+0.0015x)^{-1/2}$
	E	$0.06x(1+0.0001x)^{-1/2}$	$0.03x(1+0.0003x)^{-1}$
	F	$0.04x(1+0.0001x)^{-1/2}$	$0.016x(1+0.0003x)^{-1}$
Briggs (urban)	A-B	$0.32x(1+0.0004x)^{-1/2}$	$0.24x(1+0.001x)^{1/2}$
	C	$0.22x(1+0.0004x)^{-1/2}$	$0.20x$
10^2 m < x < 10^3 m	D	$0.16x(1+0.0004x)^{-1/2}$	$0.14(1+0.003x)^{-1/2}$
	E-F	$0.11x(1+0.0004x)^{-1/2}$	$0.08x(1+0.0015x)^{-1/2}$
Green		$\sigma_y = \frac{Kx}{\left[1+(x/a)\right]^p}$	$\sigma_z = \frac{Lx}{\left[1+(x/a)\right]^q}$
		K, L, a, p, q : coefficients for a given stability conditions, x (km)	
Martin		$\sigma_y = ax^b$	$\sigma_z = cx^d + f$
		a, b, c, d, f : coefficient for a given stability conditions, x (km)	
McMullen		$\sigma = \exp\left[I + J(\ln x) + K(\ln x)^2\right]$ I, J, K : coefficients for a given stability condition, x (km)	
Turner		$\sigma_y = \frac{1000x\tan(T)}{2.15}$	$\sigma_z = ax^b$
		T: One half Pasquill's θ (degree); is a function of x for a given stability class a,b: coefficients for a given stability condition, x (km)	

2.5.1.2 Plume Rise Determination

It is important to determine the height to which a buoyant plume with an initial exit velocity will rise. Plume rise is defined as the distance between the top of the stack and the axis of the centroid of the pollutant distribution.

It is highly dependent on terrain roughness and variable geographic effects.

All plume rise formulas contain at least one dimensionless constant that must be evaluated experimentally, and the value of these so-called constants varies from stack to stack. Table 2.6 presents some of the well-known plume rise formulas used in different model approaches (Cheremisinoff, 2002).

2.6 Air Quality Monitoring

The protection of human health and the environment from pollutants effects is the primary goal of all air pollution control programs. The protection of air quality requires accurate data on the ambient concentrations of major pollutants and emissions from air pollution sources to be available to regulatory authorities. Representations of spatial and temporal variations as well as characterizing and quantifying emissions are vital to the success of air quality monitoring. In the U.S., monitoring provides data to:

1. Determine compliance with National Ambient Air Quality Standards (NAAQSs) for seven pollutant categories in air quality control regions (AQCRs).
2. Determine long-term trends.
3. Determine human exposures.
4. Support the Air Quality Index program.
5. Support emissions reduction programs.
6. Determine effectiveness of emission control programs.
7. Support environmental assessments such as visibility impairment and degradation of watersheds.
8. Support research efforts designed to determine potential associations between pollutant levels and adverse health and environmental effects (Godish, 2004) .

Table 2.6 Examples of Plume Rise Formulas Reported in Literature (Cheremisinoff, 2002).

Investigator	Formula	Comment
Holland	$\Delta h = (1.5V_s d + 0.04Q_h)/U$ where Δh = plume rise (m), V_s = stack exit velocity (m/s), d = stack diameter (m), Q_h = heat emission rate (kcal/s), U = stack top wind speed (m/s)	Highly empirical. Requires stack testing Confirmation on case-by- Case basis
Concawe	$\Delta h = 5.53Q_h^{1/2}/U^{3/4}$	Regression formula best suited for large buoyant plumes
Stumke	$\Delta h = (d/U)[1.5V_s + 65d^{1/2}\theta^{0..25}]$ where $\theta = (T_a-T_s)/T_s$ T_a = ambient air temperature, K T_s = stack gas temperature, K	Same as Holland formula
Lucas-Moore-Spurr	$\Delta h = 135Q_h^{1/4}/U$	Regression formula with ill-defined statistics
Rauch	$\Delta h = 47.2Q_h^{1/4}/U$	Same as Lucas formula
Stone-Clark	$\Delta h = (104.2 + 0.17h_p)Q_h^{1/4}/U$ where h_p = physical stack height (m)	Modification of Lucas-Moore expression, takes into account effect of physical stack
Moses and Carson	$\Delta h = (A/U)(-0.029V_s + 5.53Q_h^{1/2})$ A = coefficient dependent on atmospheric stability: A = 2.65; Unstable A = 1.08; Neutral A = 0.68; Stable	Regression formula
Briggs	For unstable and neutral conditions: $\Delta h = 0.25Q_h^{1/3}h_p^{2/3}U$ For stable conditions: $\Delta h = 0.296[Q_h/U(\partial\theta/\partial z)]^{1/3}$ where $(\partial\theta/\partial z)$ = variation of potential temperature with height $\approx$ 0.03 K/m	Non-empirical formulation

2.7 Air Quality Monitoring Networks

Shindo and co-authors (1989) studied spatial and temporal variations of air pollution data from ambient air monitoring stations. The analysis of the actual monitoring data demonstrated that a spatio-temporal structure of air pollution field changes within several years. The variation of the meteorological conditions and the changes of locations and size of emission sources are the main cause of the changes. An optimal network based on an estimated spatial distribution or on data in a year or season is not optimal for actual pollution fields during its life span and mathematically rigorous optimality of such a network is inappropriate. The authors also proposed fundamental policies for a rational network design.

Liu and co-workers (1986) presented a methodology for determining the number and disposition of ambient air quality stations in a monitoring network for compliance with air quality standards. The developed methodology utilizes a database with real or simulated data from an air quality dispersion model for application with a two-step process for ascertaining the optimal monitoring network. The methodology is applied in a companion paper to the Las Vegas, Nevada metropolitan area for the pollutant carbon monoxide.

Arbeloa and co-authors (1993) introduced a method to design air quality monitoring networks (AQMN) for a single pollutant in which the technique leads to an optimal network. The network was able to provide maximum information with minimum measurement devices. The optimal number of stations in the network is calculated studying the variation of the coverage effectiveness and number of violations versus the number of stations in the network and the cutoff value chosen to characterize the Sphere of Influence (SOI).

Pittau and co-authors (1999) provided a study of an area in the province of Venice, in Northern Italy. The methodology is applied for two different pollutants SO_2 and NO_x. The two pollutants which have been considered characterize industrial pollution, vehicular traffic and heating plants pollution. The air quality model used is a multisource Gaussian grid model. In particular, a Plume Gaussian Model is used to simulate the dispersion of continuous emissions in steady state conditions while

instantaneous emissions are simulated by a Puff Gaussian Model. The model also takes into account the particular meteorological conditions of Northern Italy. The authors concluded that the cost of monitoring could be reduced without a reduction in the information by minimizing the number of stations.

Modak and Lohani (1985) extended their development for the Minimum Spanning Tree (MST) algorithm to consider multiple objectives in the optimum AQMN design. This extension is possible via two approaches; one based on the utility function and another based on the principles of sequential interactive compromise. The authors presented a case study of Taipei City, Taiwan. The multi-objective optimization of the AQMN has several useful implications besides optimization of network density and configuration. Optimization is then only a beginning for seeking policies in search of effective air quality management.

Demerjian (2000) presented a review of national monitoring networks in North America. The review was focused on the current state of national air quality monitoring networks. The author provided an assessment for the effectiveness and adequacy of these networks in addressing the critical needs of the various user communities they were designed to serve. Ozone, particulate matter (PM_{10} and $PM_{2.5}$) and their associate precursor compounds were the main measurements and contribution of monitoring networks from this study.

Silva and Quiroz (2003) attempted to optimize an atmospheric monitoring network of Chile's capital (Santiago) by excluding the least informative stations. The study pollutant variables were carbon monoxide (CO), airborne particulate material (PM_{10}), ozone (O_3) and sulfur dioxide (SO_2). The authors used an index of multivariate effectiveness, based on the Shannon information index and applied it to the network. The multivariate approach provided the most complete analysis from the information perspective.

Peterson (2000) presented the results of multi-scale assessment in order to develop recommendations for an ozone monitoring network for western Washington. A multi-scale assessment was a critical step in identifying a statistically rigorous and cost-effective monitoring network for air quality. The author recommended that once a

network has been established, analysis of the spatial robustness of the data should be an ongoing process as an increasingly longer time series of data is developed. In addition, periodic intensive measurements can be used to validate network design and to potentially modify the network.

Baldauf and co-authors (2001) developed a methodology which optimizes ambient air quality monitoring networks for assessments of adverse human health impacts from exposures to airborne contaminants. The proposed methodology incorporates human health risk assessment techniques. Involving risk assessment techniques as in the designed ambient air quality monitoring networks helps to limit financial and human resources to evaluate human health risks from exposures to airborne contaminants.

Bordignon and Scaglirini (2000) proposed a statistical method to detect biases in the measurement devices to improve the quality of collected data on line. The technique used by the authors was based on the joint use of stochastic modeling and statistical process control algorithms. The methodology was applied to the mean hourly ozone concentrations recorded from one monitoring site of the Bologna urban area network in Italy. The monitoring algorithm was set up through Monte Carlo simulations to detect anomalies in the data within a reasonable delay. The authors concluded that the on-line implementation of the monitoring algorithm presented in their study could lead to further improvements in the maintenance of air pollution monitoring sites if routinely implemented as a complementary tool to the usual periodic control procedures.

Ibarra-Berastegi (2006) research work focused on the prediction of hourly levels for five pollutants (SO_2, CO, NO_2, NO and O_3) in the area of Bilbao, Spain. The corresponding traffic meteorological data for air pollution network were for the years 2000 and 2001. 216 specific models based on different types of neural networks have been built using data for the year 2000. The choice of the best model has been made for each of the 216 cases simultaneously having 95% confidence level. Different architectures have been selected depending on the pollutant, location and number of hours ahead the prediction is made. For SO_2 and CO in most cases persistence of levels or linear models outperformed those based on neural networks. Predictions of NO_2 and O_3 hourly levels required in most cases linear models while MLP (Multilayer

Perceptrons Procedure), RBF (Radial Basis Function) or GRNN (Generalized Regression Neural Network) architectures were needed in few predictions. For the predictions of NO, linear models in some cases and MLP, RBF or GRNN based models in others were the major options. In spite of the different architectures and also the different explanatory mechanisms involved the performance of the selected models is very similar.

Chapter 3- Multi Objective Design of Air Quality Monitoring Network

3.1 Introduction

The US Environmental Protection Agency developed a regulation to enforce states to meet the minimum design and quality assurance requirements for air quality monitoring networks. Monitoring stations must monitor the highest pollutant concentrations, concentrations in areas of high population density, the impact of major emission sources, regional background concentrations extent of pollutant transport among populated areas, and welfare-related impacts in more rural and remote areas.

Protection of human health and the environment from pollutants effects is the primary goal of all air pollution control programs. Protection of air quality requires accurate data on ambient concentration of major pollutants and emissions from air pollution sources to be available to regulatory authorities. Representations of spatial and temporal variations as well as characterizing and quantifying emissions are vital to the success of air quality monitoring networks.
The number and locations (configurations) of air quality monitoring networks have an important role in achieving the objectives which were previously described on page 16.

Air quality monitoring networks designed to characterize the air quality of an area can become complex because they are required to provide data to allow a resolution of air quality in terms of temporal and spatial variations. Air monitoring at a carefully selected site provides a realistic picture of the air quality in the area of interest.

In this chapter, a methodology that will lead to an optimal air quality monitoring networks will be described. A mathematical model based on the Multiple Cell Approach (MCA) will be described and used to create monthly spatial distributions for the concentrations of the pollutants (CO, NO_x, and SO2) emitted from the Tabriz refinery stacks in Iran. This case study, previously studied by Fatehifar (2006a), was

selected since data is available for it. The concentration coming from the Multiple Cell Model will be employed to calculate different measures that can serve as objective functions in the optimal design of a monitoring network.

The objective of the design measures is to provide maximum information about the presence and level of atmospheric contaminants in a given area with minimum number of monitoring stations since a large number of monitoring stations is not economically acceptable.

3.2 Description of Multiple Cell Model

Atmospheric dispersion modeling is the mathematical simulation of how air pollutants disperse in the ambient atmosphere. It is performed with computer programs that solve the mathematical equations and algorithms which simulate the pollutant dispersion.

A MATLAB program of mathematical modeling of air dispersion was developed b. In this program, the Multiple Cell Model was used to predict the ground level concentration for multi pollutants (SO_x, NO_x, CO) in the network of refinery stacks (Fatehifal, 2006a).

The input consists of meteorological, emission data and stack characteristics. The output is the level of pollutant concentration observed in space. The program verification was conducted by checking the simulation results against experimental data and the Gaussian dispersion model.

The basic mathematical formulae used in the model will be given in this section and their physical meaning and model approximations will be explained.

The mathematical description of air pollution dispersion from an industrial stack should consider five major physical and chemical processes including:

(i) Horizontal transport (advection)
(ii) Horizontal diffusion
(iii) Deposition (both dry deposition and wet deposition)
(iv) Chemical reactions plus emissions
(v) Vertical transport and diffusion.

These processes can be described mathematically by using the equation of the law of conservation of mass for each pollutant and then dividing the air space into an array

of cells. Figure 3.1 shows pollutant dispersion and grid generation for a network of refinery stacks. Applying the conservation of mass of these processes leads to a system of partial differential equation.

$$\frac{\partial C^s}{\partial t} = -\frac{\partial (U_x C^s)}{\partial x} - \frac{\partial (U_y C^s)}{\partial y} - \frac{\partial (U_z C^s)}{\partial z} + \frac{\partial}{\partial x}(K_x \frac{\partial C^s}{\partial x}) + \frac{\partial}{\partial y}(K_y \frac{\partial C^s}{\partial y}) + \frac{\partial}{\partial z}(K_z \frac{\partial C^s}{\partial z}) \qquad (3.1)$$

$$+ E^s - (k_1^s + k_2^s)C^s + Q(C^s), \qquad s = 1,2,.....,q$$

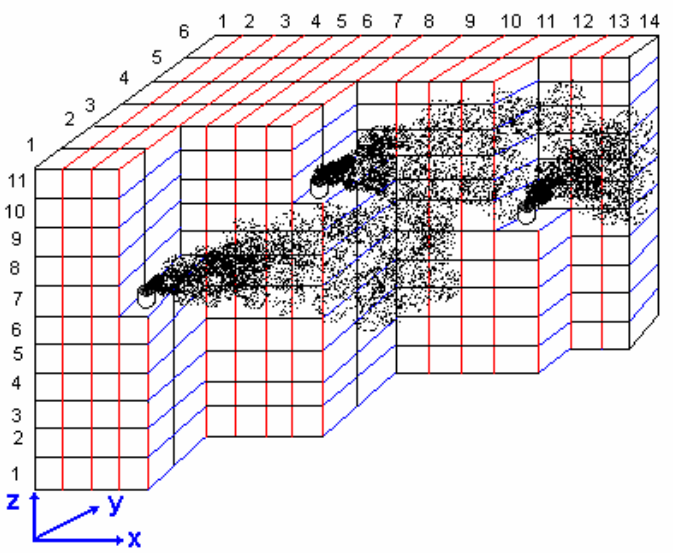

Figure 3.1 Pollutant Dispersion and Grid Generation for Network of Refinery Stacks

Where C^s - concentration of chemical species involved in the model (CO, NO_x, SO_2)

U - wind velocity

K_x, K_y, K_z - diffusion coefficients

E_s - emission sources

K_1^s, K_2^s - deposition coefficients (dry and wet deposition, respectively)

Q (C^s) - chemical reactions

3.2.1 Model Assumptions

The following assumptions are employed in deriving the model:

1- Steady state conditions ($\frac{\partial C}{\partial t} = 0$)

2- $U_y = U_z = 0$ (wind velocity in x-direction only and is a function of z)

3- Transport by bulk motion in the x-direction exceeds diffusion in the x-direction ($K_x=0$)

4- There is no deposition in the system ($K_1^s = K_2^s = 0$).

5- There is no reaction in the system (Q=0)

By applying the above assumptions, Equation 3.1 reduces to:

$$\frac{\partial (U_x C^s)}{\partial x} = \frac{\partial}{\partial y}(K_y \frac{\partial C^s}{\partial y}) + \frac{\partial}{\partial z}(K_z \frac{\partial C^s}{\partial z}) + E^s \qquad (3.2)$$

The following initial and boundary conditions are used to solve Equation 3.2:

$$\begin{aligned}
&\text{at} \quad x = 0, && C(0, j, k) = 0 \\
&\text{at} \quad y = 0, && \frac{\partial C}{\partial y} = 0 \\
&\text{at} \quad y = W, && \frac{\partial C}{\partial y} = 0 \qquad (3.3) \\
&\text{at} \quad z = 0, && \frac{\partial C}{\partial z} = 0 \\
&\text{at} \quad z = \text{mixing length}, && \frac{\partial C}{\partial z} = 0
\end{aligned}$$

3.2.2 Numerical Solution of Mathematical Model

An explicit finite difference scheme was used to solve Equation 3.2 with the initial and boundary conditions shown in Equation 3.3. The air space was divided into an array of cells where Equation 3.2 was written for each cell. Substituting the appropriate equations for the finite difference method gives the following:

$$U_{x_k} C^S_{i+1,j,k}\Delta y\Delta z + (K_y)_k \Delta x\Delta z(C^S_{i+1,j,k} - C^S_{i+1,j+1,k})/\Delta y$$

$$+ (K_y)_k \Delta x\Delta z(C^S_{i+1,j,k} - C^S_{i+1,j-1,k})/\Delta y \qquad (3.4)$$

$$+ (K_z)_{k+\frac{1}{2}} \Delta x\Delta y(C^S_{i+1,j,k} - C^S_{i+1,j,k+1})/\Delta z$$

$$+ (K_z)_{k-\frac{1}{2}} \Delta x\Delta y(C^S_{i+1,j,k} - C^S_{i+1,j,k-1})/\Delta z = U_{x_k} C^S_{i,j,k}\Delta y\Delta z + E^S_{i,j,k}\Delta y\Delta z$$

Where, the values of wind speed and eddy diffusivity are presumed known for every cell. Since an explicit algebraic formula was used, a numerical stability condition should be considered. The stability condition for the above equations is shown in Equation 3.5.

$$\Delta x \le \frac{U_x}{2K_z(\frac{5}{\Delta y^2} + \frac{1}{\Delta z^2})} \qquad (3.5)$$

3.2.3 Atmospheric Model Parameters

Atmospheric parameters like atmospheric stability, surface roughness and friction velocity, plume rise, wind velocity and dispersion coefficients and mixing height are required to solve Equation 3.4.

3.2.3.1 Atmospheric Stability

Atmospheric stability is a measure of turbulence in the ambient atmosphere. Three stability classes are considered in this dispersion model: neutral, stable and unstable class. Atmospheric stability is calculated from the following equation (Ragland, 1973):

$$L = -\frac{u^{*3} C_p \rho T}{kgH_n} \qquad (3.6)$$

Where L is the Monin-Obukhov length and is simply the height above the ground at which the production of turbulence by both mechanical and boundary forces is equal and has the units of length. u^* is the friction velocity, C_p is the specific heat of air, T is the air temperature, k is Karman's constant (k=0.4), g is the acceleration due to gravity and H_n is the net heat that enters the atmosphere. H_n for a neutral atmosphere is 0, for a stable atmosphere is -42 and for an unstable atmosphere is 175.

3.2.3.2 Surface Roughness and Friction Velocity

Friction velocity is calculated from the following equation:

$$u^* = c_g u_g \qquad (3.7)$$

Where c_g is a drag coefficient and u_g is a geostrophic wind. The geostrophic drag coefficient is a function of the surface Rossby Number ($R_0 = u_g / fZ_0$) and L, where f is the Coriolis parameter of the earth and Z_0 is surface roughness. Lettau suggests the following empirical relationship for a neutral atmosphere (Lettau, 1959):

$$c_g = 0.16/[\log_{10}(R_0) - 1.8] \qquad (3.8)$$

For stable and unstable atmosphere it must be multiplied by 0.6 and 1.2, respectively. Values of Roughness length (Z_0) and friction velocity (u^*) for several different land surfaces are presented in Table 3.1.

Table 3.1 Roughness Lengths and Friction Velocity (Heinsohn, 1999)

Surface	**Z_0 (cm)**	**u^* (m/ s)**
Very smooth (ice, mud flats)	0.001	0.16
Snow	0.0001-0.005	0.17
Smooth sea	0.0001-0.02	0.21
Level desert	0.0001-0.03	0.22
Lawn grass up to 1 cm high	0.1	0.27
Lawn grass up to 5 cm high	1-2	0.43
Lawn grass up to 50 cm high	4-9	0.60
Fully grown root crops	10-14	1.75
Tree covered	100	-
Low-density residential	200	-
Central business district	500-10000	-

3.2.3.3 Plume Rise

The effective stack height H is equal to the physical stack's height h_s plus the plume rise δh. Plume rise is defined as the height to which a buoyant plume with an initial exit velocity will rise.

$$H = h_s + \delta h \qquad (3.9)$$

Plume rise is very important and can be larger than the physical stack height in some cases. It has a significant effect on the resulting ground level pollution concentration. A schematic of an effective stack height, physical stack's height and the plume rise, is presented in Figure 3.2

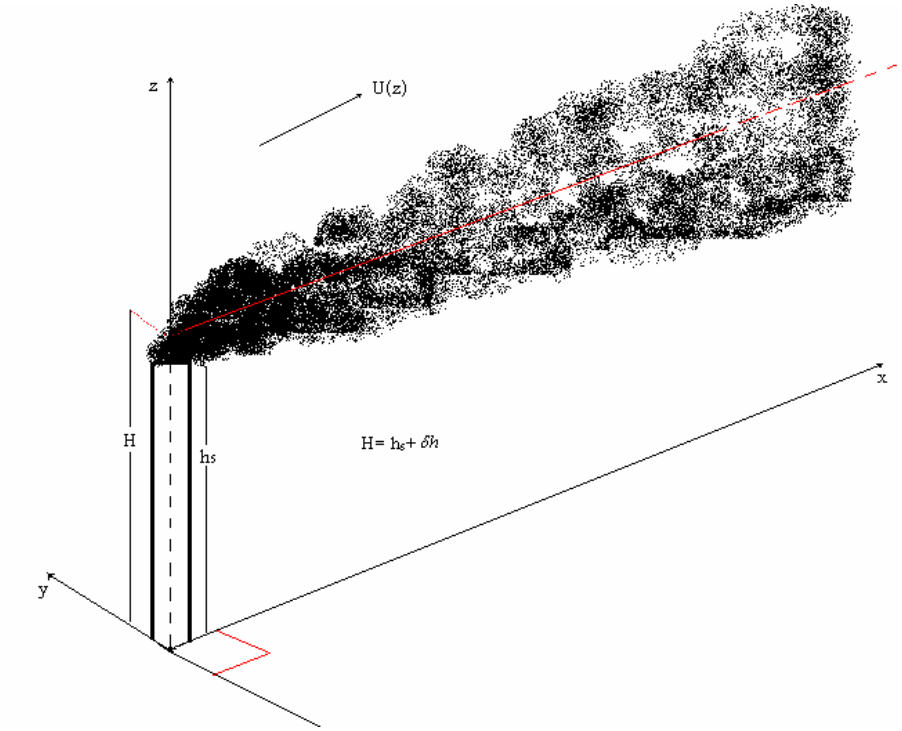

Figure 3.2 Plume Rise and Pollution Dispersion from an Industrial Stack

To determine plume rise modified Holland's equation was used. The modification has been done using regression to get a better coefficient set. The Holland equation and modified Holland equation are as the following:

$$\delta h = \frac{v_s D}{u}\left(1.5 + 2.68\times10^{-3} PD\frac{(T_s - T_a)}{T_s}\right) \qquad (3.10)$$

Where, v_s is stack exit velocity (m/s), D is stack diameter (m), u is wind velocity (m/s) measured or calculated at the height, hs, P is pressure (mbar), Ts is stack gas temperature (K) ,Ta is the atmospheric temperature (K).

For hs<35 = (Holland Eq.)-32.42+0.8576*hs

For hs<80 = (Holland Eq.)-10.1527+0.3135*hs (3.11)

For hs>=80 = (Holland Eq.)+12.39+0.17*hs

The preceding formulas are valid for neutral conditions. For unstable conditions, should be increased by a factor of 1.1 to 1.2, and for stable conditions, should be decreased by a factor of 0.8 to 0.9 (Peavy, 1985).

3.2.3.4 Wind Velocity and Dispersion Coefficients

Wind speed and eddy diffusivities for various stability classes used in this program are shown in Table 3.2.

Table 3.2 Wind Velocity and Eddy Diffusivity for Various Stability Categories (Shamsijey, 2004)

Stability	Wind velocity	Eddy diffusivity
In surface layer, $0<z<z_{sl}$		
Neutral	$\frac{u^*}{0.4}\ln(\frac{z+z_0}{z_0})$	$K_z = 0.4u_*z$ $K_y = 5K_z$
Stable	$\frac{u^*}{0.4}\left[\ln(\frac{z+z_0}{z_0})+\frac{5.2z}{L}\right]$	$K_z = 0.4u^*z/\left(1+\frac{5.2z}{L}\right)$ $K_y = 6K_z$
Unstable	$\frac{u^*}{0.4}\begin{pmatrix}2(\tan^{-1}x-\tan^{-1}x_0)+\ln(\frac{x-1}{x_0-1})\\-\ln(\frac{x+1}{x_0+1})\end{pmatrix}$ $x=[1-15(z-z_0)/L]^{1/4},\ x_0=[1-15z_0/L]^{1/4}$	$K_z = 0.4u^*z\left(1-\frac{15z}{6L}\right)^{1/4}$ $K_y = 2K_z$
Upper surface layer, $z_{sl}<z<z_m$		
Neutral	$(u_g-u_{sl})\left(\frac{z-z_{sl}}{z_m-z_{sl}}\right)^{0.2}+u_{sl}$	$K_z = 0.4u_*z_{sl}$ $K_y = 5K_z$
Stable	$(u_g-u_{sl})\left(\frac{z-z_{sl}}{z_m-z_{sl}}\right)^{0.5}+u_{sl}$	$K_z = 0.4u_*L$ $K_y = 6K_z$
Unstable	$(u_g-u_{sl})\left(\frac{z-z_{sl}}{z_m-z_{sl}}\right)^{0.2}+u_{sl}$	$K_z = 160u^{\frac{1}{2}}\left(1-\frac{6000u^*}{L}\right)^{(1/4)}$ $K_y = 2K_z$

3.2.3.5 Mixing Height

Mixing height is defined as the volume available for diluting pollutants. A minimum and maximum mixing height is calculated using Holzworth's method (Mehdizadeh, 2004). The relation between stability classes and mixing height is shown in Table 3.3.

Table 3.3 Relation between Stability Classes and Mixing Height (Beychok, 1995).

Stability Classes	Mixing Height (m)
A	1.5*AMH
B	AMH
C	AMH
D (day)	AMH
D (night)	½*(AMH+MMH)
E	MMH
F	MMH

(AMH and MMH are the afternoon and morning mixing heights)

3.2.4 Program Description

To solve the model the following equalities are substituted in equation 3.4:

$$u\Delta y\Delta z = a$$
$$K_y \Delta x\Delta z / \Delta y = e$$
$$K_z \Delta x\Delta y / \Delta z = f \qquad (3.12)$$

Equation 3.4 becomes a system of linear equations that can be arranged in a matrix as the following:

$$[A][C] = [D] \qquad (3.13)$$

Where, A is the coefficient matrix, C is the matrix of concentrations and D is the matrix of known concentrations at a previous face plus the emission rate into the grid under consideration. Figure 3.3 shows the form of matrix A for 9 grids in the y-z face.

$$\begin{bmatrix}
a1+e1+f3/2 & -e1 & 0 & -f3/2 & 0 & 0 & 0 & 0 & 0 \\
-e1 & a1+2e1+f3/2 & -e1 & 0 & -f3/2 & 0 & 0 & 0 & 0 \\
0 & -e1 & a1+2e1+f3/2 & 0 & 0 & -f3/2 & 0 & 0 & 0 \\
-f3/2 & 0 & 0 & a2+e2+f3/2+f5/2 & -e2 & 0 & -f5/2 & 0 & 0 \\
0 & -f3/2 & 0 & -e2 & a2+2e2+f3/2+f5/2 & -e2 & 0 & -f5/2 & 0 \\
0 & 0 & -f3/2 & 0 & -e2 & a2+e2+f3/2+f5/2 & 0 & 0 & -f5/2 \\
0 & 0 & 0 & -f5/2 & 0 & 0 & a3+e3+f5/2 & -e3 & 0 \\
0 & 0 & 0 & 0 & -f5/2 & 0 & -e3 & a3+2e3+f5/2 & -e3 \\
0 & 0 & 0 & 0 & 0 & -f5/2 & 0 & -e3 & a3+e3+f5/2
\end{bmatrix}$$

Figure 3.3 Matrix A for 9 Grids in yz Face

3.2.5 Model Setup

The Multiple Cell Model was used to predict the ground level concentration of multiple pollutants in the Tabriz Refinery. The model is capable of handling point sources. It was setup to cover an area of approximately 10×1.2 km^2. A matrix of 72×868 for SO_2, NO_x, and CO concentrations has been generated at the specified 868 candidate locations. The following data should be obtained in order to run the program.

3.2.5.1 Meteorological Data

The Multiple Cell Model was undertaken using the 1990-1995 Tabriz Refinery meteorological data sets. Tables 3.4 and 3.5 show the temperature and wind velocity distribution for those years (Fatehifal, 2006b).

Table 3.4 Temperature Distribution for Different Years

YEAR	JAN	FEB	MAR	APR	MAY	JUN	JUL	AUG	SEP	OCT	NOV	DEC
1995	1.2	2.8	6.8	11	17.7	21.2	25.3	27	21	12.8	6.8	8.1
1994	-0.8	0.6	6.3	13.5	16.4	21.5	24.7	23.2	19.9	14.7	7.1	-2.4
1993	-4.6	-1.3	3	10.4	15.3	21.3	25.6	24.8	21.7	13.6	3.2	0.3
1992	-4	-1.2	2	9.8	13.1	20.4	23.4	22.9	20	13.9	6.3	0.8
1991	-1.8	-0.8	5.4	12.8	13.5	22.4	26	26.5	21.2	13.1	7.3	-0.5
1990	-2.6	-0.3	4.3	10	16.9	23.4	26.5	24.8	22.2	14	8.7	1.4

Table 3.5 Wind Velocity Distribution for Different Years

YEAR	JAN	FEB	MAR	APR	MAY	JUN	JUL	AUG	SEP	OCT	NOV	DEC
1995	2.1	2.15	2.15	4.05	3.95	3.6	4.45	4.15	3.3	3.15	2.45	2.75
1994	1.65	3.05	1.55	2.6	3.65	4.3	4.55	4.75	4.2	3.3	2.3	2.55
1993	2.25	2.75	2.25	5.65	4.1	3.75	4.6	4.35	4.3	4.15	3.5	2.3
1992	1.7	2.3	3.2	4.75	3.2	3.8	3.75	4.1	3.7	4.55	3.25	3.15
1991	1.6	1.9	4.05	4.9	4.55	4.85	4.75	4.4	3.75	3.55	2.95	2.2
1990	2	2.8	3.1	4.4	3.2	4.95	4.9	4.9	3.65	2.6	1.6	2.75

3.2.5.2 Emissions Data and Stacks Characteristics

Emission data and stacks characteristics used in the modeling are presented in Table 3.6.

Table 3.6 Stacks of Tabriz Refinery (Fatehifal, 2006b)

Stack	Dia (m)	Height (m)	Temp. (°C)	Eff %	NO_2 (PPM)	NO (PPM)	CO (PPM)	SO_2 (PPM)	Q (m^3/hr)
H-101	3.58	73.2	365	76	0	86	0	1	0.5e6
H-102	2	53	460	76	_	_	_	_	0.5e6
H-151	2.38	52	430	76.4	1	70	0	0	1e6
H-152	1.5	53	455	74	_	_	_	_	1e6
H-201	2.2	36.6	400	75	0	24	111	9	10e5
H-251	3.15	36.6	696	59.5	0	69	0	1	0.25e6
H-252	3	36.6	482	70	1	19	92	3	0.25e6
H-301	2.52	52	402	73	0	35	130	0	1e6
H-402	2.34	36.6	348	77	1	45	29	1	1.5e6
H-501	1.58	36.6	320	79	2	0	7.3	3	0.5e6
H-601A	1.9	36.6	315	78	1	56	0	1	0.5e6
H-601B	2.18	36.6	343	78	1	46	17	1	0.5e6
H-602	2.18	46	333	79	0	14	2	1	0.5e6
H-603	1.81	46	399	77	0	15	34	1	1e6
H-604	0.92	36.6	682	62	2	57	127	2	2.15e5
H-701	3.57	43	280	86	0.4	76	1	0	0.5e6
B-2101	3.5	73	337	90	0	108	0	69	1e6
B-2103	3.5	73	337	83	0	98	0	13	1e5
B-2105	3.5	73	337	90	0	108	0	69	1e6

Air dispersion modeling using the Multiple Cell Model (MCM) has been conducted to predict the ground level concentrations of SO_2, NO_x, and CO resulting from Tabriz Refinery. MATLAB program was used to solve a system of partial differential equations using the finite difference method. The inputs are Meteorological data, Emission and stack characteristics data and the output is ground level concentration. Different meteorological parameters like wind velocity, ambient air temperature, atmospheric stability and surface roughness were illustrated in this program. Visualization results are shown in Figure 3.4.

After obtaining the modeling results and having pollutants concentration in every location, the design criteria that can determine the optimum structure of an Air Quality Monitoring Network (AQMN) can be calculated. This is outlined in the next section.

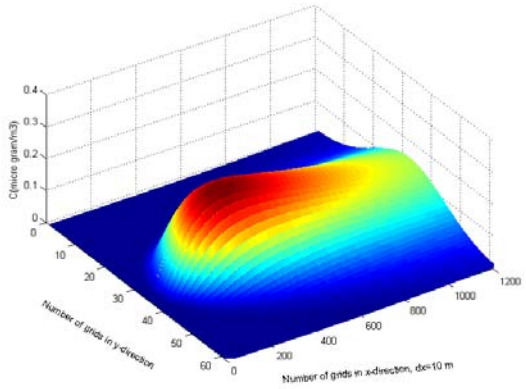

(a): SO_2 concentration distribution at ground level

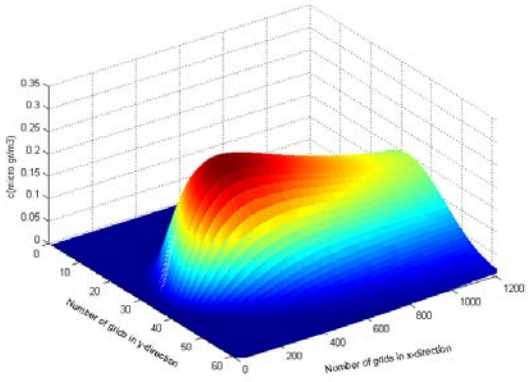

(b): NO_x concentration distribution at ground level

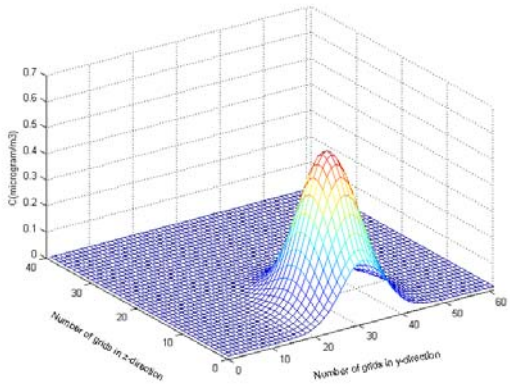

(c): NO_x concentration distribution at X=2 km

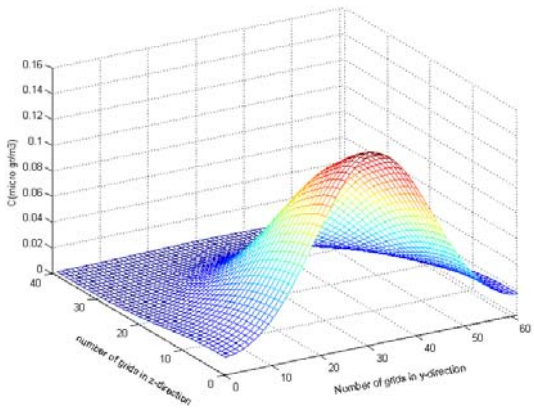

(d): SO_2 concentration distribution at X=12 km

Figure 3.4 Visualization Results from MCM Program

3.3 Air Quality Monitoring Siting Criterion

The ability to assess the air quality of an area depends on accurate data describing existing conditions. Two objectives have been considered in the monitoring network design:

1. Representation of spatial-temporal patterns.
2. Detection of violations of ambient air quality standards.

3.3.1 Methodology Description

Air quality models are important tools in air quality monitoring networks. Their use provides a relatively inexpensive air quality database. The Multiple Cell Model described in the previous section is used to generate an extensive data base to evaluate siting criterion.

However, choosing ranges of meteorological conditions under which air monitoring maybe located is necessary so that the region of interest represents different meteorological scenarios. For each of the scenarios, the air quality model is employed to produce the temporal varying air quality patterns. In this thesis, six years (monthly spatial distributions) will be considered.

Two objectives are usually of interest, the first is a representation of spatial-temporal patterns and the second is the detection of violations of ambient air quality standards.

3.3.1.1 First Objective: Spatial Coverage (N_p)

The station spatial coverage or Sphere of Influence (SOI) is defined by the surrounding area over which the air quality data for a given station can be considered to be representative (Liu, 1981). Spatial-temporal pattern is considered to be one of the most important objectives of the AQMN.

The approach used in this study to calculate the SOI is based on the similarity between the information contained in a given station compared with the rest of them. To do that, the statistical properties of the spatial distributions of the pollutant concentrations are taken into account by the mean of the spatial correlation coefficient (r), calculated from the concentration values measured (or predicted) at each monitoring station. In this way, the spatial correlation coefficient provides an indication of the relationship between stations. Assuming that $C_1 = (C_{11}, C_{12}, C_{13}, ..., C_{1n})$ and $C_2 = (C_{21}, C_{22}, C_{23}, ..., C_{2n})$ denoted the pollutant concentrations in two

different network locations measured at the same time, the spatial correlation coefficient for a sample size (n) can be expressed as :

$$r = \frac{\sum_{i=1}^{n} (C_{1i} - \overline{C}_1)(C_{2i} - \overline{C}_2)}{\sqrt{\sum_{i=1}^{n} (C_{1i} - \overline{C}_1)^2 \sum_{i=1}^{n} (C_{2i} - \overline{C}_2)^2}}, \qquad (3.14)$$

Where, $\overline{C}_1 = \frac{1}{n}\sum_{i=1}^{n} C_{1i}$ and $\overline{C}_2 = \frac{1}{n}\sum_{i=1}^{n} C_{2i}$ are the mean concentration at locations 1 and 2, respectively.

The justification for the adopted approach is based on the fact that the correlation coefficient for concentration fluctuations is expected to decrease as the distance from the first station increases, as shown in (Figure 3.5). This correlation coefficient can vary between 1 and -1.

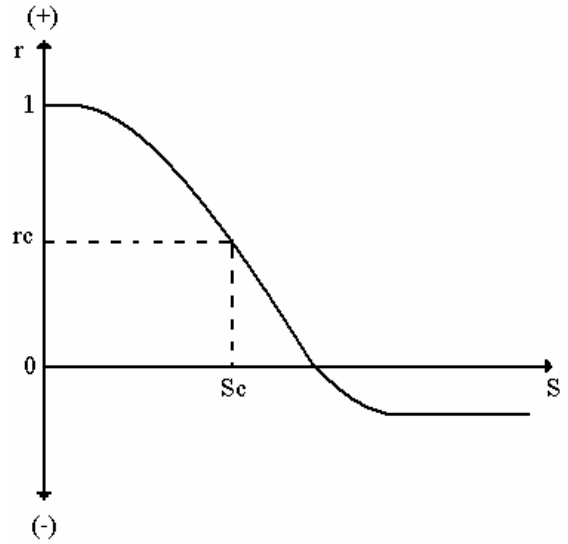

Figure 3.5 Correlation Coefficient (r) Versus Distance (S) (Liu, 1981).

Therefore, a cutoff distance S_c can be found so that the correlation coefficient is expected to be less than a certain value r_c. The assumptions implied in this approach are:

a. The data sets C_1 and C_2 are two correlated variables following a normal bivariate distribution.
b. There are no significant temporal variations that could introduce spurious autocorrelation coefficients.

After that, it can be said that the sphere of influence of a station is the area surrounding it in which the spatial correlation coefficient of this station with the neighboring points is above a certain cutoff value. This means that the air quality data measured at this station can be considered representative with a certain degree of confidence to any point in this area.

The value of r_c dose not imply a causal relationship between C_1 and C_2 but the existence of an association between both data sets such that 100 r_c^2 represents the percentage of concentration variations measured at one station explained by concentration variations measured in the other station (Ezekiel,1941).

The relation which is as follows:

$$\text{Variance explained} = r_c^2 \qquad (3.15)$$

is valid assuming a sufficient high sample size. Otherwise, it should be corrected as a function of the available number of samples.

Summarizing the characterization procedure for the SOI of a station consists of:

a. Choosing the value of the explained variance.
b. Calculating the value of r_c by Equation (3.15).
c. In the case of having few samples, correcting the previous value with tables.

Once the SOI of the station has been characterized, the Coverage Area (CA) of this sphere is defined as the number of potential monitoring sites placed inside it Which is denoted by *"a pattern score Np*".

3.3.1.2 Second Objective: Detection of Violations of Ambient Air Quality Standards (N_v)

Violation scores defined as the potential of a monitoring site for the detection of violations, denoted by N_v. A location having a high violation score is then considered to have a high potential for detection of violations. The computation of violation scores is a weighted scoring of the concentration above the prescribed thresholds. Since not all violations have the same severity, a weighting factor is used to

characterize the violations to each range for the pollutants CO, SO_2, and NO_x. The standard is given by a concentration of pollutant not to be exceeded.

The values for thresholds of CO, SO_2, and NO_x are shown in Table 3.7. In addition the weighting factor ranging from 0.5 to 5 according to the severity of threshold exceedance is also given (Fatehifar, 2006a).

Table 3.7 Air Pollution Index Assigned to Weighting Factor Values for the Violation Score.

SO_2 ($\mu g/m^3$)	NO_x ($\mu g/m^3$)	CO ($\mu g/m^3$)	Weighing factors
80	30	4000	0.5
120	80	6000	1
140	100	8000	2.5
160	130	13000	3
190	160	20000	5

Several functions have been reported to calculate the violation score such as linear functions, segmented linear functions, non linear functions, segmented non linear functions, etc. (Ott, 1977). The segmented non linear weighting function proposed in Modak and Lohani (1985) has been chosen in this research.

$$N_v^i = \sum_{i=1}^{T} \sum_{k=1}^{N_t} \frac{(w_{k+1} - w_k)(x_i - x_k)X}{(x_{k+1} - x_k)} \qquad (3.16)$$

where,

N_v^i = violation score for the i^{th} candidate location,

w_k = weighing factor corresponding to threshold x_k,

x_k = the k^{th} threshold,

X = 0 if $(x_i - x_k) \leq 0$,

X = 1 otherwise

N^t = total number of thresholds,

T = total number of simulated observations,

At this moment, we have quantified the information related to the following objectives:

1. N_p is a decision variable associated with the objective "prediction of the spatial and temporal patterns of the concentration field".
2. N_v is a decision variable associated with the objective "detection of violations over legal standards".

Starting from the two decision variables N_p and N_v which are calculated separately for each grid point using the output from Multiple Cell Model. The next step would be building up artificial neural network models that represent the two variables, pattern score and violation score as functions of (x,y) so that an optimization model can be formulated. The interest of the optimization is to achieve maximum coverage effectiveness and maximum detection of violations over ambient air standard. In order to formulate an optimization model that can be used to find the optimal network, explicit mathematical equations need to be developed for *Np* and *Nv* as functions of the spatial coordinates x and y. This will be the subject of chapter 4.

Chapter 4- Development of Artificial Neural Network Models for Predicting Violation and Pattern Scores

4.1 Introduction

In this chapter we want to characterize the relationship between the violation and pattern scores and the distance for each pollutant (NOx, SO_2, and CO) by a mathematical model and then use the model to formulate an optimization that can be utilized to find the optimum locations for monitoring stations. In order to achieve this goal, main effects and quadratic linear regression models were developed but unfortunately these models did not fit the data set well. We have therefore decided to use Artificial Neural Networks (ANNs). The data fed to the ANNs model is based on our knowledge of the following parameters that have been obtained from the Multiple Cell Model from chapter 3:

1. N_p (or pattern score) is associated with the first objective of the AQMN "prediction of the spatial and temporal patterns of the concentration field".
2. N_v (or violation score) is associated with the second objective of AQMN "detection of violations over legal standards".

Once the ANN models are appropriately trained and tested, an optimization that can identify the optimum and reasonable number of locations for the air quality monitoring networks for the given monitoring area can be formulated.

4.2 Artificial Neural Networks

A neural network is a computing tool of nonlinear static systems. It is made up of simple components called neurons or processing elements. These elements are highly interconnected and generally organized in parallel layers to transform inputs into outputs to the best of its ability. The network contains an input layer, one or more hidden layers and an output layer (Parks et. al., 1998). Figure 4.1 shows a simplified neural network with one hidden layer (Feed-Forward network). In addition a bias neuron is connected to all neurons in the hidden and output layers and its function is to supply an invariant output (Elkamel et. al., 2001). Signals travel through neurons in

these layers to generate the output. The number of neurons and hidden layers depend on the desired output.

Three important factors can identify how the neural network is computing the output and these are as the following:

4.2.1 Weight Factors

The weight factor is used to control the effect of an input to the neuron. Figure 4.2 shows a simple model of neuron. The inputs to neurons are represented here as x_1, x_2, and x_3 and weights as w_1, w_2, and w_3. Inputs are scaled by the weights before reaching the neuron. The ANN models learn by adjusting their weights to reduce the error of the output and that takes many iterations to accomplish (Baughman and Liu, 1995).

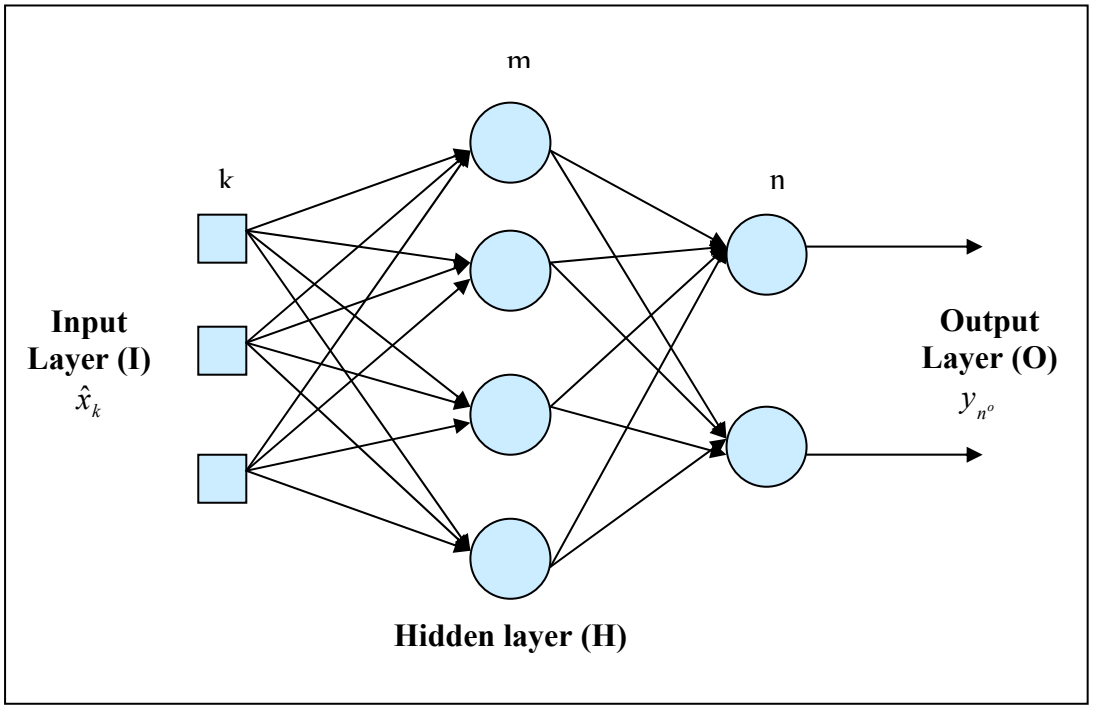

Figure 4.1 A Simplified Neural Network with One Hidden Layer (Feed-Forward)

4.2.2 Internal Thresholds

The activation of the neuron is controlled by the internal threshold and is denoted by T. The neuron calculates the summation of all of its w_i x_i's and then calculates the total activation as shown in equation 4.1(Hassoun, 1995).

$$\text{Total Activation} = \sum_{i=1}^{n}(w_i\, x_i) - T \qquad (4.1)$$

4.2.3 Transfer Functions

The output of a neuron is a function of the weighted sum of the inputs plus a bias. The non-linear transfer function is used to compute the outputs of all the neurons. The most common transfer function is the logistic sigmoid (S-shaped) function. This function is smooth, continuous and monotonically increasing and its derivative is always positive and that makes the network training easy. The sigmoid function and its derivative are:

$$f(x) = \frac{1}{1+e^{-x}} \qquad (4.2)$$

$$f'(x) = f(x) * [1 - f(x)] \qquad (4.3)$$

Other sigmoid functions are also used like the hyperbolic tangent function and the radial basis function.

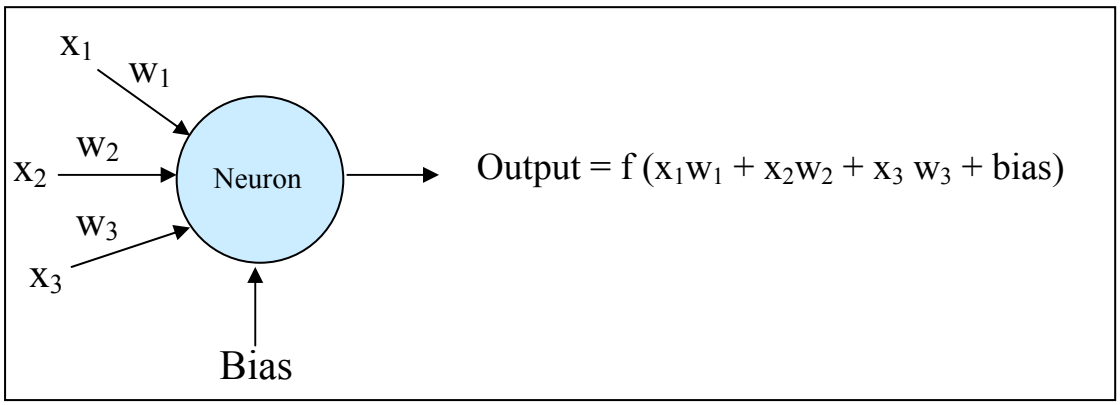

Figure 4.2 The Anatomy of the Neuron that Transfers the Input x_i to the Output through a Weight Factor w_i and a Transfer Function f

Normalizing the input and output values are recommended so that the same distribution range is achieved for every input and output variable in the data set. The following equation is used (Baughman and Liu, 1995):

$$x_{i,norm} = \frac{x_i - x_{i,\min}}{x_{i,\max} - x_{i,\min}} \qquad (4.4)$$

Where $x_{i,norm}$ is the normalized variable, $x_{i,\min}$ and $x_{i,\max}$ are the minimum and the maximum values.

Many training algorithms can be used. The most common algorithm is the back propagation algorithm (BP). There are two steps in back propagation algorithm, in the first step the input is propagated forward to the output and the error between the expected response and the actual response is calculated. The second step is a backward propagation through the net to calculate the error by using the sum of square error equation as following:

$$E_j = \sum_{j=1}^{j} \left(\hat{y}_{nj} - y^o{}_{nj} \right)^2 \qquad (4.5)$$

Where $\hat{y}_{nj}$ and y^o_{nj} are the jth desired and actual values on the outputs. After that the weight error derivatives and the desired weight changes are computed until the error function is minimized.

Developing a neural network requires two phases; the first phase is the training or learning phase. Training phase is the actual process of adjusting weights to achieve required accurate results. The second phase is the testing phase. In this phase the performance of trained network is checked.

Table 4.1 shows the input and output to the neurons for a neural network containing input, output, and one hidden layer; where w^{ih}_{km} and w^{ho}_{mn} are the weight distributing from neuron k, m, or n in the layer i, h, or o, respectively (Elkamel et. al., 2001).

Table 4.1 Input and Output to Neurons that Required in Neural Networks Computing.

Layer	Neuron	Input to the neuron	Output from the neuron
Input	k	$\hat{x}_k$	$\hat{y}_n^o = \hat{x}_k$
Hidden	m	$x_m^h = \sum_{k=0}^{I} y_k^i \, w_{km}^{ih} + b_m$	$y_m^h = \frac{1}{1+\exp\left(-x_m^h\right)}$
Output	n	$x_n^o = \sum_{m=0}^{H} y_m^h \, w_{mn}^{ho} + b_n$	$y_n^o = x_n^o$

4.3 Methodology Description

As mentioned before the main objective is to develop ANN models representing the most important parameters for designing the air quality monitoring network. The first parameter is the spatial-temporal pattern (coverage area) or pattern scores N_p and the second parameter is detection of violations of ambient air quality standards or violation scores N_v. Considering the set of the pattern scores and violations scores (N_p and N_v) that were calculated from Equations 3.14 and 3.16 for multiple pollutants CO, NO_x, and SO2 in the Tabriz refinery case study, there are 868 observations on N_p and N_v in the x-y space in the area of interest for each pollutant. We therefore have six data sets (two variables N_p and N_v for three pollutants) and we want to build up six models as functions of x and y. We have tried first main effects and quadratic linear regression models. A least squares analysis was carried out to find the best equation that fits the data we have, but unfortunately a good fit could not be found. This is explained in more details in the next section.

4.3.1 Main Effects Linear Regression Model

To characterize the violation and pattern scores as a function of the spatial co-ordinates, x and y for different pollutants (NO_x, SO_2, and CO) by a mathematical model, we first tried a main effects linear regression model. A regression analysis was carried out to fit the linear regression model for the six data sets we have. The coefficient of correlation R^2 and the standard error values for each variable are shown in Table 4.2.

The structure of the main effects linear regression models is as follows:

$$N_P = \beta_0 + \beta_1 x + \beta_2 y + \varepsilon \qquad (4.6)$$

$$N_V = \beta_0 + \beta_1 x + \beta_2 y + \varepsilon \qquad (4.7)$$

Where $\beta_0, \beta_1,$ and β_2 are the regression coefficients for the main effects linear regression models and ε is the error term. These two equations were applied for the three different pollutants. The output from the regression analysis for the linear regression models shows that the relationship between the variables is more complex and the results are not satisfactory.

Table 4.2 R^2 and standard error values for different variables that are generated from main effects linear regression models.

Variable	R^2	Standard Error
Np for NO_x	0.183	96.927
Nv for NO_x	0.359	39.1E02
Np for SO_2	0.284	50.611
Nv for SO_2	0.445	29.205E07
Np for CO	0.152	75.723
Nv for CO	0.188	67.129

4.3.2 Quadratic Linear Regression Model

Next we tried an expanded linear regression model which included an interaction and quadratic terms to determine if a better fit could be obtained. The structure of the non-linear regression models is described by the following equations:

$$N_P = \beta_0 + \beta_1 x + \beta_2 y + \beta_3 x y + \beta_4 x^2 + \beta_5 y^2 + \varepsilon \qquad (4.8)$$

$$N_V = \beta_0 + \beta_1 x + \beta_2 y + \beta_3 x y + \beta_4 x^2 + \beta_5 y^2 + \varepsilon \qquad (4.9)$$

Where $\beta_0, \beta_1, \beta_2, \beta_3, \beta_4,$ and β_5 are the regression coefficients and ε is the error term. These two equations were applied for the three different pollutants. The results from the regression show a slight improvement as shown in Table 4.3 but still are not satisfactory.

Table 4.3 R^2 and standard error values for different variables that are generated form quadratic linear regression models.

Variable	R^2	Standard Error
Np for NOx	0.541	72.776
Nv for NOx	0.725	25.663E02
Np for SO2	0.365	47.755
Nv for SO2	0.551	26.316E07
Np for CO	0.211	73.160
Nv for CO	0.292	62.797

4.3 Neural Network Model

Network models were attempted and trained using six data sets. Each data set was randomly divided into two parts: the first part consisting of 85% of the data was used for training the network, and the remaining part was used for testing the network.

Networks with one hidden layer of 7- 9 neurons were developed in order to predict *Np* and *Nv* as function of x and y for the three pollutants. A random generator initializes the weights. The back propagation algorithm was used for training. In order to check the performance of the neural network models, a testing data set was used.

The testing data set indicate that the model predictions are very good. Coefficient of correlation, R^2 values for the training and testing sets for each pollutant are shown in Table 4.4

Table 4.4 The Variables Used in the ANN Models and R^2 Values for both the Training and Testing Set.

Variable	Number of Neurons	R^2 for training set	R^2 for testing set
Np for NOx	7	0.954	0.999
Nv for NOx	7	0.998	0.999
Np for SO2	9	0.948	0.999
Nv for SO2	7	0.997	0.999
Np for CO	7	0.949	0.999
Nv for CO	7	0.992	0.999

To further check the accuracy of the network, plots of predicted and actual (from the simulation of MCM) violation scores and pattern scores versus x and y for different

pollutants CO, NOx, and SO_2 were prepared as shown in Figures 4.3, 4.5, 4.7, and 4.9.

Figures 4.4, 4.6, 4.8, and 4.10 show also the cross plot of the predicted and actual violation and pattern scores for the testing data set for each pollutant. The plots show also that a good accuracy in predictions by the ANN model is achieved.

In this chapter artificial neural network models were developed representing the violation scores and pattern scores as functions of x and y for the purpose of AQMN design. The neural network models of one hidden layer of 7-9 neurons were developed and a back propagation algorithm was used to train the networks. The ANNs model output gave very good predictions for both the training data set and testing data set. The ANN models were found to be better than the regression models previously used.

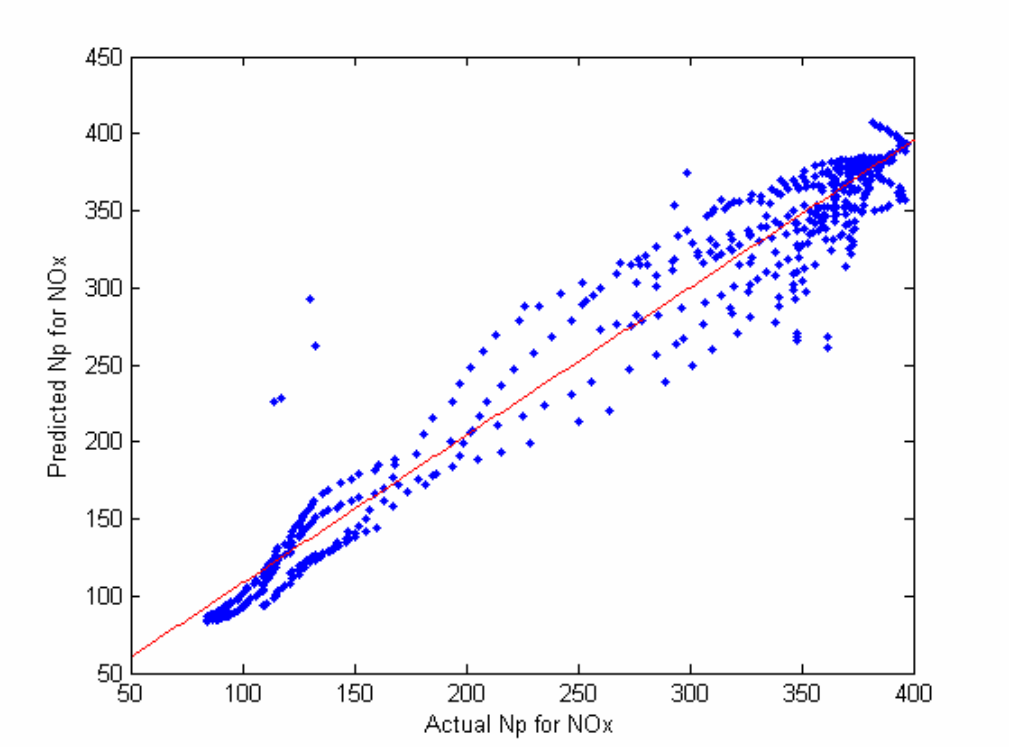

Figure 4.3 Cross Plot of Predicted and Actual *Np* (NOx) for the Training Data Set

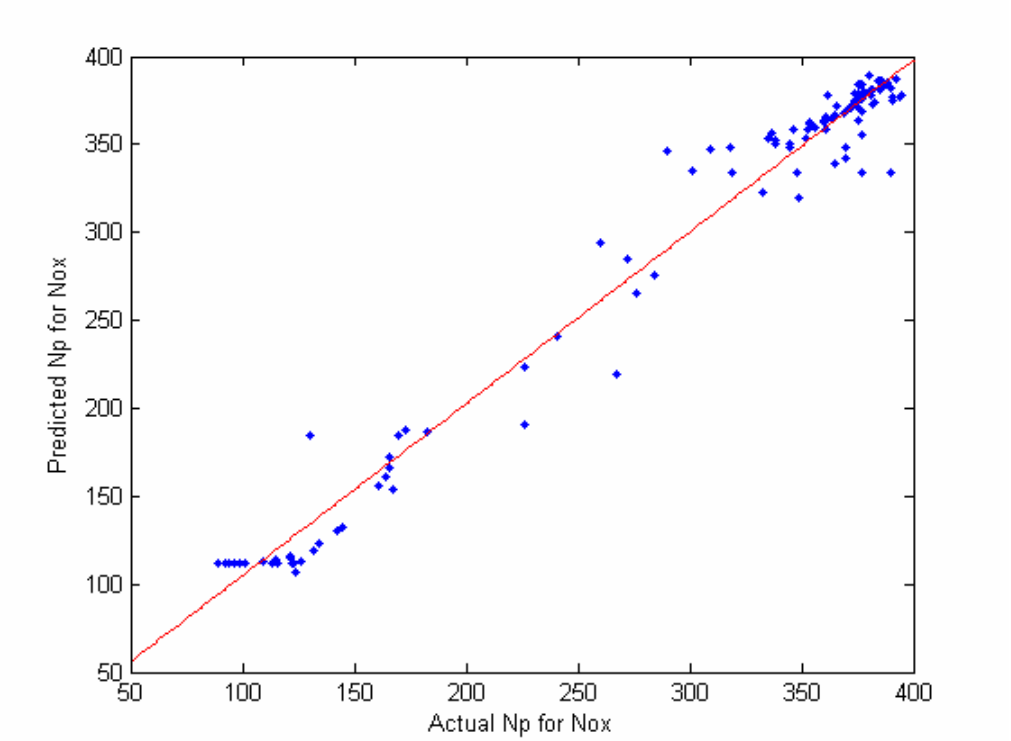

Figure 4.4 Cross Plot of Predicted and Actual *Np* (NOx) for the Testing Data Set

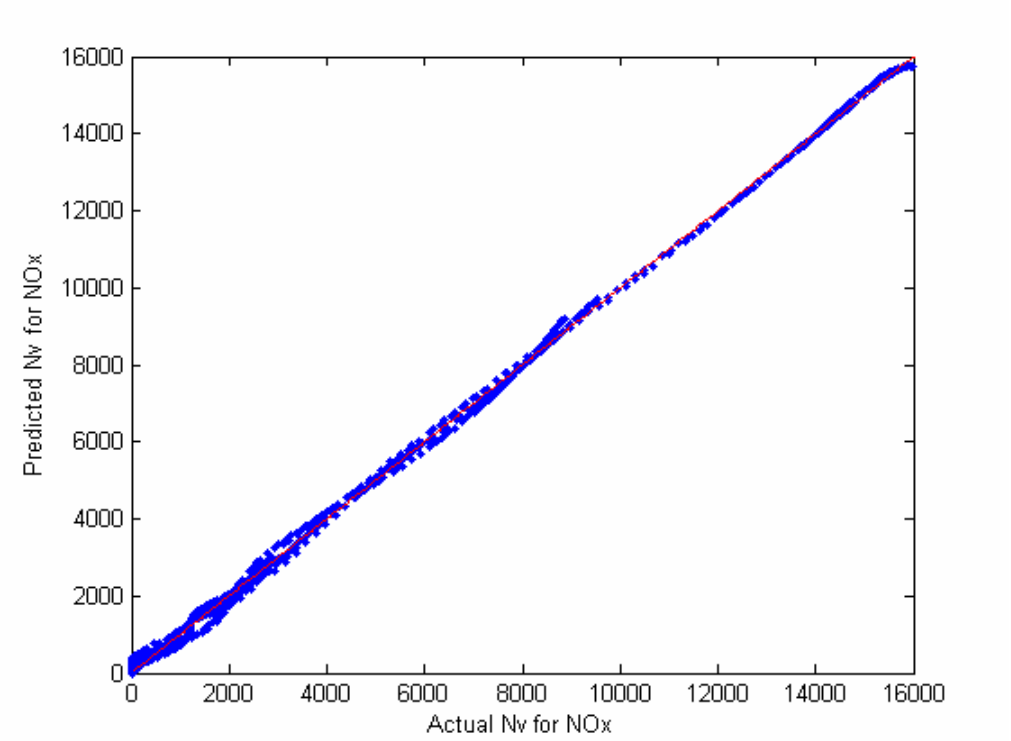

Figure 4.5 Cross Plot of Predicted and Actual *Nv* (NOx) for the Training Data Set

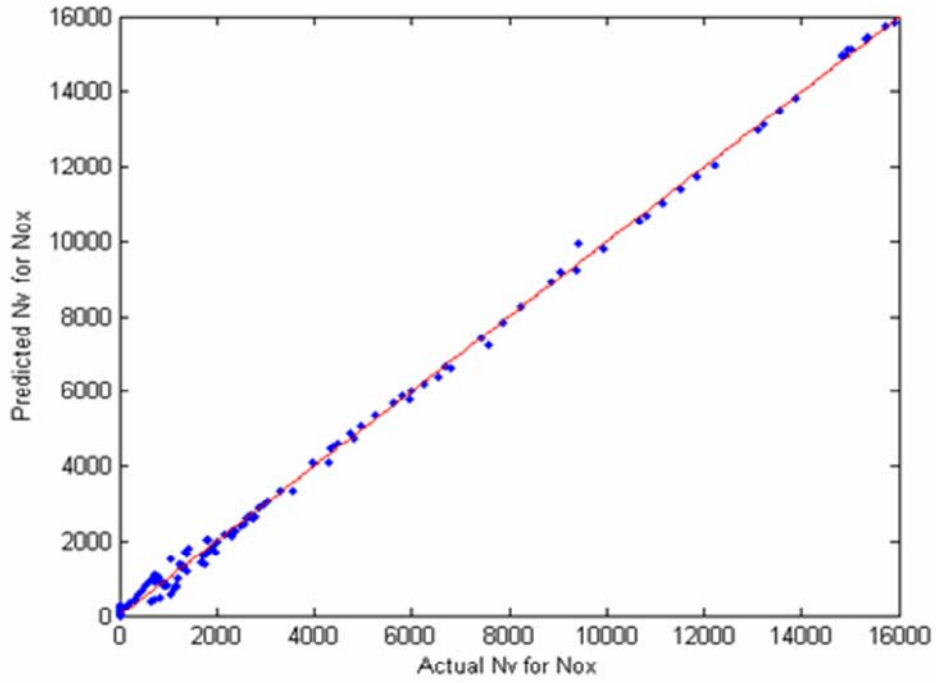

Figure 4.6 Cross Plot of Predicted and Actual *Nv* (NOx) for the Testing Data Set

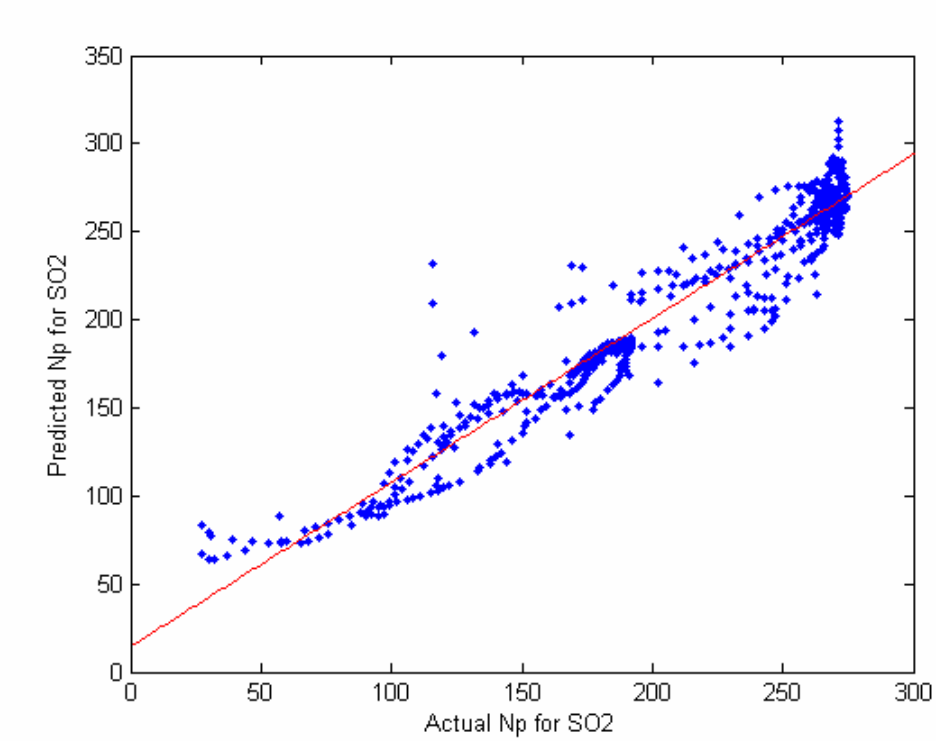

Figure 4.7 Cross Plot of Predicted and Actual *Np* (SO_2) for the Training Data Set

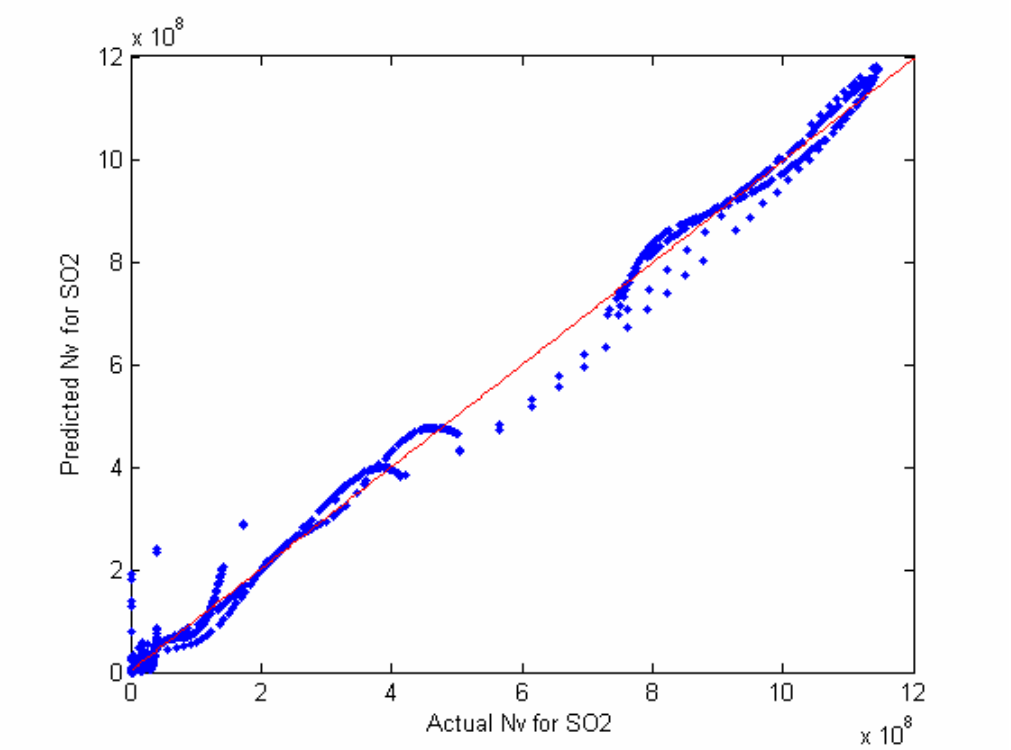

Figure 4.8 Cross Plot of Predicted and Actual *Nv* (SO_2) for the Testing Data Set

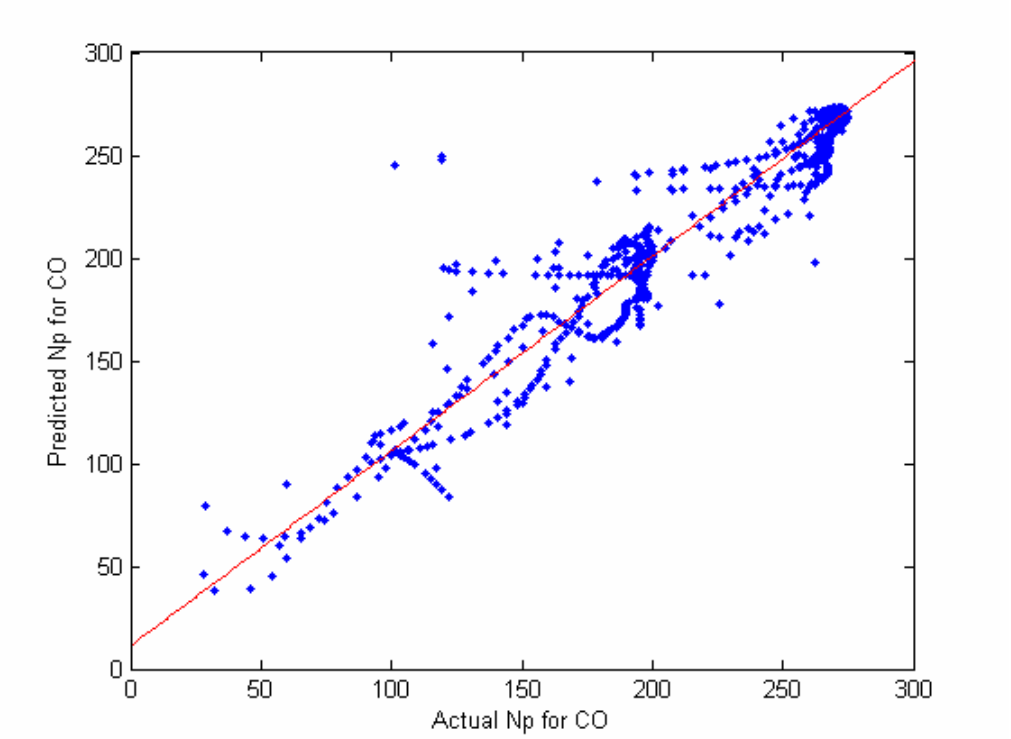

Figure 4.9 Cross Plot of Predicted and Actual *Np* (CO) for the Training Data Set

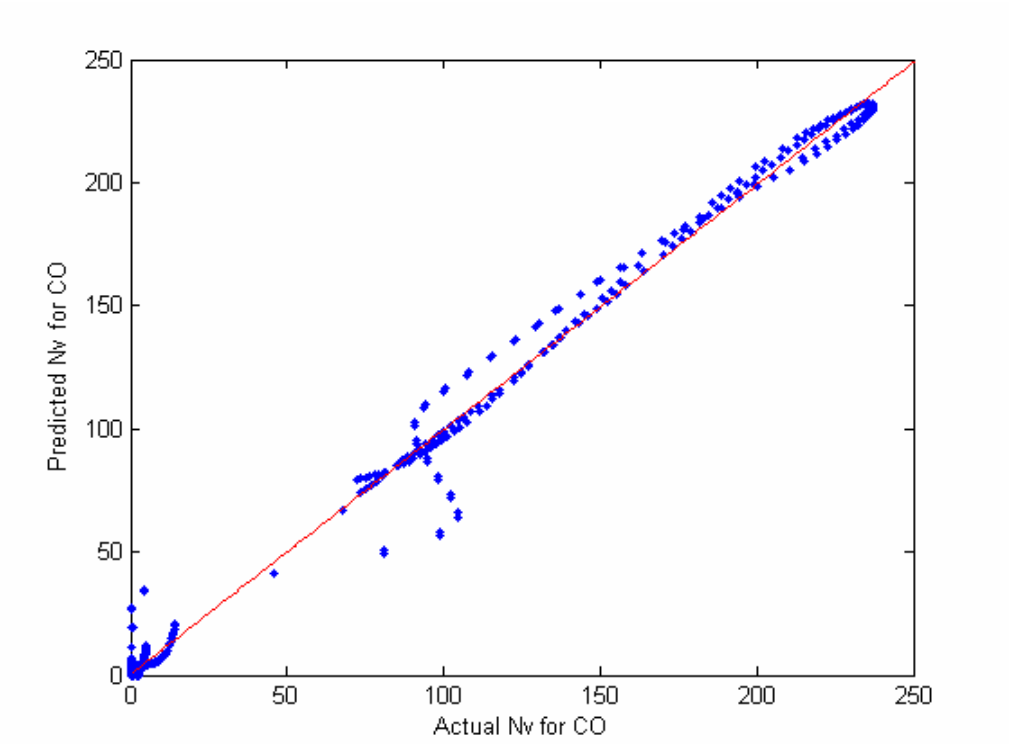

Figure 4.10 Cross Plot of Predicted and Actual *Nv* (CO) for the Testing Data Set

Chapter 5- Optimization Model Development for Locating Air Quality Monitoring Stations

5.1 Introduction

Air quality monitoring networks (AQMN) are used to characterize the presence and level of atmospheric contaminants. AQMN is an essential tool to monitor and control air pollution. Protecting human health and the environment from pollutant effects is the primary goal of all air pollution control programs. Protection of air quality requires accurate data on ambient concentration of major pollutants and emissions from air pollution sources to be available to regulatory authorities.

Air monitoring at carefully selected sites should provide a realistic picture of the air quality in the area of interest. The AQMN design objective is usually to provide maximum information about the air quality in a given area with minimum number of monitoring stations. It is required to determine the minimum number of monitoring stations due to budget constraints. Providing the minimum number of stations minimizes the installation, maintenance, and management costs.

In this study, two objectives of AQMN design have been considered; representation of spatial-temporal patterns (or pattern score) and the detection of violations of ambient air quality standard (or violation score) for multiple pollutants such as NO_x, SO_2, and CO. These two objectives were incorporated in Neural Networks (NN) models as was described in the previous chapter. The Neural networks obtained have strong predictive abilities in modeling the violation and pattern score as a function of spatial positions (x,y).

The combination of the two objectives for the multiple pollutants yields a utility function. This function should be maximized using optimization techniques in order to find optimal number and location of monitoring stations in an industrial area.

The optimization methods which were developed will be described in detail in this chapter. The first method we considered is for one station only which is the simplest scenario of solving the optimization problem. The two station scenario is more

complex in which we have account for more constraints. Then, we will describe the general method which is valid for any number of stations. The general method can be implemented and used for as many stations as needed within a prescribed budget constraint and a desired coverage area.

5.2 Mathematical Model and Model Description

5.2.1 Optimization Methodology of Neural Network Model:

To accomplish our AQMN objectives to find the optimum number and configuration of monitoring stations we have integrated the Neural Network models of violation scores and pattern scores described in chapter 4 within an optimization model. The objective function which will be described in this section was maximized and constraints were set to estimate the optimum number and locations of monitoring stations in an industrial area.

Two initial decision variables N_p and N_v were fitted to the neural network models. The objective of the neural network optimization is to achieve maximum coverage effectiveness and maximum detection of violations over ambient air standards. In order to achieve the two objectives, a utility function approach is used in this study. Different priorities will be given to each objective.

In the next section the problem formulation for this optimization problem will be explained. We start first with the simple one station case.

5.2.2 One Monitoring Station Model

The one monitoring station model predicts the location of one station only in an area of interest with the objective of maximizing detection of violations and the coverage area.

5.2.2.1 The Objective Function

The objective function for the one station model can be formulated as shown in equation (5.1).

$$\text{Maximize} \quad U = \sum_{k=1}^{n} ww_k \, N_{P_k}(x,y)_1 + \sum_{k=1}^{n} w_k \, N_{V_k}(x,y)_1 \qquad (5.1)$$

$$\text{s.t} \quad 0 \le x_1 \le L_1$$
$$0 \le y_1 \le L_2$$

Where,

k = pollutants (NO_x, SO_2 and CO)

N_{P_k} = the pattern score for pollutant k

N_{V_k} = the violation score for pollutant k

L_1, L_2 = the upper and lower bound (i.e. dimensions of coverage area)

w_k and ww_k are weight factors used to weigh the relative importance for the two objectives, violation score and pattern score, respectively.

The optimum solution will be the location of the monitoring station in the industrial area ($L_1 \times L_2 = 10 \times 1.2$ km) that achieves the composite objective described above and as shown in Figure 5.1.

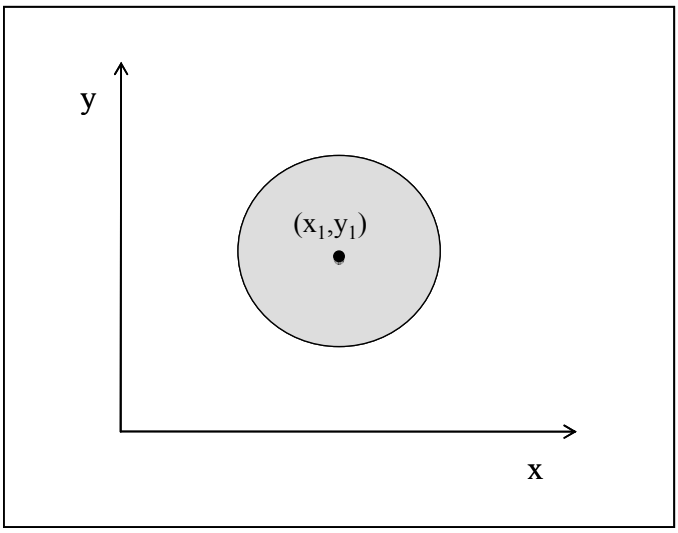

Figure 5.1 Illustration of One Monitoring Station Location and Sphere of Influence

5.2.2.2 Constraints

In order to force the sphere of influence (SOI) of the monitoring station to be inside the study area, the following constraints are added:

$$x_1 + r \le L_1$$
$$y_1 + r \le L_2$$

$$\begin{matrix} x_1 + r \le p L_1 \\ y_1 + r \le p L_2 \end{matrix} \quad \text{and} \quad \begin{matrix} x_1 - p r \ge 0 \\ y_1 - p r \ge 0 \end{matrix} \qquad (5.2)$$

Where,

r = sphere of influence radius

p = allowable percentage for the sphere of influence to be outside the area under study (i.e. p =1 means the sphere of influence must be completely in the study area)

5.2.3 Two Monitoring Station Model

If we want to find the locations of two monitoring stations simultaneously, we have to consider a sphere of influence around the location of both stations so that the surrounding area over which the air quality data for these stations is representative.

Once the sphere of influence has been identified from the neural network model, the Coverage Area (CA) of this sphere is defined as the number of potential monitoring sites placed inside it. This was denoted by a pattern score or N_p. So once the location point for the monitoring station computed by maximizing the Utility function (U) from the optimization model, we can characterize the SOI or N_p for that point from the Neural Network model.

Since the interest of the optimization problem is to achieve a maximum coverage area at a minimum overlap, we have to add constraints to minimize or avoid the overlaps between the two sphere of influence or between the effective areas for the two monitoring stations.

5.2.3.1 The Objective Function

The objective function for the two stations model is described as follows:

$$\text{Maximize } U = \sum_{k=1}^{n} ww_k \, N_{P_k}(x,y)_1 + \sum_{k=1}^{n} w_k \, N_{V_k}(x,y)_1$$

$$+ \sum_{k=1}^{n} ww_k \, N_{P_k}(x,y)_2 + \sum_{k=1}^{n} w_k \, N_{V_k}(x,y)_2 \qquad (5.3)$$

5.2.3.2 Constraint

The following constraints (5.4), (5.5) and (5.6) are used to make sure that the two monitoring stations and their sphere of influence (SOI) are inside the study area.

$$0 \le x_i \le L_1 \qquad \text{where } i = 1, 2 \qquad (5.4)$$
$$0 \le y_i \le L_2$$

$$x_1 + r_1 \le p\,L_1 \quad \text{and} \quad x_1 - p\,r_1 \ge 0 \qquad (5.5)$$
$$y_1 + r_1 \le p\,L_2 \qquad y_1 - p\,r_1 \ge 0$$

$$x_2 + r_2 \le p\,L_1 \quad \text{and} \quad x_2 - p\,r_2 \ge 0 \qquad (5.6)$$
$$y_2 + r_2 \le p\,L_2 \qquad y_2 - p\,r_2 \ge 0$$

It is important to add constraints so that the two spheres will be in different domains in our area and do not overlap. An illustration of two monitoring stations locations is given in Figure 5.2.

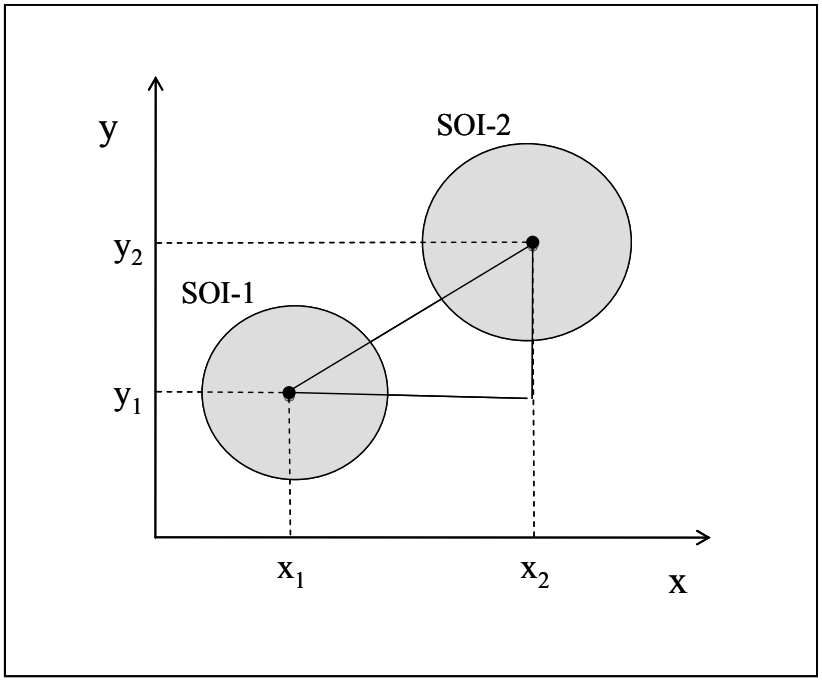

Figure 5. 2 Illustration of Two SOI for the Monitoring Stations Locations

By assuming that the SOI is a circle as shown in figure 5.2, the distance between the two points will be calculated to formulate the constraint in mathematical term as shown in the following equation.

$$\sqrt{(x_2 - x_1)^2 + (y_2 - y_1)^2} \geq \alpha (r_1 + r_2) \qquad (5.7)$$

Where, r_1 and r_2 represent the radius for the SOI-1 and SOI-2, respectively. The term (α) is used in order to allow overlaps. If α =1 then there is no overlap.

The radius of a sphere of influence is unknown so far and it is required to be estimated for the constraints described earlier (Equations 5.2 and 5.7).

Now we will attempt to find a relationship between the sphere of influence radius r and N_p. Let us assume that we have circle with potential location points inside it as shown in Figure 5.3.

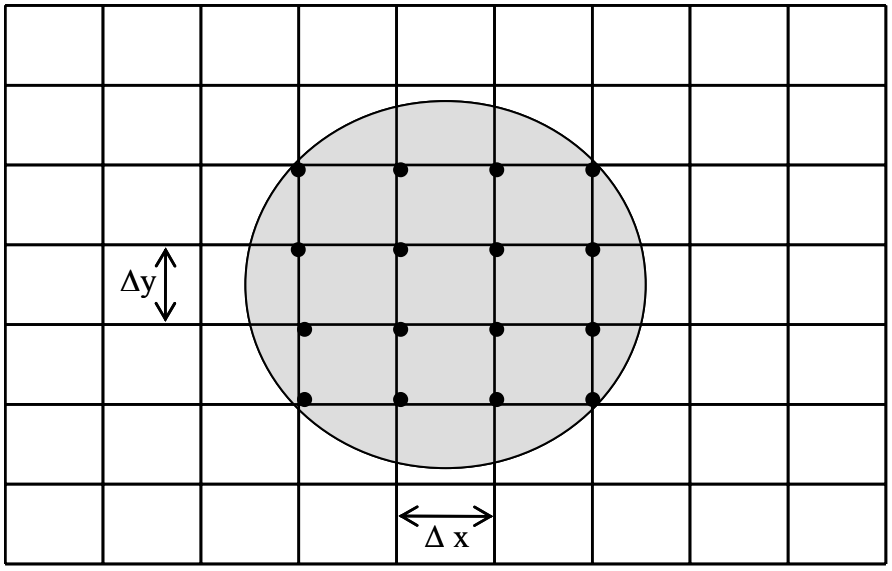

Figure 5.3 The Potential Location Points in SOI.

If we let N_p =16 and Δx, Δy be the discritizations used in the PDE finite difference method of chapter 3. In order to find the diameter of the circle, we have to assume that there is a rectangular inside the circle as shown in Figure 5.3

Assumption: $Np = 16$

We take the square root: $\sqrt{Np} = 4$

Then square root of the pattern score is used in the following equations:

Therefore the head pillar = $\left(\sqrt{N_p} - 1\right)\Delta y$ and the horizontal pillar = $\left(\sqrt{N_p} - 1\right)\Delta x$

$$r = \frac{D}{2} = \text{½ min } [\left(\sqrt{N_p} - 1\right)\Delta y, \left(\sqrt{N_p} - 1\right)\Delta x]$$

We end up with the following relation:

$$r = \text{½ mean}\left(\sqrt{N_p} - 1\right) * \min(\Delta x, \Delta y) \qquad (5.8)$$

Equation 5.8 is used to solve for the sphere of influence radius and the value is substituted in Equation 5.7. We see in equation 5.8 the radius of the sphere of influence (SOI) was calculated for the minimum (Δx, Δy) so that the equation would be considering the worst case scenario (the minimum coverage area). In order to extend Equation 5.8 to several pollutants, we use the average N_p obtained from the N_p of each pollutant.

5.2.4 General Station Model

Here the general model will be stated. The general model uses an extended objective function and more constraints. This model can be used for as many stations as required. As we increase the number of stations the coverage area will be increased.

5.2.4.1 The Objective Function

The general form for the objective function is given by:

$$\text{Maximize} \quad U = \sum_{i=1}^{M} \sum_{k=1}^{N} ww_k \, N_{P_k}(x, y)_i + \sum_{i=1}^{M} \sum_{k=1}^{N} w_k \, N_{V_k}(x, y)_i \qquad (5.9)$$

Where,

M = number of stations

N = number of pollutant

5.2.4.2 Constraints

In this case the constraints can be generalized as follows:

The first constraint (5.10) will be used to enforce the locations and their sphere of influence to be inside the study area. The second constraint (5.11) will be used to avoid overlapping between each sphere of influence.

$$\begin{matrix} x_i + r_i \le p\,L_1 \\ y_i + r_i \le p\,L_2 \end{matrix} \quad \text{and} \quad \begin{matrix} x_i - p\,r_i \ge 0 \\ y_i - p\,r_i \ge 0 \end{matrix} \qquad (5.10)$$

$$\sqrt{\left(x_i - x_j\right)^2 + \left(y_i - y_j\right)^2} \ge \alpha\left(r_i + r_j\right) \qquad (5.11)$$

$\forall\, i, j = 1,.....,M$ and $i \ne j$

In addition we have:

$$\begin{matrix} 0 \le x_i \le L_1 \\ 0 \le y_i \le L_2 \end{matrix} \qquad \forall\, i = 1,2,.....,M \qquad (5.12)$$

5.3 Methodology Description of Allocation of AQMN

Here we will show the main steps and procedure used to find the optimum number and configuration of the AQMN. The intention of this section is to summarize and provide the reader with an outline of the methodology used.

The optimization problem considered in the last section is a Nonlinear Programming Problem (NLP) which can be solved using the "fmincon" function of Matlab. Figure 5.4 gives a flow chart of the calculation procedure. First the pattern scores and violation scores are evaluated for a given number of stations using the developed Neural Network models of chapter 4. These are then combined to formulate an objective function of theNLP model. The constraints are also set at this stage. Once the NLP model is ready, we make use of the "fmincon" function of Matlab. An initial guess is required in order to start the optimization procedure. We describe below a simple heuristic procedure that we employed in order to get this guess. The flow chart for this heuristic is given in Figure 5.5.

A description of the optimization algorithm using a heuristic method (Elkamel et.al., 2007) is as follows:

1. Starting from the concentration data obtained through the mathematical model i.e., Multiple Cell Model of the pollution phenomena, a network formed by matrix of M x N where M is the number of observed (or predicted) concentrations at a potential locations numbered from 1 to N.
2. The correlation coefficients matrix $r_{i,j}$ are calculated, being i = 1, 2, …N; j = 1, 2, … N.
3. The SOI_i are calculated, being i = 1, 2, …N where the SOI_i is the set formed by locations m and correlated with location i in which correlation coefficient $r_{i,m} \geq r_c$.
4. The violation score N^i_v are calculated, being i = 1, 2,…, N using equation (3.16) and the coefficients shown in table 3.7.
5. The coverage area in term of pattern score N^i_p are formed for each SOI obtained, being i = 1, 2,…, N.
6. The utility function UF_i are calculated, being i = 1, 2,…, N with a suitable value for b as shown in Figure 5.5.
7. The ith location (station) of a maximum UF is chosen.
8. In order to avoid overlaps, the ith location(s) (stations) belonging to the SOI of the station being selected in step 7 are deleted from all sets SOI_i to which they belonged.
9. Back to step 5. The loop ends when the number of stations is adequate.

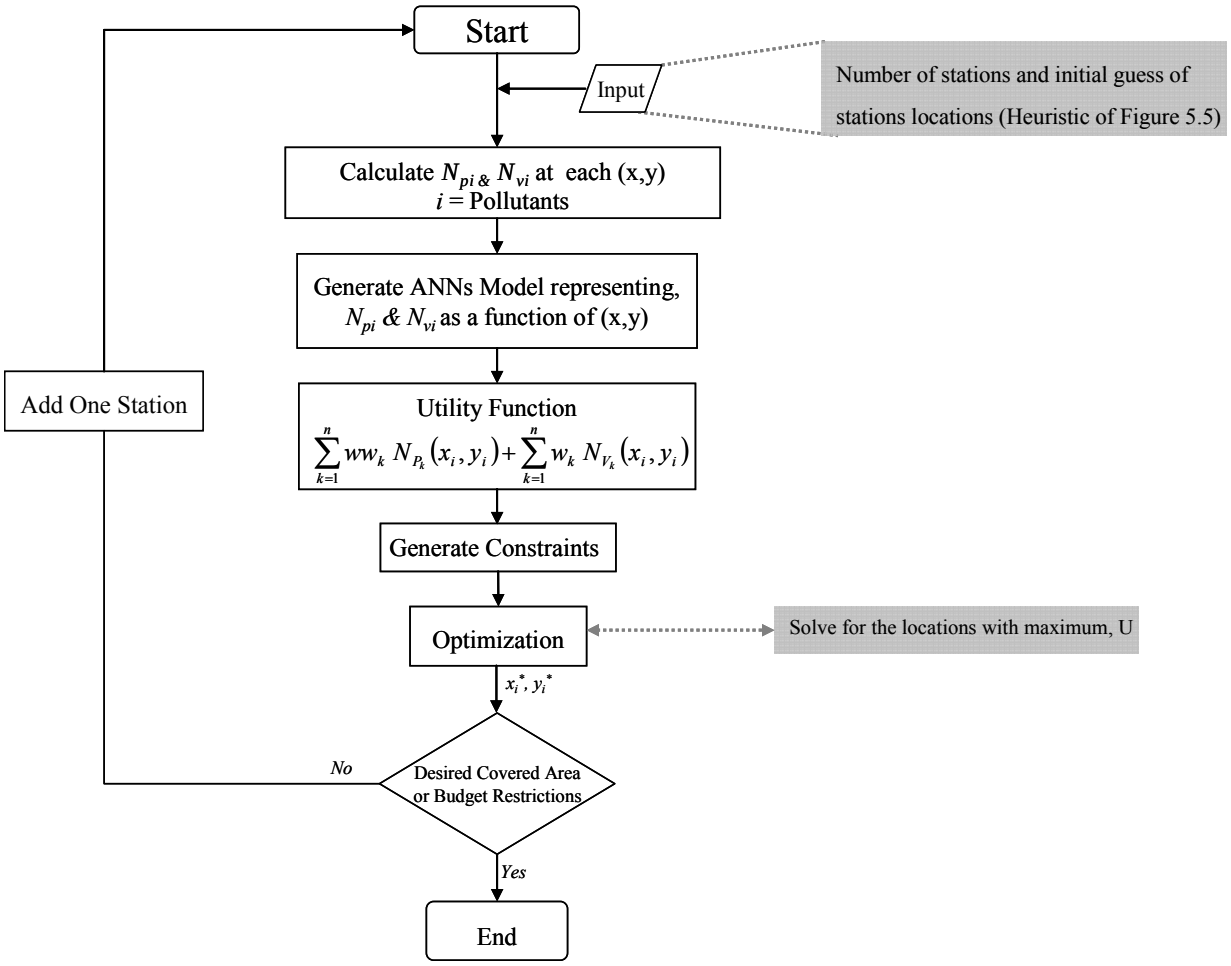

Figure 5.4 Flow Chart for AQMN Using Mathematical Programming Approach

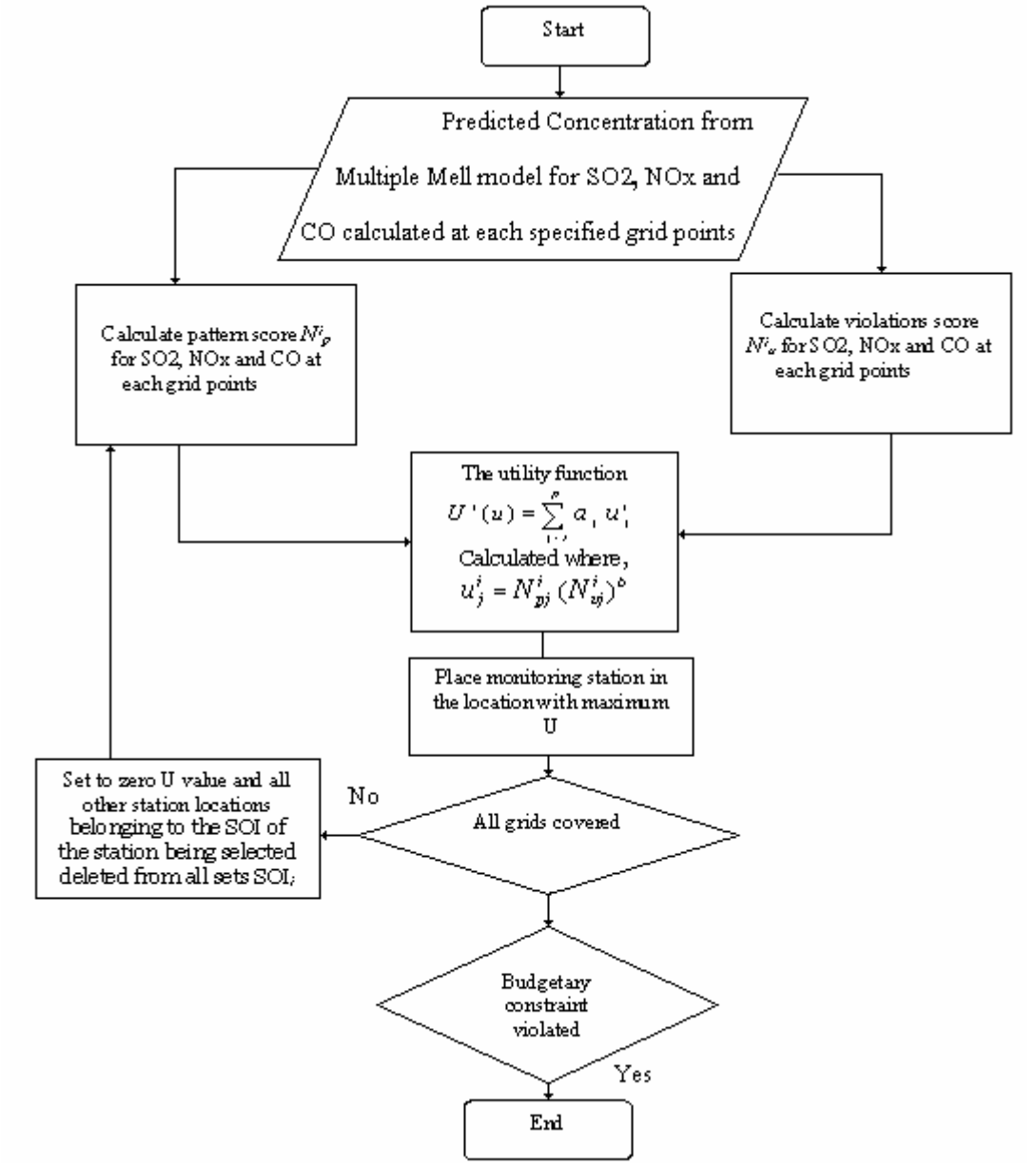

Figure 5.5 Flowchart Determination Procedure for Allocation of Monitoring Stations (Heuristic). (Elkamel et.al., 2007)

5.4 Results and Discussion

The optimization models discussed in this chapter were used to identify the optimal locations of the monitoring stations for sulfur dioxide (SO_2), nitrogen oxide (NOx), and carbon monoxide (CO) within the vicinity under study. Presented here is the model output for one, two, three, four, five, six, and seven station models. As discussed previously, the developed model objective is to predict the optimum location that maximizes two AQMN objectives. The first is the representation of the spatial temporal patterns (coverage area). The second objective is the detection of violations of ambient air quality standard. The results of this study shows the influence of changing the pattern score (*Np*) and violation score (*Nv*) weights for the one station and two station models. The influence of changing the weight factors of SO_2, NOx, and CO are studied for all the proposed models. The coverage area which could be covered by the monitoring stations will also be discussed. The presented tables in the following results show the influence of increasing the weight factors of the pattern score and violation score on the location of monitoring station and sphere of influence radius. From this radius we can calculate the coverage area. Knowing that as we increase the numbers of monitoring stations the coverage area will increase. Since many results can be generated from the model, the effect of pattern score and violation score for each pollutant (NOx, SO_2 and CO) by changing the weight factor are shown in Appendix instead.

5.4.1 One Station Model

5.4.1.1 Effect of the Importance of *Nv* and *Np*

Table 5.1 shows the effects of changing the weight factor of the pattern score on the location of the monitoring station, SOI radius and the coverage area. It is noticed that by increasing the weight factor of the pattern score from 1 to 10,000 the coverage area increased by 0.0015%. Increasing the weight factor of the pattern score had therefore a negligible effect on the location for this case of a single station.

Table 5.2 shows the effect of changing the weight factor of the violation score (*Nv*). By increasing the weight factor of the violation score it is shown that an increase in

the coverage area percentage by 0.0057% is obtained. The location changes also slightly in (x) and (y) by 3.364% and 0.014% respectively.

Table 5.1 Influence of Changing Pattern Score Weight (ww)

w	ww	(x,y)	*r*	CA%
1	1	(4.1317,0.4949)	0.4949	9.2345
1	10	(4.1317,0.4949)	0.4949	9.2345
1	100	(4.1316,0.4949)	0.4949	9.2345
1	1000	(4.1313,0.4949)	0.4949	9.2345
1	10000	(4.1276,0.4950)	0.4950	9.2360

where,

w : weight factor of the violation score(*Nv*).
ww : weight factor of pattern score (*Np*).
(x,y) : represents the location.
r : radius of the sphere of influence (SOI).
CA% : percentage of coverage area.

Table 5. 2 Influence of Changing Violation Score Weight (w)

w	ww	(x,y)	*r*	CA%
10	1	(4.1317,0.4949)	0.4949	9.2345
100	1	(4.1317,0.4949)	0.4949	9.2345
1000	1	(4.1317,0.4949)	0.4949	9.2345
10000	1	(4.2707,0.5089)	0.4951	9.2402

5.4.1.2 Effect of Importance of Pollutants

The importance of the specified pollutant was evaluated by using different weight factors for the violation scores and pattern scores at the same time. This was done for the three pollutants. Table 5.3 shows the output after increasing the weight factor of nitrogen oxide from 10 to 10,000. The coverage area decreased in size by 0.0657%. The location was also affected. It is noticed that in the (x) direction there was a change by 4.19% when we have increased the weight factor of NOx from 10 to 10,000. In the (y) direction the change is small and is around 0.34%.

Table 5.3 Influence of Changing the Weight Factor of Nitrogen Oxide (NOx)

Weight Factor	**(x,y)**	***r***	**CA%**
10	(4.1318,0.4949)	0.4949	9.2345
100	(4.1335,0.4949)	0.4949	9.2345
1000	(4.1497,0.4947)	0.4947	9.2278
10000	(4.3051,0.4932)	0.4932	9.1688

The influence and effect of increasing the weight factor of sulfur dioxide is shown in Table 5.4. The coverage area percentage was not affected by this change. The location had negligible change in the (x) direction only.

Table 5.4 Influence of Changing the Weight Factor of Sulfur Dioxide (SO_2)

Weight Factor	**(x,y)**	***r***	**CA%**
10	(4.1316,0.4949)	0.4949	9.2345
100	(4.1316,0.4949)	0.4949	9.2345
1000	(4.1316,0.4949)	0.4949	9.2345
10000	(4.1317,0.4949)	0.4949	9.2345

Table 5.5 shows the influence of increasing the weight factor of carbon monoxide on the location and coverage area percentage. The location in the (x) direction had a minor increase by increasing the weight factor in this case. While the coverage area percentage expressed no change.

Table 5.5 Influence of Changing the Weight Factor of Carbon Monoxide (CO).

Weight Factor	**(x,y)**	***r***	**CA%**
10	(4.1317,0.4949)	0.4949	9.2345
100	(4.1317,0.4949)	0.4949	9.2345
1000	(4.1323,0.4949)	0.4949	9.2345
10000	(4.1384,0.4949)	0.4949	9.2345

5.4.2 Two Station Model

5.4.2.1 Effect of Importance of *Np* and *Nv*

Table 5.6 shows the influence of increasing the weight of the pattern score for the two station model. It is clear that there is a minor increase in the coverage area percentage as a result of increasing the weight of the pattern score. The first location $(x,y)_1$ did not show any change to be considered in this case whereas the second location $(x,y)_2$ had a change in the (x) direction only.

Table 5.6 Influence of Changing Pattern Score Weight (ww)

w	ww	$(x,y)_1$	$(x,y)_2$	r_1	r_2	CA%
1	1	(9.6486, 0.8257)	(4.1317, 0.4949)	0.3514	0.4949	13.8888
1	10	(9.6486, 0.8257)	(4.1317, 0.4949)	0.3514	0.4949	13.8888
1	100	(9.6486, 0.8257)	(4.1316, 0.4949)	0.3514	0.4949	13.8889
1	1000	(9.6486, 0.8257)	(4.1313, 0.4949)	0.3514	0.4949	13.8890
1	10000	(9.6486, 0.8256)	(4.1276, 0.4950)	0.3514	0.4950	13.8907

The effect of changing the violation score weight is shown in Table 5.7. We see that the coverage area percentage did not change and was not affected by increasing the weight factor of the violation score. The first location and the second location showed no change in this case.

Table 5.7 Influence of Changing Violation Score Weight (w)

w	ww	$(x,y)_1$	$(x,y)_2$	r_1	r_2	CA%
10	1	(9.6486, 0.8257)	(4.1317,0.4949)	0.3514	0.4949	13.8888
100	1	(9.6486, 0.8257)	(4.1317,0.4949)	0.3514	0.4949	13.8888
1000	1	(9.6486, 0.8257)	(4.1317,0.4949)	0.3514	0.4949	13.8888
10000	1	(9.6486, 0.8257)	(4.1317,0.4949)	0.3514	0.4949	13.8888

5.4.2.2 Effect of Importance of Pollutants

The influence of increasing the weight factor of nitrogen oxide is shown in Table 5.8. The first location was affected by increasing the weight factor of NOx in this case by 50% for (x) and 40.8% for (y). The second location got influenced and the change in the (x) direction for this location is 7.2% and 0.55% in the (y) direction. The area coverage percentage increased by 4.435%. The area coverage and the location expressed dramatic effect on the weighting factor on NOx for this particular instance.

Table 5.8 Influence of Changing the Weight Factor of Nitrogen Oxide (NOx)

Weight Factor	**$(x,y)_1$**	**$(x,y)_2$**	***r_1***	***r_2***	**CA%**
10	(9.6486, 0.8257)	(4.1318,0.4949)	0.3514	0.4949	13.8888
100	(9.6486, 0.8256)	(4.1335,0.4949)	0.3514	0.4949	13.8888
1000	(4.6357, 0.4899)	(3.6471, 0.4988)	0.4899	0.4988	18.4262
10000	(4.8207, 0.4883)	(3.8348, 0.4976)	0.4883	0.4976	18.3239

Table 5.9 shows the influence of increasing the weight factor of sulfur dioxide in the two station model. It is noticed that there is no change recorded in the coverage area percentage or the estimated locations in this case.

Table 5.9 Influence of Changing the Weight Factor of Sulfur Dioxide (SO_2)

Weight Factor	**$(x,y)_1$**	**$(x,y)_2$**	***r_1***	***r_2***	**CA%**
10	(9.6486, 0.8257)	(4.1316, 0.4949)	0.3514	0.4949	13.8889
100	(9.6486, 0.8257)	(4.1316, 0.4949)	0.3514	0.4949	13.8889
1000	(9.6486, 0.8257)	(4.1316, 0.4949)	0.3514	0.4949	13.8889
10000	(9.6486, 0.8257)	(4.1316, 0.4949)	0.3514	0.4949	13.8889

Table 5.10 shows the effect of increasing the weight factor of carbon monoxide. The first location was not influenced by the weight factor increase and the second location had a minor change in the (x) direction only. The coverage area percentage showed also no change.

Table 5.10 Influence of Changing the Weight Factor of Carbon Monoxide (CO)

Weight Factor	$(x,y)_1$	$(x,y)_2$	r_1	r_2	CA%
10	(9.6486, 0.8257)	(4.1317,0.4949)	0.3514	0.4949	13.8889
100	(9.6486, 0.8257)	(4.1317,0.4949)	0.3514	0.4949	13.8889
1000	(9.6486, 0.8257)	(4.1323, 0.4949)	0.3514	0.4949	13.8889
10000	(9.6486, 0.8255)	(4.1384, 0.4949)	0.3514	0.4949	13.8889

5.4.3 Three Station Model

5.4.3.1 Location and Coverage Area of Monitoring Stations

Now we will be studying the output results for the three station model. Table 5.11 shows the output results from the Three Station Model without considering the weight factor (weight factor =1). The coverage area percentage was 27.5% in this case.

Table 5.11 Three Station Model Output with no Consideration of Weight Factor

$(x,y)_1$	$(x,y)_2$	$(x,y)_3$	r_1	r_2	r_3	CA%
(3.0717, 0.4974)	(4.0647, 0.4956)	(5.0471, 0.4869)	0.4974	0.4956	0.4869	27.5243

5.4.3.2 Effect of Importance of Pollutants

Table 5.12 gives the influence of increasing the weight factor from 10 to 10,000 of Nitrogen Oxide on the coverage area percentage and the estimated locations. The coverage area percentage is affected by the increase of the weight factor of NOx. We notice a decrease in the coverage area percentage by 0.24%. The first location $(x,y)_1$ changed in the positive direction with respect to (x) and negative direction with respect to (y). The second location $(x,y)_2$ has a minor change in the positive direction with respect to (y) only. The third location $(x,y)_3$ moved to the positive direction with respect to (x) and negative direction with respect to (y) by increasing the weight factor of NOx .

Table 5.12 Influence of Changing the Weight Factor of Nitrogen Oxide (NOx)

Weight Factor	**$(x,y)_1$**	**$(x,y)_2$**	**$(x,y)_3$**	***r_1***	***r_2***	***r_3***	**CA%**
10	(3.6249,0.4989)	(5.5720,0.4328)	(4.6139,0.4901)	0.4989	0.4328	0.4901	25.5001
100	(3.6270,0.4989)	(4.6159,0.4901)	(5.5720,0.4328)	0.4989	0.4901	0.4328	25.4993
1000	(3.1034,0.4978)	(4.0964,0.4953)	(5.0784,0.4867)	0.4978	0.4953	0.4867	27.5209
10000	(4.3051,0.4932)	(5.5720,0.4333)	(6.4926,0.4891)	0.4932	0.4333	0.4891	25.2624

Table 5.13 shows the effects of increasing the weight factor of sulfur dioxide. The coverage area had the maximum change by increasing the weight factor of SO_2 from 10 to 100. The maximum increase of the coverage area in this case is 2.02%. The maximum decrease is noticed when we increase the weight factor from 10 to 1000. The coverage area percentage was not influenced by the change from 10 to 10,000 and maintained its original value.

There is no influence on the three estimated locations when the weight factor is changed from 10 to 10,000. On the other hand, some changes are noticeable when the weight factor for SO_2 is changed from 10 to 100 and 1000.

Table 5.13 Influence of Changing the Weight Factor of Sulfur Dioxide (SO2)

Weight Factor	**$(x,y)_1$**	**$(x,y)_2$**	**$(x,y)_3$**	***r_1***	***r_2***	***r_3***	**CA%**
10	(3.6247,0.4989)	(4.6137,0.4901)	(5.5720,0.4328)	0.4989	0.4901	0.4328	25.5002
100	(3.0716,0.4974)	(4.0646,0.4956)	(5.0471,0.4869)	0.4974	0.4956	0.4869	27.5243
1000	(4.1316,0.4949)	(5.5720,0.4328)	(6.4046,0.4380)	0.4949	0.4328	0.3997	22.3207
10000	(3.6247,0.4989)	(4.6137,0.4901)	(5.5720,0.4328)	0.4989	0.4901	0.4328	25.5002

Table 5.14 shows the influence of changing the weight factor of carbon monoxide from 10 to 10,000 for the three station model. We notice an increase in the coverage area percentage by 2.02% when we increase the weight factor in this case from 10 to 10,000. The first location moved to the negative direction with respect to (x) and (y) as a result of increasing the weight factor of CO from 10 to 10,000. The second and third locations changed in the negative direction for (x) and positive direction in (y).

Table 5.14 Influence of Changing the Weight Factor of Carbon Monoxide (CO).

Weight Factor	$(x,y)_1$	$(x,y)_2$	$(x,y)_3$	r_1	r_2	r_3	CA%
10	(3.6248,0.4989)	(4.6137,0.4901)	(5.5720,0.4328)	0.4989	0.4901	0.4328	25.5002
100	(3.0717,0.4974)	(4.0648,0.4956)	(5.0472,0.4869)	0.4974	0.4956	0.4869	27.5242
1000	(3.6255,0.4989)	(4.6144,0.4901)	(5.5720,0.4328)	0.4989	0.4901	0.4328	25.4999
10000	(3.0810,0.4975)	(4.0740,0.4955)	(5.0563,0.4868)	0.4975	0.4955	0.4868	27.5234

5.4.4 Four Station Model

5.4.4.1 Location and Coverage Area of Monitoring Stations

The Four Station Model output results will be presented in terms of coverage area percentage and the estimated locations. Table 5.15 shows the output from the Four Station Model without considering the weight factor (weight factor =1). The coverage area percentage in this case is 34.5%.

Table 5.15 Four Station Model Output with no Consideration of Weight Factor

$(x,y)_1$	$(x,y)_2$	$(x,y)_3$	$(x,y)_4$	r_1	r_2	r_3	r_4	CA%
(3.6247, 0.4989)	(4.6137, 0.4901)	(6.4922, 0.4891)	(5.5720, 0.4328)	0.4989	0.4901	0.4891	0.4328	34.5173

5.4.4.2 Effect of Importance of Pollutants

The results presented in Table 5.16 show that by increasing the weight factor of nitrogen oxide from 10 to 10,000 the coverage area percentage decreased by 1.78%. The first location change by increasing the weigh factor in this case as it shows a change with respect to both (x) and (y). The second, third and fourth locations show a change with respect to (x) and a small change with respect to (y).

Table 5.16 Influence of Changing the Weight Factor of Nitrogen Oxide (NOx)

w	$(x,y)_1$	$(x,y)_2$	$(x,y)_3$	$(x,y)_4$	r_1	r_2	r_3	r_4	CA%
10	(2.4632, 0.4754)	(4.4289, 0.4919)	(5.4068, 0.4860)	(3.4377, 0.4994)	0.4754	0.4919	0.4860	0.4994	35.9484
100	(3.6670, 0.4987)	(4.6553, 0.4897)	(5.575,0 .4319)	(2.6790, 0.4893)	0.4987	0.4897	0.4319	0.4893	34.4740
1000	(2.6796, 0.4893)	(4.6559, 0.4897)	(5.5756, 0.4318)	(3.6675, 0.4987)	0.4893	0.4897	0.4318	0.4987	34.4718
10000	(2.9034, 0.4948)	(4.8802, 0.4879)	(5.7869, 0.4388)	(3.8952, 0.4971)	0.4948	0.4879	0.4201	0.4971	34.1721

It is observed from Table 5.17 that by increasing the weight factor of sulfur dioxide from 10 to 10,000 the coverage area percentage stay at the same value. The first location has a change in (x) and (y) directions while locations two and three seem to be not influenced by changing the weight factor from 10 to 10,000 for SO_2. The fourth location show a change in both (x) and (y) directions.

Table 5.17 Influence of Changing the Weight Factor of Sulfur Dioxide (SO_2)

w	$(x,y)_1$	$(x,y)_2$	$(x,y)_3$	$(x,y)_4$	r_1	r_2	r_3	r_4	CA%
10	(3.4376, 0.4994)	(4.4289, 0.4919)	(5.4068, 0.4860)	(2.4631, 0.4754)	0.4994	0.4919	0.4860	0.4754	35.9483
100	(2.4631, 0.4754)	(4.4289, 0.4919)	(5.4068, 0.4860)	(3.4376, 0.4994)	0.4754	0.4919	0.4860	0.4994	35.9483
1000	(2.4631, 0.4754)	(4.4289, 0.4919)	(5.4068, 0.4860)	(3.4376, 0.4994)	0.4754	0.4919	0.4860	0.4994	35.9483
10000	(2.4631, 0.4754)	(4.4289, 0.4919)	(5.4068, 0.4860)	(3.4376, 0.4994)	0.4754	0.4919	0.4860	0.4994	35.9483

Table 5.18 shows the influence of increasing the weight factor of carbon monoxide from 10 to 10,000 for the Four Station Model. We notice a minor increase of 0.002% in the coverage area percentage and small changes of the locations of the four stations.

Table 5.18 Influence of Changing the Weight Factor of Carbon Monoxide (CO)

w	$(x,y)_1$	$(x,y)_2$	$(x,y)_3$	$(x,y)_4$	r_1	r_2	r_3	r_4	CA%
10	(2.4631, 0.4754)	(4.4289, 0.4919)	(5.4068, 0.4860)	(3.4376, 0.4994)	0.4754	0.4919	0.4860	0.4994	35.9483
100	(2.4632, 0.4754)	(4.4289, 0.4919)	(5.4068, 0.4860)	(3.4377, 0.4994)	0.4754	0.4919	0.4860	0.4994	35.9483
1000	(2.4633, 0.4754)	(4.4290, 0.4919)	(5.4069, 0.4860)	(3.4378, 0.4994)	0.4754	0.4919	0.4860	0.4994	35.9483
10000	(3.4388, 0.4994)	(5.4079, 0.4860)	(4.4300, 0.4919)	(2.4642, 0.4755)	0.4994	0.4860	0.4919	0.4755	35.9503

5.4.5 Five Station Model

5.4.5.1 Location and Coverage Area of Monitoring Stations

The Five Station Model output results are presented in terms of coverage area percentage and locations of the stations. Table 5.19 shows the output results for the locations of the five stations for a weight factor of 1. The coverage area percentage is shown in Table 5.20. In this case the coverage area percentage is 41.95%.

Table 5.19 Five Station Model Output for Location Estimates (Weight Factors=1)

$(x,y)_1$	$(x,y)_2$	$(x,y)_3$	$(x,y)_4$	$(x,y)_5$
(2.3160, 0.4695)	(4.2766, 0.4935)	(6.1452, 0.4355)	(3.2841, 0.4991)	(5.2562, 0.4862)

Table 5.20 Five Station Model Output for Sphere of Influence Radius and Coverage Area Percentage (Weight Factors=1)

r_1	r_2	r_3	r_4	r_5	CA%
0.4695	0.4935	0.4043	0.4991	0.4862	41.9509

5.4.5.2 Effect of Importance of Pollutants

Table 5.21 shows the influence of increasing the weight factor of nitrogen oxide from 10 to 10,000 for the Five Station Model. It is observed that the first and third locations are shifted to the negative direction with respect to (x) and (y). Whereas the second

location was affected by increasing the weight of NOx and showed a change in the positive direction with respect to (x) and (y). The fourth location showed a negative move in the (x) direction and a minor positive change in the (y) direction. The fifth location had a positive change in the (x) direction and a small negative change in the (y) direction.

Table 5.22 reveals that by increasing the weigh factor for NOx in the Five Station Model we have some increase in the coverage area percentage by 1.24%.

Table 5.21 Influence of Changing the Weight Factor of Nitrogen Oxide (NOx) on the Stations Locations

w	$(x,y)_1$	$(x,y)_2$	$(x,y)_3$	$(x,y)_4$	$(x,y)_5$
10	(3.4377,0.4994)	(2.4632,0.4754)	(9.6486,0.8257)	(5.4068,0.4860)	(4.428,0.4919)
100	(2.6757,0.4892)	(4.6520,0.4897)	(5.5725,0.4326)	(3.6636,0.4987)	(6.4924,0.4891)
1000	(2.5586,0.4852)	(4.5243,0.4931)	(7.3459,0.4456)	(3.4565,0.4884)	(5.2021,0.4567)
10000	(2.4586,0.4752)	(4.4241,0.4919)	(6.2829,0.4469)	(3.4329,0.4994)	(5.4021,0.4860)

Table 5.22 Influence of Changing the Weight Factor of Nitrogen Oxide (NOx) on Sphere of Influence Radius and Coverage Area Percentage

w	r_1	r_2	r_3	r_4	r_5	CA%
10	0.4994	0.4754	0.3514	0.4860	0.4919	40.6027
100	0.4892	0.4897	0.4326	0.4987	0.4891	43.5109
1000	0.4434	0.4344	0.32344	0.4900	0.5191	40.6027
10000	0.4752	0.4919	0.3957	0.4994	0.4860	41.8428

Table 5.23 presents the results from the Five Station Model by increasing the weight factor for the sulfur dioxide from 10 to 10,000. Location one, three and four show positive changes in the (x) and (y) directions. Location two and five show positive changes in the (x) direction and some negative change in the (y) direction.

Table 5.24 presents the result of increasing the weigh factor of SO_2. We notice from this table that the coverage area percentage is increased by 4.2%.

Table 5.23 Influence of Changing the Weight Factor of Sulfur Dioxide (SO_2) on the Stations Locations

Weight Factor	**$(x,y)_1$**	**$(x,y)_2$**	**$(x,y)_3$**	**$(x,y)_4$**	**$(x,y)_5$**
10	(2.3306, 0.4700)	(4.2918, 0.4933)	(6.2460, 0.4887)	(3.2993, 0.4992)	(5.2712, 0.4861)
100	(2.3159, 0.4695)	(4.2766, 0.4935)	(5.2562, 0.4862)	(3.2840, 0.4991)	(6.1452, 0.4355)
1000	(2.3159, 0.4695)	(3.2840, 0.4991)	(6.1452, 0.4355)	(5.2562, 0.4862)	(4.2766, 0.4935)
10000	(2.4631, 0.4754)	(4.4289, 0.4919)	(9.6486, 0.8257)	(3.4376, 0.4994)	(5.4068, 0.4860)

Table 5.24 Influence of Changing the Weight Factor of Sulfur Dioxide (SO_2) on Sphere of Influence Radius and Coverage Area Percentage

Weight Factor	**r_1**	**r_2**	**r_3**	**r_4**	**r_5**	**CA%**
10	0.4700	0.4933	0.4887	0.4992	0.4861	44.8074
100	0.4695	0.4935	0.4862	0.4991	0.4043	41.9509
1000	0.4695	0.4991	0.4043	0.4862	0.4935	41.9509
10000	0.4754	0.4919	0.4919	0.4994	0.4860	40.6026

Table 5.25 shows the influence of increasing the weight factor of carbon monoxide on the five generated locations. The first location has a change in the negative direction in terms of (x) and (y). The second location has a positive change in (x) direction and a minor negative change in the (y) direction. The fourth location has a positive change in both (x) and (y) directions. The third and fifth locations show positive changes in the (x) direction only.

Table 5.26 shows the effects of increasing the weight factor of CO on the sphere of influence radius and the coverage area percentage. We see that the coverage area percentage undergoes a very small increase of 0.0059% in this case.

Table 5.25 Influence of Changing the Weight Factor of Carbon Monoxide (CO) on the Station Locations

Weight Factor	$(x,y)_1$	$(x,y)_2$	$(x,y)_3$	$(x,y)_4$	$(x,y)_5$
10	(3.2993, 0.4992)	(4.2918, 0.4933)	(6.2460, 0.4887)	(2.3306, 0.4700)	(5.2712, 0.4861)
100	(4.2918, 0.4933)	(5.2712, 0.4861)	(2.3307, 0.4700)	(3.2994, 0.4992)	(6.2461, 0.4887)
1000	(4.6519, 0.4897)	(3.6635, 0.4987)	(5.5724, 0.4326)	(2.6756, 0.4892)	(6.4048, 0.4380)
10000	(2.3362, 0.4702)	(4.2975, 0.4932)	(6.2517, 0.4887)	(3.3051, 0.4992)	(5.2769, 0.4861)

Table 5.26 Influence of Changing the Weight Factor of Carbon Monoxide (CO) on Sphere of Influence Radius and Coverage Area Percentage

Weight Factor	r_1	r_2	r_3	r_4	r_5	CA%
10	0.4992	0.4933	0.4887	0.4700	0.4861	44.8075
100	0.4933	0.4861	0.4700	0.4992	0.4887	44.8075
1000	0.4897	0.4987	0.4326	0.4892	0.3998	40.5211
10000	0.4702	0.4932	0.4887	0.4992	0.4861	44.8134

5.4.6 Six Station Model

5.4.6.1 Location and Coverage Area of Monitoring Stations

Now we will discuss the Six Station Model output results in terms of coverage area percentage and the location of the monitoring stations. Tables 5.27 and 5.28 show the output results for the obtained locations and coverage area percentage, respectively, from the Six Station Model with weight factor of one. The coverage area percentage in this case was 50.59% and is shown in Table 5.28.

Table 5.27 Six Station Model Output for Stations Locations (Weight Factors=1)

$(x,y)_1$	$(x,y)_2$	$(x,y)_3$	$(x,y)_4$	$(x,y)_5$	$(x,y)_6$
(4.9910, 0.4872)	(3.0149, 0.4967)	(5.9657, 0.4875)	(2.0581, 0.4607)	(4.0077, 0.4961)	(6.8543, 0.4402)

Table 5.28 Six Station Model Output for Sphere of Influence Radius and Coverage Area Percentage (Weight Factors=1)

r_1	r_2	r_3	r_4	r_5	r_6	CA%
0.4872	0.4967	0.4875	0.4607	0.4961	0.4023	50.592

5.4.6.2 Effect of Importance of Pollutants

Table 5.29 shows the influence of increasing the weight factor of nitrogen oxide from 10 to 10,000 for the Six Location Model to determine the locations of the monitoring stations. We notice from this table that the first location changes in the negative direction with respect to (x) and (y). The second, third and sixth locations show changes in the negative direction with respect to (x) and positive changes in the (y) direction. The fourth location show a positive move in the (x) direction and a negative one in the (y) direction. The fifth location undergoes a positive change in (x) and (y) directions.

Table 5.30 shows that the coverage area percentage increases by 2.26% when we increase the weight factor of NOx from 10 to 10,000.

Table 5.29 Influence of Changing the Weight Factor of Nitrogen Oxide (NOx) on the Location Estimates

Weight Factor	$(x,y)_1$	$(x,y)_2$	$(x,y)_3$	$(x,y)_4$	$(x,y)_5$	$(x,y)_6$
10	(4.0259, 0.4960)	(5.9053, 0.4353)	(6.7158, 0.4401)	(3.0331, 0.4969)	(2.0755, 0.4613)	(5.0089, 0.4871)
100	(5.1783, 0.5160)	(4.2217, 0.4939)	(6.8073, 0.4634)	(2.2362, 0.4481)	(3.2279, 0.4999)	(5.9755, 0.4764)
1000	(3.0444, 0.4971)	(5.0201, 0.4870)	(6.8799, 0.4431)	(4.0373, 0.4958)	(2.0863, 0.4617)	(5.9948, 0.4877)
10000	(2.3415, 0.4704)	(5.2823, 0.4861)	(6.2571, 0.4887)	(7.1233, 0.4621)	(4.3030, 0.4932)	(3.3106, 0.4992)

Table 5.30 Influence of Changing the Weight Factor of Nitrogen Oxide (NOx) on Sphere of Influence Radius and Coverage Area Percentage

Weight Factor	r_1	r_2	r_3	r_4	r_5	r_6	**CA%**
10	0.4960	0.4107	0.3998	0.4969	0.4613	0.4871	47.9360
100	0.4899	0.4946	0.3921	0.4661	0.4983	0.4868	50.5511
1000	0.4971	0.4870	0.3985	0.4958	0.4617	0.4877	50.5130
10000	0.4704	0.4861	0.4887	0.3778	0.4932	0.4992	50.1993

Table 5.31 shows the influence of increasing the weight factor of sulfur dioxide on the stations locations. We notice that the first location changes both the (x) and (y) directions. Locations two, three and six undergo positive changes in the (x) and (y) directions. The fourth location undergoes a positive change in the (x) direction and a negative one in the (y) direction. The fifth location shows a negative change in the (x) and (y) directions.

Table 5.32 shows the influence of increasing the weight factor for SO_2 on the Sphere of Influence Radius and Coverage Area Percentage. We notice that the coverage area percentage increase by 2.66% as we increase the weight factor from 10 to 10,000.

Table 5.31 Influence of Changing the Weight Factor of Sulfur Dioxide (SO_2) on the Stations Locations

Weight Factor	$(x,y)_1$	$(x,y)_2$	$(x,y)_3$	$(x,y)_4$	$(x,y)_5$	$(x,y)_6$
10	(4.0257, 0.4960)	(2.0752, 0.4613)	(6.7156, 0.4401)	(3.0328, 0.4969)	(5.0087, 0.4871)	(5.9050, 0.4353)
100	(2.0581, 0.4607)	(3.0149, 0.4967)	(6.8542, 0.4402)	(4.0077, 0.4961)	(4.9909, 0.4872)	(5.9657, 0.4875)
1000	(4.0256, 0.4960)	(5.9052, 0.4349)	(6.7173, 0.4393)	(2.0752, 0.4613)	(3.0327, 0.4969)	(5.0086, 0.4871)
10000	(3.0149, 0.4967)	(4.9909, 0.4872)	(6.8542, 0.4402)	(4.0077, 0.4961)	(2.0581, 0.4607)	(5.9657, 0.4875)

Table 5.32 Influence of Changing the Weight Factor of Sulfur Dioxide (SO_2) on Sphere of Influence Radius and Coverage Area Percentage

Weight Factor	r_1	r_2	r_3	r_4	r_5	r_6	**CA%**
10	0.4960	0.4613	0.3999	0.4969	0.4871	0.4108	47.9372
100	0.4607	0.4967	0.4023	0.4961	0.4872	0.4875	50.5921
1000	0.4960	0.4108	0.3999	0.4613	0.4969	0.4871	47.9411
10000	0.4967	0.4872	0.4023	0.4961	0.4607	0.4875	50.5921

Table 5.33 shows the influence of increasing the weight factor of CO from 10 to 10,000 on the stations locations. The first, second and sixth locations undergo positive changes in the (x) and (y) directions. Location three undergoes minor positive change in the (x) direction and a negative change in the (y) direction. The fourth location undergoes a negative change with respect to the (x) and (y) directions. The fifth location undergoes a negative change in the (x) direction and a positive in the (y) direction.

Table 5.34 shows the influence of increasing the weight factor of CO from 10 to 10,000. The table shows the changes in the sphere of influence radius and the coverage area percentage. The coverage area percentage in this case increases slightly by 0.088%.

Table 5.33 Influence of Changing the Weight Factor of Carbon Monoxide (CO) on the Station Locations

Weight Factor	$(x,y)_1$	$(x,y)_2$	$(x,y)_3$	$(x,y)_4$	$(x,y)_5$	$(x,y)_6$
10	(3.0149, 0.4967)	(2.0581, 0.4607)	(6.8543, 0.4402)	(4.0077, 0.4961)	(5.9657, 0.4875)	(4.9910, 0.4872)
100	(4.0078, 0.49612)	(2.0582, 0.4607)	(4.9910, 0.4872)	(3.0150, 0.4967)	(5.9658, 0.4875)	(6.8544, 0.4402)
1000	(2.0588, 0.4608)	(4.9916, 0.4872)	(6.8552, 0.4400)	(4.0084, 0.4961)	(3.0156, 0.4967)	(5.9664, 0.4875)
10000	(3.0219, 0.4968)	(4.9979, 0.4872)	(6.8638, 0.4386)	(2.0648, 0.4610)	(4.0147, 0.4961)	(5.9726, 0.4876)

Table 5.34 Influence of Changing the Weight Factor of Carbon Monoxide (CO) on Sphere of Influence Radius and Coverage Area Percentage

Weight Factor	r_1	r_2	r_3	r_4	r_5	r_6	CA%
10	0.4967	0.4607	0.4023	0.4961	0.4875	0.4872	50.5921
100	0.4961	0.4607	0.4872	0.4967	0.4875	0.4023	50.5929
1000	0.4608	0.4872	0.4026	0.4961	0.4967	0.4875	50.6009
10000	0.4968	0.4872	0.4049	0.4610	0.4961	0.4876	50.6801

5.4.7 Seven Station Model

5.4.7.1 Location and Coverage Area of Monitoring Stations

The Seven Station Model results are presented here and the discussion focuses on the coverage area percentage and the stations locations. Table 5.35 shows the output results for the stations locations from the Seven Station Model with a weight factor of one. The coverage area percentage is shown in Table 5.36. In this case the coverage area percentage is 56.8378%.

Table 5.35 Seven Station Model Output for Stations Locations (Weight Factors=1)

$(x,y)_1$	$(x,y)_2$	$(x,y)_3$	$(x,y)_4$	$(x,y)_5$	$(x,y)_6$	$(x,y)_7$
(3.9646, 0.4965)	(2.9720, 0.4961)	(6.7924, 0.4535)	(4.9485, 0.4874)	(2.0173, 0.4594)	(5.9233, 0.4874)	(7.6053, 0.4308)

Table 5.36 Seven Station Model Output for Sphere of Influence Radius and Coverage Area Percentage (Weight Factors=1)

r_1	r_2	r_3	r_4	r_5	r_6	r_7	CA%
0.4976	0.4923	0.3905	0.4888	0.4546	0.4867	0.4274	56.8378

5.4.7.2 Effect of Importance of Pollutants

Table 5.37 shows the influence of increasing the weight factor of nitrogen oxide from 10 to 10,000 for the Seven Station Model on the locations for the monitoring stations. We notice from this table that the first location undergoes a negative change in the (x)

and (y) directions. Locations two and three undergo negative changes in the (x) direction and positive ones in the (y) direction. The fourth, fifth and sixth locations show a positive changes in the (x) direction and negative changes in the (y) direction. The seventh location show positive change in both the (x) and (y) directions.

Table 5.38 shows the changes in the sphere of influence radius and the coverage area percentage as we increased the weight factor for NOx from 10 to 10,000. It can be noticed that the coverage area percentage decrease by 1.85% in this case.

Table 5.37 Influence of Changing the Weight Factor of Nitrogen Oxide (NOx) on the Location Estimates

Weight Factor	$(x,y)_1$	$(x,y)_2$	$(x,y)_3$	$(x,y)_4$	$(x,y)_5$	$(x,y)_6$	$(x,y)_7$
10	(4.0259, 0.4960)	(5.9053, 0.4353)	(6.7158, 0.4401)	(3.0331, 0.4969)	(2.0755, 0.4613)	(5.0089, 0.4871)	(1.5499, 0.4543)
100	(1.8227, 0.4534)	(2.7671, 0.4917)	(7.3974, 0.4410)	(4.7439, 0.4889)	(3.7569, 0.4981)	(5.7194, 0.4866)	(6.5941, 0.4474)
1000	(1.8499, 0.4543)	(5.7482, 0.4867)	(4.7728, 0.4887)	(6.6220, 0.4485)	(2.7959, 0.4924)	(3.7862, 0.4979)	(7.4202, 0.4446)
10000	(2.1733, 0.4645)	(5.1099, 0.4866)	(6.0012, 0.4400)	(4.1284, 0.4950)	(3.1353, 0.4981)	(6.7892, 0.4565)	(7.5480, 0.4695)

Table 5.38 Influence of Changing the Weight Factor of Nitrogen Oxide (NOx) on Sphere of Influence Radius and Coverage Area Percentage

Weight Factor	r_1	r_2	r_3	r_4	r_5	r_6	r_7	**CA%**
10	0.4994	0.4860	0.4919	0.4755	0.4867	0.4887	0.3880	54.564
100	0.4534	0.4917	0.4143	0.4889	0.4981	0.4866	0.3890	56.3347
1000	0.4543	0.4867	0.4887	0.3880	0.4924	0.4979	0.4102	56.2180
10000	0.4645	0.4866	0.4058	0.4950	0.4981	0.3824	0.3765	52.7184

Table 5.39 shows the influence of increasing the weight of sulfur dioxide on the stations locations. We see that the first and sixth locations undergo negative changes with respect to the (x) and (y) directions. The second and seventh locations undergo negative changes in (x) direction and positive changes in the (y) direction. The third and fourth locations undergo positive changes in the (x) direction and negative

changes in the (y) direction. Location five undergoes positive changes with respect to both the (x) and (y) directions.

Table 5.40 shows the influence of increasing the weight factor for SO_2 on the sphere of influence radius and coverage area percentage. The coverage area decreases by 2.16% as the weight factor increases from 10 to 10,000.

Table 5.39 Influence of Changing the Weight Factor of Sulfur Dioxide (SO_2) on the Stations Locations

Weight Factor	$(x,y)_1$	$(x,y)_2$	$(x,y)_3$	$(x,y)_4$	$(x,y)_5$	$(x,y)_6$	$(x,y)_7$
10	(2.7639, 0.4916)	(4.7408, 0.4890)	(6.5911, 0.4473)	(3.7537, 0.4982)	(1.8197, 0.4534)	(5.7163, 0.4866)	(7.3949, 0.4406)
100	(1.5611, 0.4456)	(4.4501, 0.4917)	(3.4591, 0.4994)	(5.4277, 0.4860)	(2.4831, 0.4769)	(6.3082, 0.4422)	(7.1106, 0.4412)
1000	(2.656, 0.4612)	(4.4561, 0.534)	(5.561, 0.4678)	(6.456, 0.4653)	(1.5789, 0.4563)	(3.675, 0.4545)	(7.564, 0.493)
10000	(1.8755, 0.4550)	(3.8137, 0.4977)	(7.3240, 0.4408)	(4.7999, 0.4885)	(2.8229, 0.4931)	(5.7087, 0.4324)	(6.5209, 0.4462)

Table 5.40 Influence of Changing the Weight Factor of Sulfur Dioxide (SO_2) on Sphere of Influence Radius and Coverage Area Percentage

Weight Factor	r_1	r_2	r_3	r_4	r_5	r_6	r_7	**CA%**
10	0.4916	0.4890	0.3891	0.4982	0.4534	0.4866	0.4148	56.3476
100	0.4456	0.4917	0.4994	0.4860	0.4769	0.3955	0.4070	55.6211
1000	0.4456	0.4887	0.4991	0.4860	0.4691	0.3901	0.4020	55.123
10000	0.4550	0.4977	0.4127	0.4885	0.4931	0.4220	0.3903	54.1879

Table 5.41 shows the influence of increasing the weight factor of carbon monoxide on monitoring stations locations with the Seven Station Model. We notice that location one and seven have negative changes in the (x) and (y) directions. Location two show a negative change in the (x) direction and a positive changes with respect to the (y) direction. The third and fourth location show positive changes in the (x) direction and

negative in the (y) direction. The fifth and sixth locations show positive changes in both the (x) and (y) directions.

Table 5.42 shows the influence of changing the weight factor of CO on the sphere of influence radius and coverage area percentage. The coverage area increase by 5.17% as we increase the weight factor from 10 to 10,000.

Table 5.41 Influence of Changing the Weight Factor of Carbon Monoxide (CO) on the Station Locations

Weight Factor	$(x,y)_1$	$(x,y)_2$	$(x,y)_3$	$(x,y)_4$	$(x,y)_5$	$(x,y)_6$	$(x,y)_7$
10	(4.6516, 0.4897)	(7.2004, 0.4410)	(6.3980, 0.4439)	(3.6632, 0.4987)	(2.6753, 0.4892)	(5.5722, 0.4327)	(9.6486, 0.8257)
100	(2.8230, 0.4931)	(1.8756, 0.4550)	(6.5210, 0.4462)	(4.8000, 0.4885)	(3.8138, 0.4977)	(5.7087, 0.4324)	(7.3241, 0.4408)
1000	(4.6515, 0.4897)	(2.6752, 0.4892)	(8.1787, 0.4376)	(5.5722, 0.4327)	(3.6631, 0.4987)	(6.4922, 0.4891)	(7.3626, 0.4623)
10000	(1.8259, 0.4535)	(4.7473, 0.4889)	(7.4051, 0.4382)	(3.7603, 0.4981)	(2.7704, 0.4918)	(5.7228, 0.4866)	(6.5978, 0.4471)

Table 5.42 Influence of Changing the Weight Factor of Carbon Monoxide (CO) on Sphere of Influence Radius and Coverage Area Percentage

Weight Factor	r_1	r_2	r_3	r_4	r_5	r_6	r_7	**CA%**
10	0.4897	0.4093	0.3931	0.4987	0.4892	0.4327	0.3514	51.2951
100	0.4931	0.4550	0.3903	0.4885	0.4977	0.4220	0.4128	54.1888
1000	0.4897	0.4892	0.4348	0.4327	0.4987	0.4891	0.3817	56.1346
10000	0.4535	0.4889	0.4181	0.4981	0.4918	0.4866	0.3893	56.4664

It is observed from the proposed models as we have moved from the one station to the seven station model the coverage area percentage increases from 9.2345% to 56.8378%. The model could be extended to include as many monitoring stations as required to meet our objectives.

Figure 5.6 shows the effect of increasing the number of stations on the coverage area. As is expected, as we increase the number of stations the coverage area increases. This of course comes at the expense of increased cost.

We have examined the effect of different weighting pattern score, violation score and the pollutant weight on the performance of the optimization method for the AQMN design. We notice that the coverage area showed only minor changes as we increased the weighting factors for the seven models described earlier independently. By knowing that each scenario had slight changes in the coverage area and location as we increase the weight factors we can say that the developed model in this work is providing us with accurate predictions for the monitoring station locations and their coverage area.

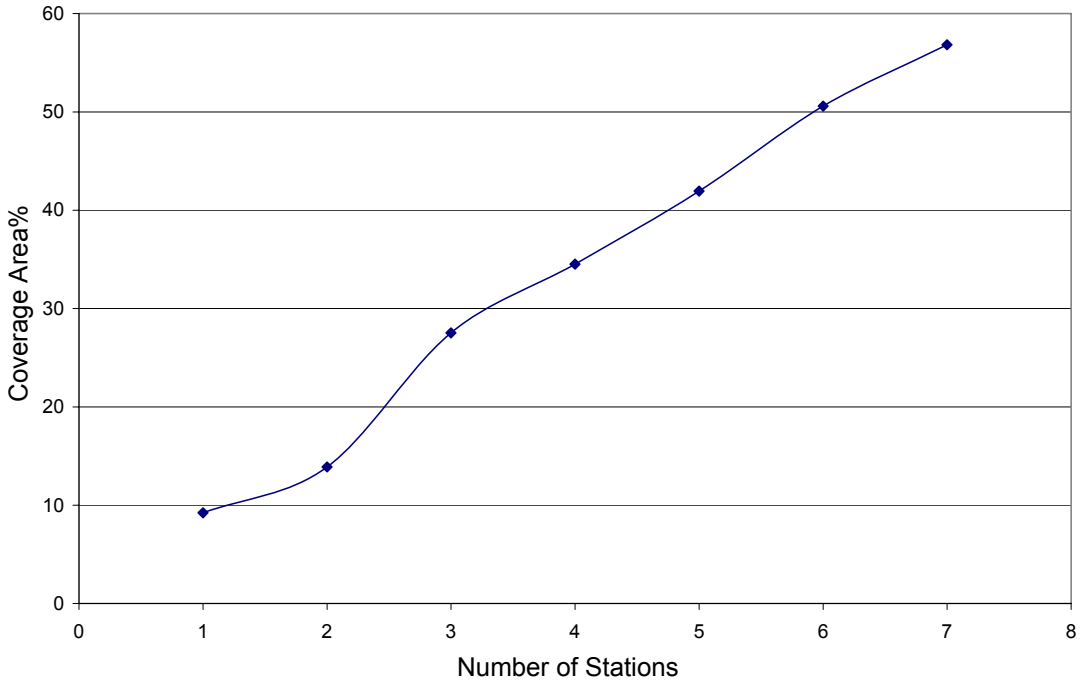

Figure 5.6 Effect of Increasing Number of Stations on the Coverage Area

Chapter 6- Conclusions

In this work we have described optimization models for identifying and determining the optimal location and configuration of Air Quality Monitoring Networks in an industrial area for different pollutants such as sulfur dioxide (SO_2), nitrogen oxide (NOx), and carbon monoxide (CO).

A mathematical model based on Multiple Cell Approach (MCA) was used to provide an air quality data base for monthly spatial distributions for the concentrations of the pollutants (CO, NO_x, and SO2) emitted from Tabriz refinery stacks. The output of the Multiple Cell model was used to measure the AQMN objectives in an industrial area.

One of the major problems related to the AQMN design is the definition of the spacing between the monitoring locations; such definition must be capable of identifying and predicting the parameters of AQMN design criteria. For this purpose ANN models were developed in order to model the scores *Np* and *Nv* as a function of spatial coordinates (x,y). Neural network models of one hidden layer of 7-9 neurons were developed and a back propagation algorithm was used to train the networks. The ANN model output gave very good predictions for both the training data set and testing data set. The ANN models were found to be better than linear regression and non-linear regression models and presented important results on their computational capabilities.

A multiple objective design criteria for multi pollutants were incorporated in a weighted utility function consisting of *Np* and *Nv*. An optimization model with appropriate constraints for maximizing the predicting ability of the spatial and temporal patterns of the concentration field and maximizing the ability of detection of violations over legal standards while minimizing overlaps between the effective areas of the monitoring stations was developed.

The presented optimization model can be used for as many stations as required. As we increased the number of stations the coverage area increased. The optimization models were successfully used in order to locate air quality monitoring stations.

Recommendations for future work:

- Extend the research work to consider different cutoff correlation coefficient in spatial analysis to determine the effective area of the monitoring stations for the optimum siting of ambient air monitors.

- Consider different structure of the utility function that combines the AQMN two objectives. Several forms of UF could be attempted as of interest to maintain the optimization models.

- Consider different types of pollutants (reactive pollutants such as ozone and hydrocarbons) in the optimization procedures.

- Expand the research work with a decision support system (DSS) to manage and evaluate the optimization technique for monitoring locations

References

Arbeloa, F. J. Seron; Caseirs, C.Perez; Andres, M.Latorre, 1993, Air Quality Monitoring: Optimization of a Network Around a Hypothetical Potash Plant in Open Countryside, Atmospheric Environment, 27A, No. 5, 729-738.

Baldauf, Richard W.; Lane, Dennis D.; Marote, Glen A., 2001, Ambient Air Quality Monitoring Networking Design for Assessing Human Health Impacts from Exposures to Airborne Contaminants, Environmental Monitoring and Assessment, 66, 63–76.

Baughman, D.R.; Liu, Y.A., 1995. Neural Networks in Bioprocessing and Chemical Engineering. Academic Press.

Beychok, M. R. ,1995, Fundamentals of Stack Gas Dispersion, Milton R. Beychok, Third Edition.

Bordignon, Silvano; Scaglirini, Michele, 2000, Monitoring Algorithms for Detecting Changes in the Ozone Concentrations, Environmetrics, 11, 125-137.

Bretschneider, B.; Kurfurst, J. 1987, Fundamental Aspects of Pollution and Environmental Science 8: Air Pollution Control Technology, Elsevier.

Cheremisinoff, N., 2002, Handbook of Air Pollution Prevention and Control, Elsevier science.

Cooper, C.; Alley, F., 2002, Air Pollution Control: A Design Approach, Third Edition, Waveland Press, Inc

Demerjian, Kenneth L., 2000, A Review of National Monitoring Networks in North America, Atmospheric Environment, 34, 1861-1884.

Elkamel, A.; Abdul-Wahab, S.; Bohamra, W.; Alper, A., 2001. Measurement and prediction of ozone levels around a heavily industrised area: a neural network approach. Advances in Environmental Research, 5, 47-59

Elkamel, A.; Fatehifar, E.; Taheri, M.; Al-Rashidi, M.S.; Lohi, A., 2007.A heuristic optimization approach for Air Quality Monitoring Network design with the simultaneous consideration of multiple pollutants. Journal of Environmental Management.

Ezekiel M., 1941, Methods of Correlation Analysis, John Wiley and Sons, London.

Fatehifar, E., 2006a, Development of an Optimal Design of a Multi-Pollutant Air Quality Monitoring Network, Ph.D.Thesis, Shiraz University.

Fatehifar, E., 2006b, Personal Communication.

Godish, T., 2004, Air Quality, Fourth Edition, CRC Press LLC.

Hassoun, M.H., 1995, Fundamentals of Artificial Neural Networks, The MIT Press.

Heinsohn, R. J.; Kabel, R. L., 1999, Sources and Control of Air Pollution, Printice Hall.

Ibarra-Berastegi, G., 2006, Short-term prediction of air pollution levels using neural networks, WIT Transactions on Ecology and the Environment, Air Pollution XIV, Vol 86, 23-31.

Liu, M. K.; Avrin, J., 1981, Methodology for designing an optimal air quality monitoring network, EPA-600/4-81-002, U.S. Environmental Protection Agency, Las Vegas, Nevada.

Liu, M. K.; Avrin, J.; Pollack, R. I.; Behar, J. V.; McElroy, J. L., 1986, Methodology for Designing Air Quality Monitoring Networks: I. Theoretical Aspects, Environmental Monitoring and Assessment, 6, 1-11.

Mehdizadeh, F.; Rifai, H. S., 2003, Modelling Point Source Plumes at High Altitudes Using a Modified Gaussian Model, Atmospheric Environment, 38, pp. 821-831.

Modak, P. M.; Lohani, B. N., 1985a, Optimization of ambient air quality monitoring networks: PartI, Environmental Monitoring and Assessment, 5, 1.

Modak, P. M.; Lohani, B. N., 1985b, Optimization of ambient air quality monitoring networks: Part II, Environmental Monitoring and Assessment, 5, 21.

Modak, P. M.; Lohani, B. N., 1985c, Optimization of ambient air quality monitoring networks: Part III, Environmental Monitoring and Assessment 5, 39.

Ott, W. J., 1977, Development of Criteria for Siting Air Monitoring Stations, Journal of the Air Pollution Control Association, 27, 543-547.

Parks, R.W.; Levine, D.S.; Long, D.L., 1998, Fundamentals of Neural Network Modeling, The MIT Press.

Peavy, H. S., 1985, Environmental Engineering, McGraw-Hill, Inc.

Peterson, David L., 2000, Monitoring Air Quality in Mountains: Designing an Effective Network, Environmental Monitoring and Assessment, 64, 81–91.

Pittau, Maria Grazia; Romano, Daniela; Cirillo, Marco C.; Coppi, Renato, 1999, An Optimal Design for Air Pollution Monitoring Network, Environmetrics, 10, 351-360.

Ragland, K. W., 1973, Multiple Box Model for Dispersion of Air Pollutants from Area Sources, Atmospheric Environment, 7, pp. 1017-1032.

Seigneur, C. March, 1992, Understand the Basics of Air Quality Modeling, Chemical Engineering Progress.

Shamsijey, M., 2004, Simulation of Pollutant Emitted from Cement Factory Over the City of Shiraz, M. Sc. Thesis, Shiraz University, Shiraz, Iran.

Shindo, Junko; O, Ko; Matsumoto, Yukio, 1989, Considerations on Air Pollution Monitoring Network Design in the Light of Spatio-Temporal Variations of Data, Air Pollution Monitoring Design, 335-342.

Silvaa, Claudio; Quirozb, Alexis, 2003, Optimization of the Atmospheric Pollution Monitoring Network at Santiago de Chile, Atmospheric Environment, 37, 2337–2345.

Stern, A.; Boubel, R.; Turner, D.; Fox, D., 1984, Fundamentals of Air Pollution, Second Edition, Academic Press, Inc.

Wark, K.; Warner, C.; Davis, W., 1998, Air Pollution: Its Origin and Control, Third Edition, Addison Wesley Longman, Inc.

Appendix

Results for one station:

Table 1. Influence of Changing Pattern Score Weight (ww)

w	ww	N_p	N_v
1	1	250.6613 151.8111 143.1888	8849.5 1.2171e9 256.01
1	10	250.6617 151.8110 143.1886	8849.5 1.2171e9 256.01
1	100	250.6652 151.8104 143.1871	8849.4 1.2171e9 256.01
1	1000	250.7014 151.8043 143.1723	8848.7 1.2171e9 256
1	10000	251.0640 151.7427 143.0233	8841.5 1.2171e9 255.89

Table 2. Influence of Changing Violation Score Weight (w)

w	ww	N_p	N_v
10	1	250.6613 151.8111 143.1888	8849.5 1.2171e+009 256.01
100	1	250.6612 151.8111 143.1888	8849.5 1.2171e+009 256.01
1000	1	250.6612 151.8111 143.1888	8849.5 1.2171e+009 256.01
10000	1	238.3608 153.6316 151.2222	9107.7 1.2186e+009 261.4

Table 3. Influence of Changing the Weight Factor of Nitrogen Oxide (NOx)

Weight Factor	N_p	N_v
10	250.6451 151.8138 143.1954	8849.8 1.2171e+009 256.01
100	250.4827 151.8411 143.2624	8853 1.2171e+009 256.06
1000	248.8776 152.1047 143.9313	8885 1.2171e+009 256.51
10000	234.2815 153.9391 150.6446	9182.5 1.2155e+009 260.69

Table 4. Influence of Changing the Weight Factor of Sulfur Dioxide (SO_2)

Weight Factor	N_p	N_v
10	250.6630 151.8108 143.1881	8849.4 1.2171e+009 256.01
100	250.6631 151.8107 143.1880	8849.4 1.2171e+009 256.01
1000	250.6632 151.8107 143.1880	8849.4 1.2171e+009 256.01
10000	250.6568 151.8118 143.1906	8849.6 1.2171e+009 256.01

Table 5. Influence of Changing the Weight Factor of Carbon Monoxide (CO).

Weight Factor	N_P	N_V
10	250.6607 151.8112 143.1890	8849.5 1.2171e+009 256.01
100	250.6548 151.8122 143.1915	8849.6 1.2171e+009 256.01
1000	250.5949 151.8222 143.2161	8850.8 1.2171e+009 256.03
10000	249.9978 151.9220 143.4631	8862.7 1.2171e+009 256.2

Results for two stations:

Table 6. Influence of Changing Pattern Score Weight (ww)

w	ww	Pollutants	N_{P1}	N_{P2}	N_{V1}	N_{V2}
1	1	NOx SO2 CO	92.301 55.946 150.44	250.66 151.81 143.19	10442 2.7683e+008 1.3285	8849.5 1.2171e+009 256.01
1	10	NOx SO2 CO	92.301 55.945 150.44	250.66 151.81 143.19	10442 2.7683e+008 1.3285	8849.5 1.2171e+009 256.01
1	100	NOx SO2 CO	92.301 55.945 150.45	92.301 55.945 150.45	10442 2.7683e+008 1.3285	8849.4 1.2171e+009 256.01
1	1000	NOx SO2 CO	92.3 55.938 150.46	250.7 151.8 143.17	10442 2.7683e+008 1.3287	8848.7 1.2171e+009 256
1	10000	NOx SO2 CO	92.292 55.871 150.6	251.06 151.74 143.02	10445 2.7683e+008 1.3299	8841.5 1.2171e+009 255.89

Table 7. Influence of Changing Violation Score Weight (w)

w	ww	Pollutants	N_{P1}	N_{P2}	N_{V1}	N_{V2}
10	1	NOx	92.301	250.66	10442	8849.5
		SO2	55.946	151.81	2.7683e+008	1.2171e+009
		CO	150.44	143.19	1.3285	256.01
100	1	NOx	92.301	250.66	10442	8849.5
		SO2	55.946	151.81	2.7683e+008	1.2171e+009
		CO	150.44	143.19	1.3285	256.01
1000	1	NOx	92.301	250.66	10442	8849.5
		SO2	55.946	151.81	2.7683e+008	1.2171e+009
		CO	150.44	143.19	1.3285	256.01
10000	1	NOx	92.301	250.66	10442	8849.5
		SO2	55.946	151.81	2.7683e+008	1.2171e+009
		CO	150.44	143.19	1.3285	256.01

Table 8. Influence of Changing the Weight Factor of Nitrogen Oxide (NOx)

Weight Factor	Pollutants	N_{P1}	N_{P2}	N_{V1}	N_{V2}
10	NOx	92.301	250.65	10442	8849.8
	SO2	55.943	151.81	2.7683e+008	1.2171e+009
	CO	150.45	143.2	1.3286	256.01
100	NOx	92.298	250.48	10443	8853
	SO2	55.916	151.84	2.7683e+008	1.2171e+009
	CO	150.51	143.26	1.329	256.06
1000	NOx	207.32	304.67	9780.9	7811.9
	SO2	154.68	136.77	1.2041e+009	1.2055e+009
	CO	166.55	126.77	268.38	241.18
10000	NOx	194.5	282.43	10104	8235.6
	SO2	154.05	144.28	1.1932e+009	1.2126e+009
	CO	175.99	132.3	271.64	247.25

Table 9. Influence of Changing the Weight Factor of Sulfur Dioxide (SO_2)

Weight Factor	**Pollutants**	N_{P1}	N_{P2}	N_{V1}	N_{V2}
10	NOx	92.301	250.66	10442	8849.4
	SO2	55.946	151.81	2.7683e+008	1.2171e+009
	CO	150.44	143.19	1.3285	256.01
100	NOx	92.301	250.66	10442	8849.4
	SO2	55.946	151.81	2.7683e+008	1.2171e+009
	CO	150.44	143.19	1.3285	256.01
1000	NOx	92.301	250.66	10442	8849.4
	SO2	55.946	151.81	2.7683e+008	1.2171e+009
	CO	150.44	143.19	1.3285	256.01
10000	NOx	92.301	250.66	10442	8849.4
	SO2	55.946	151.81	2.7683e+008	1.2171e+009
	CO	150.44	143.19	1.3285	256.01

Table 10. Influence of Changing the Weight Factor of Carbon Monoxide (CO)

Weigh Factor	**Pollutants**	N_{P1}	N_{P2}	N_{V1}	N_{V2}
10	NOx	92.301	250.66	10442	8849.5
	SO2	55.945	151.81	2.7683e+008	1.2171e+009
	CO	150.44	143.19	1.3285	256.01
100	NOx	92.301	250.65	10442	8849.6
	SO2	55.944	151.81	2.7683e+008	1.2171e+009
	CO	150.45	143.19	1.3286	256.01
1000	NOx	92.299	250.6	10442	8850.8
	SO2	55.93	151.82	2.7683e+008	1.2171e+009
	CO	150.48	143.22	1.3288	256.03
10000	NOx	92.282	250	10448	8862.7
	SO2	55.787	151.92	2.7683e+008	1.2171e+009
	CO	150.78	143.46	1.3314	256.2

Results for three stations:

Table 11. Three Station Model Output with no Consideration of Weight Factor

Pollutants	N_{P1}	N_{P2}	N_{P3}	N_{V1}	N_{V2}	N_{V3}
NOx	372.97	257.42	180.97	6290.2	8716.2	10496
SO2	103.93	150.57	153.07	1.1682e+009	1.2168e+009	1.1757e+009
CO	116.64	140.52	187.48	216.79	254.11	274.11

Table 12. Influence of Changing the Weight Factor of Nitrogen Oxide (NOx)

Weight Factor	Pollutants	N_{P1}	N_{P2}	N_{P3}	N_{V1}	N_{V2}	N_{V3}
10	NOx	307.37	204.72	208.93	7760	9232.6	9742.4
	SO2	135.76	151.4	154.73	1.2045e+009	1.1643e+009	1.2052e+009
	CO	126.19	78.315	165.45	240.42	332.37	267.93
100	NOx	307.12	208.79	204.71	7764.7	9745.9	9232.9
	SO2	135.85	154.72	151.4	1.2046e+009	1.2051e+009	1.1643e+009
	CO	126.24	165.55	78.33	240.49	267.98	332.37
1000	NOx	369.68	254.18	179.29	6384.3	8779.8	10551
	SO2	105.95	151.19	152.96	1.1707e+009	1.217e+009	1.173e+009
	CO	116.93	141.77	189.02	218.54	255.02	274.29
10000	NOx	234.28	203.91	138.22	9182.5	9251.2	12937
	SO2	153.94	151.39	165.81	1.2155e+009	1.1643e+009	1.0114e+009
	CO	150.64	79.394	226.39	260.69	332.32	237.38

Table 13. Influence of Changing the Weight Factor of Sulfur Dioxide (SO_2)

Weight Factor	Pollutants	N_{P1}	N_{P2}	N_{P3}	N_{V1}	N_{V2}	N_{V3}
10	NOx	307.4	208.95	204.72	7759.4	9742	9232.6
	SO2	135.75	154.73	151.4	1.2045e+009	1.2052e+009	1.1643e+009
	CO	126.18	165.44	78.313	240.42	267.93	332.37
100	NOx	372.97	257.42	180.97	6290.1	8716.2	10496
	SO2	103.93	150.57	153.07	1.1682e+009	1.2168e+009	1.1757e+009
	CO	116.64	140.51	187.48	216.79	254.11	274.11
1000	NOx	250.66	204.71	150.45	8849.4	9232.9	10716
	SO2	151.81	151.4	168.15	1.2171e+009	1.1643e+009	1.0556e+009
	CO	143.19	78.331	59.995	256.01	332.37	337.33
10000	NOx	307.4	208.95	204.72	7759.4	9742	9232.6
	SO2	135.75	154.73	151.4	1.2045e+009	1.2052e+009	1.1643e+009
	CO	126.18	165.44	78.313	240.42	267.93	332.37

Table 14. Influence of Changing the Weight Factor of Carbon Monoxide (CO).

Weight Factor	Pollutants	N_{P1}	N_{P2}	N_{P3}	N_{V1}	N_{V2}	N_{V3}
10	NOx	307.39	208.95	204.72	7759.5	9742.1	9232.6
	SO2	135.75	154.73	151.4	1.2045e+9	1.2052e+009	1.1643e+009
	CO	126.18	165.44	78.313	240.42	267.93	332.37
100	NOx	372.96	257.41	180.97	6290.5	8716.4	10496
	SO2	103.94	150.57	153.07	1.1682e+009	1.2168e+009	1.1757e+009
	CO	116.64	140.52	187.48	216.79	254.12	274.11
1000	NOx	307.3	208.89	204.72	7761.2	9743.4	9232.7
	SO2	135.78	154.73	151.4	1.2045e+009	1.2052e+009	1.1643e+009
	CO	126.2	165.48	78.323	240.44	267.95	332.37
10000	NOx	372.02	256.47	180.47	6317.9	8735	10512
	SO2	104.52	150.75	153.04	1.169e+009	1.2169e+009	1.1749e+009
	CO	116.72	140.88	187.93	217.31	254.38	274.17

Results for four stations:

Table 15. Four Station Model Output with no Consideration of Weight Factor

Pollutants	N_{P1}	N_{P2}	N_{P3}	N_{P4}	N_{V1}	N_{V2}	N_{V3}	N_{V4}
NOx	307.39	208.95	138.23	204.72	7759.5	9742.1	12936	9232.6
SO2	135.75	154.73	165.8	151.4	1.2045e9	1.2052e9	1.0115e9	1.1643e9
CO	126.18	165.44	226.4	78.315	240.42	267.93	237.39	332.37

Table 16. Influence of Changing the Weight Factor of Nitrogen Oxide (NOx)

Weight Factor	Pollutants	N_{P1}	N_{P2}	N_{P3}	N_{P4}
10	NOx	381.36	381.36	381.36	330.52
	SO2	66.755	66.755	66.755	126.16
	CO	120.08	120.08	120.08	121.89
100	NOx	302.25	205.88	206.19	402.53
	SO2	137.67	154.64	151.47	79.36
	CO	127.3	167.54	76.138	115.06
1000	NOx	402.5	205.84	206.3	302.18
	SO2	79.392	154.64	151.47	137.69
	CO	115.06	167.57	75.97	127.32
10000	NOx	388.39	190.71	176.96	275.59
	SO2	93.165	153.79	154.91	146.24
	CO	115.53	179.04	76.706	134.31

Table 17. Influence of Changing the Weight Factor of Nitrogen Oxide (NOx)

Weight Factor	Pollutants	N_{V1}	N_{V2}	N_{V3}	N_{V4}
10	NOx	4121.3	9411.1	11127	7300.6
	SO2	1.1265e+009	1.2125e+009	1.1406e+009	1.1942e+009
	CO	158.4	263.79	273.34	233.65
100	NOx	7858.4	9815.4	9196.9	5026.8
	SO2	1.2064e+009	1.2031e+009	1.1641e+009	1.1345e+009
	CO	241.85	268.77	332.52	187.72
1000	NOx	5028.6	9816.4	9194.3	7859.6
	SO2	1.1346e+009	1.2031e+009	1.164e+009	1.2064e+009
	CO	187.77	268.78	332.54	241.86
10000	NOx	5770.2	10207	9838.3	8365.8
	SO2	1.1547e+009	1.189e+009	1.1356e+009	1.2142e+009
	CO	206.18	272.47	334.83	249.11

Table 18. Influence of Changing the Weight Factor of Sulfur Dioxide (SO_2)

Weight Factor	Pollutants	N_{P1}	N_{P2}	N_{P3}	N_{P4}
10	NOx	330.53	223.56	164.3	381.36
	SO2	126.16	154.63	152.54	66.752
	CO	121.88	156.38	203.97	120.08
100	NOx	381.36	223.56	164.3	330.53
	SO2	66.752	154.63	152.54	126.16
	CO	120.08	156.38	203.97	121.88
1000	NOx	381.36	223.56	164.3	330.53
	SO2	66.752	154.63	152.54	126.16
	CO	120.08	156.38	203.97	121.88
10000	NOx	381.36	223.56	164.3	330.53
	SO2	66.752	154.63	152.54	126.16
	CO	120.08	156.38	203.97	121.88

Table 19. Influence of Changing the Weight Factor of Sulfur Dioxide (SO_2)

Weight Factor	Pollutants	N_{V1}	N_{V2}	N_{V3}	N_{V4}
10	NOx	7300.5	9411	11127	4121.2
	SO2	1.1942e+009	1.2125e+009	1.1406e+009	1.1265e+009
	CO	233.65	263.79	273.34	158.39
100	NOx	4121.2	9411	11127	7300.5
	SO2	1.1265e+009	1.2125e+009	1.1406e+009	1.1942e+009
	CO	158.39	263.79	273.34	233.65
1000	NOx	4121.2	9411	11127	7300.5
	SO2	1.1265e+009	1.2125e+009	1.1406e+009	1.1942e+009
	CO	158.39	263.79	273.34	233.65
10000	NOx	4121.2	9411	11127	7300.5
	SO2	1.1265e+009	1.2125e+009	1.1406e+009	1.1942e+009
	CO	158.39	263.79	273.34	233.65

Table 20. Influence of Changing the Weight Factor of Carbon Monoxide (CO)

Weight Factor	Pollutants	N_{P1}	N_{P2}	N_{P3}	N_{P4}
10	NOx	381.36	223.56	164.3	330.53
	SO2	66.753	154.63	152.54	126.16
	CO	120.08	156.38	203.97	121.88
100	NOx	381.36	223.56	164.3	330.53
	SO2	66.753	154.63	152.54	126.16
	CO	120.08	156.38	203.97	121.88
1000	NOx	381.37	223.55	164.3	330.51
	SO2	66.759	154.63	152.54	126.17
	CO	120.08	156.38	203.98	121.89
10000	NOx	330.38	164.26	223.46	381.47
	SO2	126.22	152.54	154.64	66.811
	CO	121.91	204.02	156.43	120.05

Table 21. Influence of Changing the Weight Factor of Carbon Monoxide (CO)

Weight Factor	Pollutants	N_{V1}	N_{V2}	N_{V3}	N_{V4}
10	NOx	4121.2	9411	11127	7300.5
	SO2	1.1265e9	1.2125e9	1.1406e9	1.1942e9
	CO	158.39	263.79	273.34	233.65
100	NOx	4121.2	9411	11127	7300.5
	SO2	1.1265e9	1.2125e9	1.1406e9	1.1942e9
	CO	158.39	263.79	273.34	233.65
1000	NOx	4121.6	9411.2	11127	7300.8
	SO2	1.1265e9	1.2125e9	1.1406e9	1.1942e9
	CO	158.41	263.79	273.34	233.65
10000	NOx	7303.4	11129	9413.1	4125.6
	SO2	1.1942e9	1.1405e9	1.2125e9	1.1266e9
	CO	233.69	273.33	263.81	158.55

Results for five stations:

Table 22. Five Station Model Output with no Consideration of Weight Factor

Pollutants	N_{P1}	N_{P2}	N_{P3}	N_{P4}	N_{P5}
NOx	379.11	236.86	160.67	349.26	170.58
SO2	59.797	153.69	162.67	117.23	152.52
CO	121.14	149.37	62.252	119.18	197.45

Pollutants	N_{V1}	N_{V2}	N_{V3}	N_{V4}	N_{V5}
NOx	3602.9	9128.8	10233	6895.9	10861
SO2	1.105e9	1.216e9	1.0897e9	1.184e9	1.1563e9
CO	139.3	259.94	339.21	227.33	274.46

Table 23. Influence of Changing the Weight Factor of Nitrogen Oxide (NOx)

Weight Factor	Pollutants	N_{P1}	N_{P2}	N_{P3}	N_{P4}	N_{P5}
10	NOx	330.52	381.36	92.301	164.3	223.55
	SO2	126.16	66.755	55.943	152.54	154.63
	CO	121.89	120.08	150.45	203.98	156.38
100	NOx	402.67	206.13	205.19	302.66	138.23
	SO2	79.165	154.65	151.41	137.51	165.81
	CO	115.06	167.37	77.664	127.21	226.4
1000	NOx	411.67	223.13	245.19	334.66	128.23
	SO2	75.161	184.65	131.42	127.51	175.81
	CO	135.06	187.37	73.661	177.21	236.4
10000	NOx	380.96	223.95	149.95	331.12	164.48
	SO2	66.513	154.62	164.68	125.89	152.53
	CO	120.18	156.15	57.733	121.79	203.78

Table 24. Influence of Changing the Weight Factor of Nitrogen Oxide (NOx)

Weight Factor	Pollutants	N_{V1}	N_{V2}	N_{V3}	N_{V4}	N_{V5}
10	NOx	7300.6	4121.3	10442	11127	9411.1
	SO2	1.1942e9	1.1265e9	2.7683e8	1.1406e9	1.2125e9
	CO	233.65	158.4	1.3286	273.34	263.79
100	NOx	5015.4	9809.5	9221.6	7850.4	12936
	SO2	1.1342e9	1.2033e9	1.1643e9	1.2063e9	1.0115e9
	CO	187.4	268.7	332.41	241.73	237.38
1000	NOx	4315.4	9509.5	9431.6	7980.4	19836
	SO2	1.1342e9	1.2033e9	1.1643e9	1.2063e9	1.0115e9
	CO	197.4	278.7	342.52	2341.73	297.38
10000	NOx	4103.1	9402.4	10940	7288.2	11119
	SO2	1.1262e+009	1.2127e+009	1.0689e+009	1.1939e+009	1.1411e+009
	CO	157.74	263.67	330.73	233.46	273.39

Table 25. Influence of Changing the Weight Factor of Sulfur Dioxide (SO_2)

Weight Factor	Pollutants	N_{P1}	N_{P2}	N_{P3}	N_{P4}	N_{P5}
10	NOx	379.11	235.49	142.44	347.44	169.91
	SO2	60.427	153.83	161.12	118.15	152.5
	CO	121.1	150.04	225.76	119.42	198.13
100	NOx	379.11	236.87	170.58	349.26	160.67
	SO2	59.796	153.69	152.52	117.22	162.67
	CO	121.14	149.37	197.45	119.18	62.254
1000	NOx	379.11	349.26	160.67	170.58	236.87
	SO2	59.796	117.22	162.67	152.52	153.69
	CO	121.14	119.18	62.254	197.45	149.37
10000	NOx	381.36	223.56	92.301	330.53	164.3
	SO2	66.752	154.63	55.946	126.16	152.54
	CO	120.08	156.38	150.44	121.88	203.97

Table 26. Influence of Changing the Weight Factor of Sulfur Dioxide (SO_2)

Weight Factor	Pollutants	N_{V1}	N_{V2}	N_{V3}	N_{V4}	N_{V5}
10	NOx	3652.2	9157.4	12579	6937.3	10888
	SO2	1.1076e+009	1.2158e+009	1.0406e+009	1.1851e+009	1.1548e+009
	CO	141.17	260.34	247.16	228	274.4
100	NOx	3602.8	9128.8	10861	6895.8	10233
	SO2	1.105e+009	1.216e+009	1.1563e+009	1.184e+009	1.0897e+009
	CO	139.3	259.94	274.46	227.33	339.21
1000	NOx	3602.8	6895.8	10233	10861	9128.8
	SO2	1.105e+009	1.184e+009	1.0897e+009	1.1563e+009	1.216e+009
	CO	139.3	227.33	339.21	274.46	259.94
10000	NOx	4121.2	9411	10442	7300.5	11127
	SO2	1.1265e+009	1.2125e+009	2.7683e+008	1.1942e+009	1.1406e+009
	CO	158.39	263.79	1.3285	233.65	273.34

Table 27. Influence of Changing the Weight Factor of Carbon Monoxide (CO)

Weight Factor	Pollutants	N_{P1}	N_{P2}	N_{P3}	N_{P4}	N_{P5}
10	NOx	347.43	235.48	142.44	379.11	169.91
	SO2	118.15	153.83	161.12	60.428	152.5
	CO	119.42	150.05	225.76	121.1	198.13
100	NOx	235.48	169.91	379.11	347.43	142.44
	SO2	153.83	152.5	60.43	118.15	161.12
	CO	150.05	198.13	121.1	119.42	225.76
1000	NOx	206.13	302.68	205.13	402.68	150.48
	SO2	154.65	137.51	151.41	79.158	168.16
	CO	167.37	127.21	77.743	115.06	60.085
10000	NOx	379.11	234.97	142.34	346.74	169.66
	SO2	60.67	153.88	161.22	118.49	152.5
	CO	121.08	150.3	225.81	119.51	198.38

Table 28. Influence of Changing the Weight Factor of Carbon Monoxide (CO)

Weight Factor	Pollutants	N_{V1}	N_{V2}	N_{V3}	N_{V4}	N_{V5}
10	NOx	6937.3	9157.4	12579	3652.3	10888
	SO2	1.1851e+009	1.2158e+009	1.0406e+009	1.1076e+009	1.1547e+009
	CO	228	260.34	247.16	141.18	274.4
100	NOx	9157.5	10888	3652.5	6937.5	12580
	SO2	1.2158e+009	1.1547e+009	1.1076e+009	1.1851e+009	1.0406e+009
	CO	260.34	274.4	141.18	228	247.16
1000	NOx	9809.3	7850.2	9223	5015	10714
	SO2	1.2033e+009	1.2062e+009	1.1643e+009	1.1342e+009	1.0556e+009
	CO	268.7	241.73	332.4	187.39	337.37
10000	NOx	3671.1	9168.2	12588	6953	10898
	SO2	1.1085e+009	1.2157e+009	1.0399e+009	1.1855e+009	1.1542e+009
	CO	141.89	260.49	246.92	228.25	274.38

Results for six stations:

Table 29. Six Station Model Output with no Consideration of Weight Factor

Pollutants	N_{P1}	N_{P2}	N_{P3}	N_{P4}	N_{P5}	N_{P6}
NOx	184.11	378.58	148.01	377.32	263.36	140.84
SO2	153.3	100.29	156.71	50.798	149.3	176.46
CO	184.67	116.18	221.46	121.09	138.34	64.32

Pollutants	N_{V1}	N_{V2}	N_{V3}	N_{V4}	N_{V5}	N_{V6}
NOx	10399	6118.8	12116	2769.6	8600.6	11410
SO2	1.1804e9	1.1638e9	1.075e9	1.0507e9	1.2163e9	9.9842e8
CO	273.68	213.47	258.81	105.66	252.46	328.34

Table 30. Influence of Changing the Weight Factor of Nitrogen Oxide (NOx)

Weight Factor	Pollutants	N_{P1}	N_{P2}	N_{P3}	N_{P4}	N_{P5}	N_{P6}
10	NOx	261.44	173.3	143.12	376.82	377.54	183.09
	SO2	149.73	157.47	174.13	101.46	51.279	153.22
	CO	139.03	65.483	61.281	116.32	121.15	185.57
100	NOx	178.08	247.79	137.6	378.85	362.51	144.43
	SO2	152.22	152.28	177.48	55.251	110.02	159.12
	CO	197.69	144.38	54.075	122.35	117.55	221.36
1000	NOx	375.71	182.46	139.8	260.25	377.67	147.38
	SO2	102.18	153.18	176.65	149.98	51.588	157.11
	CO	116.41	186.13	60.398	139.46	121.18	222.05
10000	NOx	379.11	169.42	142.24	132.91	234.47	346.08
	SO2	60.903	152.49	161.32	178.96	153.92	118.82
	CO	121.06	198.63	225.86	41.31	150.55	119.6

Table 31. Influence of Changing the Weight Factor of Nitrogen Oxide (NOx)

Weight Factor	Pollutants	N_{V1}	N_{V2}	N_{V3}	N_{V4}	N_{V5}	N_{V6}
10	NOx	8637.9	9865.9	11230	6174.1	2823.4	10430
	SO2	1.2165e9	1.121e9	1.0156e9	1.1652e9	1.0549e9	1.1789e9
	CO	253	337.59	331.52	214.56	107.95	273.84
100	NOx	10531	8906.7	11909	3209.9	6573.5	12468
	SO2	1.1731e9	1.217e9	9.8373e8	1.0861e9	1.1753e9	1.052e9
	CO	280.35	256.81	315.34	123.73	221.88	246.56
1000	NOx	6208.3	10449	11572	8661	2857.1	12166
	SO2	1.1661e9	1.178e9	9.9469e8	1.2166e9	1.0575e9	1.0714e9
	CO	215.23	273.92	324.71	253.32	109.37	257.67
10000	NOx	3688.9	10907	12597	12678	9178.5	6967.8
	SO2	1.1094e9	1.1536e9	1.0393e9	9.5899e8	1.2156e9	1.1859e9
	CO	142.56	274.35	246.69	283.65	260.63	228.49

Table 32. Influence of Changing the Weight Factor of Sulfur Dioxide (SO_2)

Weight Factor	Pollutants	N_{P1}	N_{P2}	N_{P3}	N_{P4}	N_{P5}	N_{P6}
10	NOx	261.47	377.53	143.13	376.85	183.1	173.33
	SO2	149.72	51.272	174.13	101.44	153.23	157.46
	CO	139.02	121.15	61.316	116.32	185.56	65.489
100	NOx	377.32	378.58	140.84	263.36	184.11	148.01
	SO2	50.797	100.29	176.46	149.3	153.3	156.71
	CO	121.09	116.18	64.324	138.34	184.67	221.46
1000	NOx	261.5	173.52	143.14	377.53	376.88	183.12
	SO2	149.71	157.47	174.13	51.263	101.42	153.23
	CO	139	65.476	61.366	121.15	116.31	185.54
10000	NOx	378.58	184.11	140.84	263.36	377.32	148.01
	SO2	100.29	153.3	176.46	149.3	50.797	156.71
	CO	116.18	184.67	64.324	138.34	121.09	221.46

Table 33. Influence of Changing the Weight Factor of Sulfur Dioxide (SO_2)

Weight Factor	Pollutants	N_{V1}	N_{V2}	N_{V3}	N_{V4}	N_{V5}	N_{V6}
10	NOx	8637.3	2822.6	11228	6173.3	10430	9865.2
	SO2	1.2165e9	1.0548e9	1.0156e9	1.1652e9	1.179e9	1.1211e9
	CO	252.99	107.91	331.55	214.55	273.83	337.59
100	NOx	2769.5	6118.7	11410	8600.6	10399	12116
	SO2	1.0507e9	1.1638e9	9.9842e8	1.2163e9	1.1804e9	1.075e9
	CO	105.66	213.47	328.35	252.46	273.68	258.81
1000	NOx	8636.7	9857.7	11226	2821.6	6172.3	10429
	SO2	1.2165e9	1.1211e9	1.0157e9	1.0548e9	1.1652e9	1.179e9
	CO	252.98	337.64	331.58	107.87	214.53	273.83
10000	NOx	6118.7	10399	11410	8600.6	2769.5	12116
	SO2	1.1638e9	1.1804e9	9.9842e8	1.2163e9	1.0507e9	1.075e9
	CO	213.47	273.68	328.35	252.46	105.66	258.81

Table 34. Influence of Changing the Weight Factor of Carbon Monoxide (CO)

Weight Factor	Pollutants	N_{P1}	N_{P2}	N_{P3}	N_{P4}	N_{P5}	N_{P6}
10	NOx	378.58	377.32	140.84	263.36	148.01	184.1
	SO2	100.3	50.798	176.46	149.3	156.71	153.3
	CO	116.18	121.09	64.323	138.34	221.46	184.67
100	NOx	263.35	377.32	184.1	378.57	148.01	140.84
	SO2	149.31	50.8	153.3	100.3	156.71	176.46
	CO	138.34	121.09	184.67	116.18	221.46	64.349
1000	NOx	377.33	184.07	140.86	263.29	378.51	147.99
	SO2	50.816	153.3	176.49	149.32	100.34	156.72
	CO	121.09	184.71	64.607	138.36	116.19	221.48
10000	NOx	377.9	183.71	141.08	377.4	262.61	147.86
	SO2	100.75	153.27	176.73	50.982	149.47	156.8
	CO	116.23	185.02	67.172	121.11	138.6	221.61

Table 35. Influence of Changing the Weight Factor of Carbon Monoxide (CO)

Weight Factor	Pollutants	N_{V1}	N_{V2}	N_{V3}	N_{V4}	N_{V5}	N_{V6}
10	NOx	6118.8	2769.6	11410	8600.7	12116	10399
	SO2	1.1638e9	1.0507e9	9.9842e8	1.2163e9	1.075e9	1.1804e9
	CO	213.48	105.66	328.34	252.46	258.81	273.68
100	NOx	8600.8	2769.8	10399	6119	12116	11410
	SO2	1.2163e9	1.0507e9	1.1804e9	1.1638e9	1.075e9	9.9841e8
	CO	252.47	105.67	273.68	213.48	258.8	328.36
1000	NOx	2771.7	10400	11404	8602.1	6120.9	12117
	SO2	1.0508e9	1.1804e9	9.9833e8	1.2163e9	1.1638e9	1.0749e9
	CO	105.75	273.69	328.47	252.48	213.52	258.78
10000	NOx	6140.2	10411	11348	2790.4	8615.1	12128
	SO2	1.1643e9	1.1799e9	9.9752e8	1.0523e9	1.2164e9	1.0741e9
	CO	213.9	273.74	329.53	106.55	252.67	258.54

Results for seven stations:

Table 36. Seven Station Model Output with no Consideration of Weight Factor

Pollutants	N_{P1}	N_{P2}	N_{P3}	N_{P4}	N_{P5}	N_{P6}	N_{P7}
NOx	286.2	394.77	142.97	196.98	373.96	152.96	134.22
SO2	143	87.187	172.12	154.17	46.495	154.4	183.51
CO	131.04	114.83	52.015	174.41	119.72	216.47	98.43

Pollutants	N_{V1}	N_{V2}	N_{V3}	N_{V4}	N_{V5}	N_{V6}	N_{V7}
NOx	8161.2	5474.7	11391	10037	2179.5	11755	11698
SO2	1.2111e9	1.14479	1.0243e9	1.1958e9	9.9708e8	1.1e9	9.2917e8
CO	246.05	199.32	326.92	271.32	79.541	266.02	313.8

Table 37. Influence of Changing the Weight Factor of Nitrogen Oxide (NOx)

Weight Factor	Pollutants	N_{P1}	N_{P2}	N_{P3}	N_{P4}	N_{P5}	N_{P6}	N_{P7}
10	NOx	261.5	173.52	143.14	377.53	376.88	183.12	163.65
	SO2	149.71	157.47	174.13	51.263	101.42	153.23	159.15
	CO	139	65.476	61.366	121.15	116.31	185.54	64.477
100	NOx	373.13	397.93	133.01	199.63	291.49	154.06	143.35
	SO2	45.962	84.641	182.8	154.36	141.42	154.04	171.2
	CO	119.08	115.13	81.345	172.06	129.87	215.17	50.68
1000	NOx	373.73	153.28	197.66	142.62	396.15	288.05	132
	SO2	46.364	154.29	154.25	171.66	86.414	142.54	182.87
	CO	119.44	216.02	173.54	49.786	115.19	130.77	76.556
10000	NOx	378.52	177.64	163.65	250.98	366.26	138.51	125.08
	SO2	54.328	152.85	159.15	151.76	107.98	174.13	183.11
	CO	121.32	190.56	64.477	143.06	117.26	45.077	42.574

Table 38. Influence of Changing the Weight Factor of Nitrogen Oxide (NOx)

Weight Factor	Pollutants	N_{V1}	N_{V2}	N_{V3}	N_{V4}	N_{V5}	N_{V6}	N_{V7}
10	NOx	8600.8	2769.8	10399	6119	12116	11410	11535
	SO2	1.2163e9	1.0507e9	1.1804e9	1.1638e9	1.075e9	9.9841e8	1.1014e9
	CO	252.47	105.67	273.68	213.48	258.8	328.36	286.27
100	NOx	2074.4	5324.4	12082	9970.4	8063.5	11684	11394
	SO2	9.8539e8	1.1428e9	9.343e8	1.1981e9	1.2101e9	1.1049e9	1.029e9
	CO	74.673	195.61	308.3	270.4	244.79	267.1	326.13
1000	NOx	2151.3	11735	10021	11478	5420.2	8128.9	12263
	SO2	9.9369e8	1.1014e9	1.1963e9	1.0252e9	1.1454e9	1.2111e9	9.3114e8
	CO	78.252	266.27	270.89	324.2	198.01	245.73	302.8
10000	NOx	3133.3	10605	10218	8843.1	6477.7	12039	13423
	SO2	1.0772e9	1.1702e9	1.1076e9	1.2171e9	1.1731e9	1.0013e9	9.0842e8
	CO	120.79	274.43	336.45	255.92	220.23	307.38	245.34

Table 39. Influence of Changing the Weight Factor of Sulfur Dioxide (SO_2)

Weight Factor	Pollutants	N_{P1}	N_{P2}	N_{P3}	N_{P4}	N_{P5}	N_{P6}	N_{P7}
10	NOx	398.12	199.84	143.44	291.87	373.06	154.15	133.12
	SO2	84.448	154.37	171.15	141.29	45.92	154.02	182.8
	CO	115.13	171.9	50.782	129.78	119.04	215.07	81.878
100	NOx	365.88	221.78	327.84	163.49	384.16	151.22	136.94
	SO2	43.959	154.69	127.35	152.57	67.862	165.67	179.97
	CO	113.71	157.4	122.33	204.84	119.45	56.201	70.666
1000	NOx	385.44	250. 3	261.5	173.52	143.14	377.53	398.12
	SO2	50.786	128.78	149.71	157.47	174.13	51.263	84.448
	CO	116.64	140.77	139	65.476	61.366	121.15	115.13
10000	NOx	374.26	284.86	134.07	195.86	394.37	192.12	145
	SO2	46.778	143.54	182.19	154.14	88.092	153.76	169.83
	CO	119.74	131.63	78.839	174.93	115.25	70.417	51.868

Table 40. Influence of Changing the Weight Factor of Sulfur Dioxide (SO_2)

Weight Factor	Pollutants	N_{V1}	N_{V2}	N_{V3}	N_{V4}	N_{V5}	N_{V6}	N_{V7}
10	NOx	5313.8	9964.8	11384	8056.3	2066	11678	12062
	SO2	1.1426e9	1.1983e9	1.0294e9	1.2099e9	9.8446e8	1.1052e9	9.3464e8
	CO	195.34	270.35	326.33	244.69	74.28	267.18	308.86
100	NOx	1389.2	9450	7355.4	11165	4208.4	10767	11760
	SO2	8.9636e8	1.2119e9	1.1955e9	1.1383e9	1.1275e9	1.0671e9	9.6731e8
	CO	40.547	264.3	234.47	273.08	161.52	335	319.81
1000	NOx	8600.8	2769.8	10399	6119	12116	11410	11394
	SO2	1.2163e9	1.0507e9	1.1804e9	1.1638e9	1.075e9	9.9841e8	1.0294e9
	CO	252.47	105.67	273.68	213.48	258.8	328.36	326.33
10000	NOx	2224.4	8189.5	11991	10068	5509.4	9433.3	11240
	SO2	1.0013e9	1.212e9	9.4264e8	1.1945e9	1.1478e9	1.1469e9	1.0387e9
	CO	81.615	246.59	311.81	271.32	200.18	335.26	328.86

Table 41. Influence of Changing the Weight Factor of Carbon Monoxide (CO)

Weight Factor	Pollutants	N_{P1}	N_{P2}	N_{P3}	N_{P4}	N_{P5}	N_{P6}	N_{P7}
10	NOx	206.16	135.72	148.3	302.71	402.69	204.97	92.301
	SO2	154.65	180.98	167.46	137.5	79.142	151.4	55.945
	CO	167.35	73.894	54.281	127.2	115.06	77.975	150.44
100	NOx	394.36	374.26	145	195.86	284.85	192.11	134.07
	SO2	88.098	46.78	169.83	154.14	143.54	153.76	182.19
	CO	115.25	119.74	51.868	174.93	131.63	70.416	78.878
1000	NOx	206.16	402.69	121.87	204.93	302.72	138.23	129.42
	SO2	154.65	79.138	186.31	151.4	137.49	165.8	181.72
	CO	167.35	115.06	119.25	78.036	127.2	226.4	45.836
10000	NOx	373.2	199.39	133.45	291.08	397.73	153.97	143.37
	SO2	46.007	154.34	182.96	141.55	84.848	154.07	171.3
	CO	119.13	172.23	86.059	129.98	115.14	215.27	50.934

Table 42. Influence of Changing the Weight Factor of Carbon Monoxide (CO)

Weight Factor	Pollutants	N_{V1}	N_{V2}	N_{V3}	N_{V4}	N_{V5}	N_{V6}	N_{V7}
10	NOx	9808.8	11861	10968	7849.5	5014	9226.8	10442
	SO2	1.2033e9	9.5683e8	1.0551e9	1.2062e9	1.1342e9	1.1643e9	2.7683e8
	CO	268.69	316.6	332.81	241.72	187.36	332.39	1.3285
100	NOx	5509.7	2224.6	11240	10068	8189.7	9433.5	11991
	SO2	1.1478e9	1.0013e9	1.0387e9	1.1945e9	1.212e9	1.1469e9	9.4263e8
	CO	200.18	81.626	328.86	271.32	246.59	335.26	311.83
1000	NOx	9808.7	5013.8	12680	9227.9	7849.3	12936	12949
	SO2	1.2033e9	1.1342e9	8.5412e8	1.1643e9	1.2062e9	1.0115e9	9.3188e8
	CO	268.69	187.35	265.8	332.39	241.71	237.39	272.38
10000	NOx	2083.3	9976.3	11966	8071.2	5335.7	11690	11385
	SO2	9.8637e8	1.1979e9	9.3382e8	1.2102e9	1.1432e9	1.1045e9	1.0287e9
	CO	75.093	270.46	310.88	244.9	195.9	267	326.44